Biogenesis and functions of phosphatidylserine and phosphatidylthreonine in *Toxoplasma gondii*

D i s s e r t a t i o n

eingereicht an der

Lebenswissenschaftliche Fakultät

der Humboldt Universität zu Berlin

Zur Erlangung des Akademischen Grades

Doctor rerum naturalium

(Dr. rer. nat.)

im Fach Biologie

von MSc-Biologe Ruben D. Arroyo-Olarte

Präsidentin/Präsident der Humboldt Universität zu Berlin:

Prof. Dr. Jan-Hendrik Olbertz

Dekan der Lebenswissenschaftlichen Fakultät:

Prof. Dr. Richard Lucius

Gutachter/in: 1. Prof. Richard Lucius

2. Prof. Jos Brouwers

3. Prof. Frank Seeber

Tag der mündlichen Prüfung: 04.11.2014

Acknowledgements

First, I would like to thank my supervisor Dr. Nishith Gupta, for his constant support.

I am grateful to Prof. Richard Lucius for his support and the opportunity to work in his department.

Moreover, I want to thank Prof. Frank Seeber, Prof. Jos Brouwers, and Prof. Richard Lucius for agreeing to review this thesis.

I would like to thank Prof. Bernd J. Helms and Prof. Jos Brouwers for the oportunity to establish a successful collaboration and introducing me into the the fascinating field of lipidomics. Also thanks to the members of Prof. Helms's lab at the Institute of Biomembranes of Utrecht University for the friendly atmosphere and assistance.

To our collaborator Dr. Ildiko R. Dunay of the Department om medical microbiology of Magdeburg University, who contributed with the *in vivo* part of this research, also thanks to Aindrila Biswas for providing the brain histological data and to Friederike Hoffmann for her assistance with the Ca^{2+} measurements.

Special thanks to Boehringer-Ingelheim and Elsa-Neumann Stiftung des Landes Berlin for supporting my stay in Helm's Lab and the final phase of my PhD, respectively.

I want to thank all the members of the department of Molecular Parasitology. Special thanks to Grit for her support and for managing the lab. I also thank all other PhD colleagues, Master and Bachelor students for their support and clarifications.

Also thanks to my friends for helping me out through the difficult times.

Finally, I would like to thank my family for their unconditional support from the distance.

Abstract

Toxoplasma gondii is arguably the most succesful parasite in Earth and a major cause of abortion and opportunistic infections in humans and livestock. Understanding the metabolic flexibility of this parasite is essential to comprehend its adaptability. Lipids are basic components of biological membranes. However, in the last decades non-customary roles for lipids beyond membrane biogenesis have been recognized. Here we report for the first time phosphatidylthreonine (PtdThr) as a major phospholipid in *T. gondii* and show its relationship with its archetypical analog, phosphatidylserine (PtdSer). We also identify a novel parasite enzyme (*Tg*PTS), which diverged from the mainstream PtdSer-synthase family to produce this otherwise rare lipid. Genetic ablation of *Tg*PTS not only abolished PtdThr synthesis, but also impaired severely the lytic cycle of *T. gondii*, particularly the egress but also the invasion into host cells without affecting the parasite replication. Our work indicates that, either a lower Ca^{2+} pool and/or a diminished Ca^{2+} mobilization from the parasite endoplasmic reticulum cause a reduced gliding motility, which underlies the observed phenotypes.

Moreover, the mutant parasites lacking PtdThr (*Δtgpts*) are avirulent and exert full protection against both, acute and chronic toxoplasmosis in a murine model. These results highlight the importance of parasite lipids as therapeutic targets and of genetically-attenuated strains in the development of effective vaccines against coccidian parasites.

Our work also identified the parasite enzyme that is responsible for PtdSer synthesis in *T. gondii* (*Tg*PSS). Contrary to *Tg*PTS, we were unable to ablate *Tg*PSS gene, suggesting its essentiality for *T. gondii*. By using a degradation-domain internal tagging approach, we were however able to downregulate *Tg*PSS protein, which translated into a 60-70% reduction in PtdSer synthesis and content in *T. gondii*, without perturbing significantly the parasite fitness in both, wild-type and *Δtgpts* strains. Lipid analyses show that *T. gondii* can recompense for the reduction in PtdSer by increasing proportionally the levels of phosphatidylinositol, and for the loss of PtdThr by upregulating its PtdSer synthesis. Taken together, these results demonstrate the metabolic flexibility of *T. gondii* regarding its anionic phospholipid metabolism to maintain a normal membrane biogenesis and parasite replication. However, such compensatory mechanisms are unable to complement for the abscence of PtdThr concerning virulence, egress and invasion, demonstrating that *T. gondii* has evolved *Tg*PTS and its product, PtdThr, as an adaptation to optimize its parasitic lifestyle.

Zusammenfassung

Toxoplasma gondii ist wohl der am besten an den Menschen und Tieren angepasste Parasit der Welt und eine der Hauptursachen für Abtreibungen und opportunistsiche Infektionen. Das Verständnis der Stoffwechselflexibilität dieses Parasiten ist essentiel um seine Anpassungsfähigkeit nachzuvollziehen. Lipide sind Grundbestandteile der biologischen Membranen. Doch in den letzten Jahrzehnten sind neben der Biogenese der Membranen noch weitere Funktionen entdeckt worden. Hier berichten wir zum ersten Mal über Phosphatidylthreonin (PtdThr) als Hauptphospholipid von *T. gondii* und zeigen seine Beziehung mit seinem archetypischen Analogon, Phosphatidylserin (PtdSer). Wir identifizieren auch ein neues Parasitenenzym (*Tg*PTS), welches von der regulären PtdSer-Synthase-Familie abgewichen ist und dieses sonst selten vorkommende Lipid synthetisiert. Die Gendeletion von *Tg*PTS stoppte nicht nur die Synthese von PtdThr, sondern auch stark beeinträchtigt den lytischen Zyklus von *T. gondii*, insbesondere beim Aus- und Eintritt in die Wirtszellen, ohne dabei die Replikation des Parasiten zu verhindern. Unsere Arbeit zeigt, dass entweder ein niedriger Ca^{2+}-Pool oder eine verminderte Ca^{2+}-Mobilisierung aus dem endoplasmatischen Retikulum des Parasiten eine reduzierte Motilität verursachen, welche den beobachteten Phänotypen zugrunde liegt.

Darüber hinaus fehlt es den mutierten Parasiten an PtdThr (*Δtgpts*), sie sind avirulent und üben vollständigen Schutz gegen akute und chronische Toxoplasmose in einem Mausmodell aus. Diese Ergebnisse verdeutlichen die Bedeutung der Parasitenlipide als therapeutisches Ziel und von genetisch abgeschwächten Stämmen für die Entwicklung von wirksamen Impfstoffen gegen Kokzidien.

Unsere Arbeit konnte auch das Parasiten-Enzym identifizieren, welches verantwortlich für die Synthese von PtdSer in *T. gondii* (*Tg*PSS) ist. Im Gegensatz zu *Tg*PTS, waren wir nicht in der Lage das *Tg*PSS Gen zu entfernen, das seine Essentialität für *T. gondii* andeutet. Durch die Verwendung einer gezielten Degradation-Domain-Tagging-Methode waren wir jedoch in der Lage das *Tg*PSS Protein herunter zu regeln, was zu einer Reduzierung von 60 bis 70% in der PtdSer-Synthese und -Gehalt in *T. gondii* führte, ohne die Fitness im Wildtyp und Δ*tgtps*-Stämmen erheblich zu stören. Lipid-Analysen zeigen, dass *T. gondii* für die Reduzierung von PtdSer proportional Phosphatidylinositol erhöht und durch den Verlust an PtdThr die Synthese von PtdSer hochreguliert wird. Zusammengenommen zeigen diese Ergebnisse die

metabolische Flexibilität von *T. gondii* hinsichtlich seines anionischen Phospholipid-Stoffwechsels, um eine normale Membranbiogenese und Replikation der Parasiten beizubehalten. Allerdings sind solche Ausgleichsmechanismen nicht fähig die Abwesenheit an PtdThr bezüglich der Virulenz und dem Ein-und Austritt zu kompensieren. Wir können zusammenfassen, dass *T. gondii Tg*PTS und seine Produkte (PtdThr) sich entwickelten, um seine Anpassung an den parasitären Lebensstil zu optimieren.

TABLE OF CONTENTS

LIST OF FIGURES

LIST OF APPENDICES

ABBREVIATIONS

ATc	Anhydro-tetracycline
ATP	Adenosine triphosphate
CAT	Chloramphenicol acetyltransferase
CCT	Choline cytidylyltransferase
cDNA	Complementary deoxyribonucleic acid
$CHCl_3$	Chloroform
CK	Choline kinase
CPT	CDP-choline phosphotransferase
DAPI	4',6-diamidino-2-phenylindole
DHFR-TS	Dihydrofolate reductase thymidylate synthase
DMEM	Dulbeccos's modified Eagle medium
DNA	Deoxyribonucleic acid
EDTA	Ethylendiamine tetraacetate
EK	Ethanolamine kinase
ER	Endoplasmic reticulum
EtOH	Ethanol
FAS I/II	Fatty acid synthase type I/II
FCS	Fetal calf serum
FUdR	5-Fluoro-2'-deoxyuridine
GSH	Glutathione (reduced)
HFF	Human foreskin fibroblast
HPLC	High-Performance Liquid Chromatography
HXGPRT	Hypoxanthine-xanthine-guanine phosphoribosyl transferase
IEM	Immunoelectron microscopy
IFA	Indirect immunofluorescence assay
IMC	Inner membrane complex
IPTG	Isopropyl-ß-D-1-thiogalactopyranoside
LDL	Low-density lipoprotein
LiAc	Lithium acetate
MeOH, (CH_3OH)	Methanol

MS	Mass spectrometry
NADH	Nicotinamide adenine dinucleotide
NBD	7-nitrobenz-2-oxa-1,3-diazol-4-yl
ORF	Open reading frame
PBS	Phosphate buffered saline
PCR	Polymerase chain reaction
PEG	Polyethylene glycol
PEMT	Phosphatidylethanolamine methyltransferase
PSD	Phosphatidylserine decarboxylase
Petn-Cer	Phosphoethanolamine ceramide
PSS	Phosphatidylserine synthase
PtdCho	Phosphatidylcholine
PtdEtn	Phopshatidylethanolamine
PtdGro	Phosphatidylglycerol
PtdIns	Phosphatidylinositol
PtdOH	Phosphatidic acid
PtdSer	Phosphatidylserine
PV	Parasitophorous vacuole
PVM	PV membrane
RNA	Ribonucleic acid
RT-PCR	Reverse-transcriptase PCR
SDS	Sodium dodecyl sulfate
SM	Sphyngomyelin
TaTi	Trans-activator trap identified
TLC	Thin layer chromatography
UPRT	Uracil phosphoribosyl transferase
UTR	Untranslated region

1. Introduction

1.1. *Toxoplasma gondii*: Life cycle, distribution and pathogenesis

T. gondii is an obligate intracellular parasite of cosmopolitan distribution. The life cycle of *T. gondii* consist in two phases: one sexual phase which occurs only in the cat intestine, and an asexual phase which unlike most unicellular parasites, can occur in nearly all warm-blooded vertebrates, due in part to *T. gondii* special ability to differentiate into dormant stages or tissue cysts, where it remains largely protected from the host's immune system (Black and Boothroyd, 2000) (Fig. 1).

The sexual phase of *T. gondii* life cycle starts in the feline intestine after ingestion of contaminated meat with tissue cysts that release bradyzoites which then differentiate into sexual stages. Gametes undergo fertilization and resulting zygotes differentiate into oocysts containing 4 sporozoites, which are released in the cat feces to the environment. During the asexual phase, intermediate hosts, including humans, can acquire the parasite after ingestion of contaminated food or water with tissue cysts or environment-resistant oocysts (Dubey, 1998). Recently, alternative routes of infection have been proposed, including toxoplasmosis as a potential sexually-transmited disease in both, animals (Lopes et al., 2013) and humans (Flegr et al., 2014), strengthening the evolutionary success of this cosmopolitan parasite.

Initially, either sporozoites (from oocysts) or bradyzoites (from tissue cysts) differentiate into the fast replicating stage or tachyzoite (Greek *tachy*: fast). Tachyzoites replicate within their host cell every 6-8 hours until reaching 64 to 128 parasites per host cell, which is then lysed releasing infective parasites (Radke and White, 1998). This lytic behavior is responsible for the acute phase of toxoplasmosis, which characterizes by tissue necrosis and inflammatory response (Mordue et al., 2001). Depending on genetic factors of both, the host and the parasite, acute infection either continues uncontrolled resulting in the death of the host or is put in check by the host's immune system causing the differentiation of tachyzoites into slow-replicating bradyzoites inside tissue cysts (Behnke et al., 2012; Cavaillès et al., 2006; Jensen et al., 2013; Niedelman et al., 2012). These are found mainly in muscles and brain tissue, where they remain for the lifetime of the host. However, when the host immune system is immature (e.g. neonates (Torgerson and Mastroiacovo, 2013)) or compromised (e.g. AIDS (Navia et al., 1986), organ transplants (Wendum et al., 2002)), bradyzoites differentiate again

into fast growing tachyzoites, which lead to severe disease in different organs (brain, liver, eye, etc), with a potential lethal outcome.

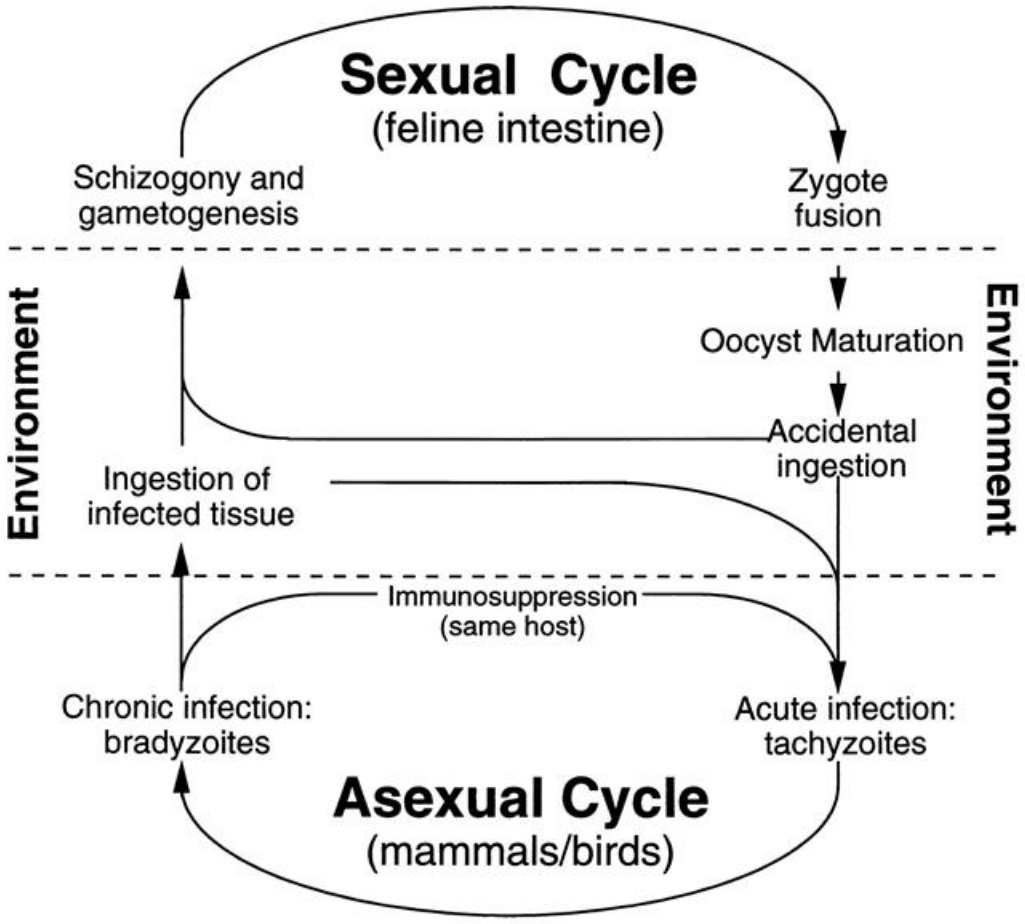

Fig. 1. Life cycle of *Toxoplasma gondii*. Taken from (Black and Boothroyd, 2000).

During the acute phase of infection, the parasite undergoes the so-called lytic cycle (Fig. 2). This begins when the extracellular parasite seeks for its host cell, attaches to it and actively invades it. Replication of *T. gondii* occurs exclusively within its host cell inside a non-fusogenic parasitophorous vacuole (PV), which the parasite secludes from the host lysosomal network. The PV is also actively modified by the parasite to enhance the nutrition acquisition from the host organelles, like mitochondria, Golgi and endoplasmic reticulum, which get in close contact with it and supply among others sugars, nucleotide precursors, cholesterol and phospholipids (Blume et al., 2009; Chaudhary et al., 2004; Coppens et al., 2000; Iltzsch,

1993; Romano et al., 2013a, 2013b). After several rounds of intracellular replication the parasites become motile and initiate the egress from its host cell, thereby causing its lysis.

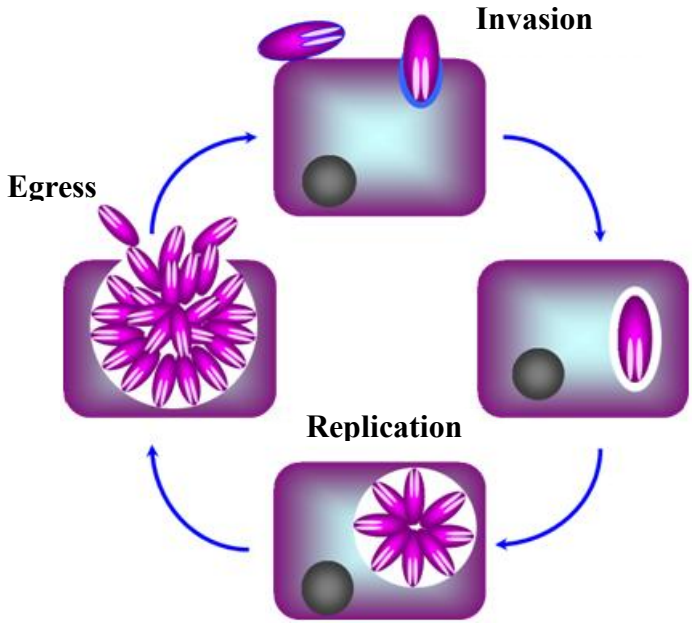

Fig. 2. Lytic cycle of *T. gondii*. Adapted from (Arroyo-Olarte et al. 2014, under submission).

Intracellular replication has been the most commonly targeted phase of the lytic cycle by current drug treatments. In *T. gondii* it occurs through a special mode of cell division known as endodyogeny, in which the two daughter cells are formed within the scaffold of the mother cell, following a hierarchical sequence of organelle partioning and leaving behind a residual body (Fig. 3). The other two phases of the lylic cycle of *T. gondii*, however, invasion and egress, although also fundamental for the pathogenesis, have been disregarded as therapeutic targets.

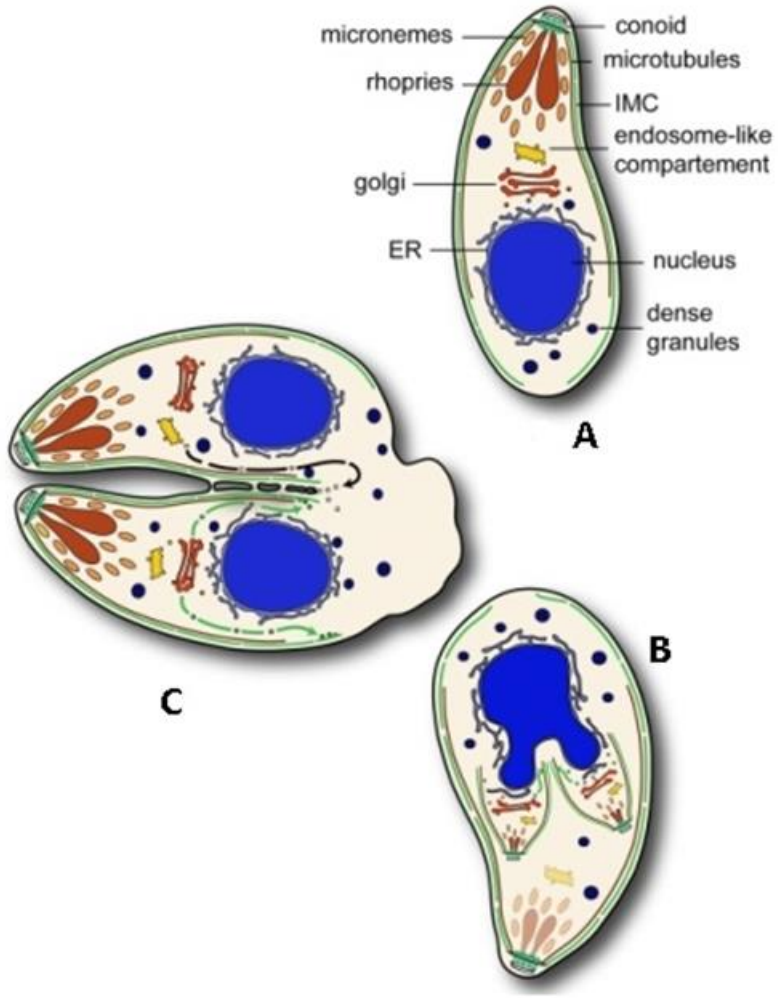

Fig 3. *Schematic representation of endodyogeny and cell structure of T. gondii.* **(A)** Mother cell. **(B)** developing daughter cells within mother cell, IMC (inner membrane complex) scaffolds are shown in green. **(C)** Cytokinesis. Adapted from (Agop-Nersesian et al., 2010).

1.1.1. Regulation of the lytic cycle: Calcium signaling, motility and exocytosis in apicomplexan parasites

Apicomplexan parasites are an ancient group of unicellular eukaryotic organisms, mostly related to other protozoans like dinoflagelates and ciliates (Baldauf, 2003). Apicomplexans often contain many plant-like genes probably resulting from their ancient origin pre-dating the plant-animal split, but mostly due to the acquisition of an algae-derived secondary plastid endosymbiont, called the apicoplast (Janouskovec et al., 2010; Oborník et al., 2009; Sato,

2011). Due to the particular origin and parasitic nature of apicomplexans, calcium signaling pathways regulating the lytic cycle of *T. gondii* and related parasites are unique and offer potential therapeutic targets (Nagamune and Sibley, 2006; Nagamune et al., 2008a; Plattner et al., 2012).

It has been shown that calcium plays a central role in the regulation of the invasion and egress stages of *T. gondii* lytic cycle by controlling parasite secretion and motility (Billker et al., 2009; Lourido et al., 2010; McCoy et al., 2012; Meissner et al., 2002). The rapid release from intracellular calcium storages into the cytosol where it is normally maintained at very low levels (ranging the nanomolar concentrations), is thus a potent trigger to initiate multitude of signaling cascades (Nagamune et al., 2008a). In the same way, released calcium must be quickly dampened to avoid toxic effects in the cells. Taken together, apicomplexans, and particularly *T. gondii*, has developed elaborated molecular mechanisms to control the calcium fluxes and the subsequent signaling pathways regulating its lytic cycle (Fig 4).

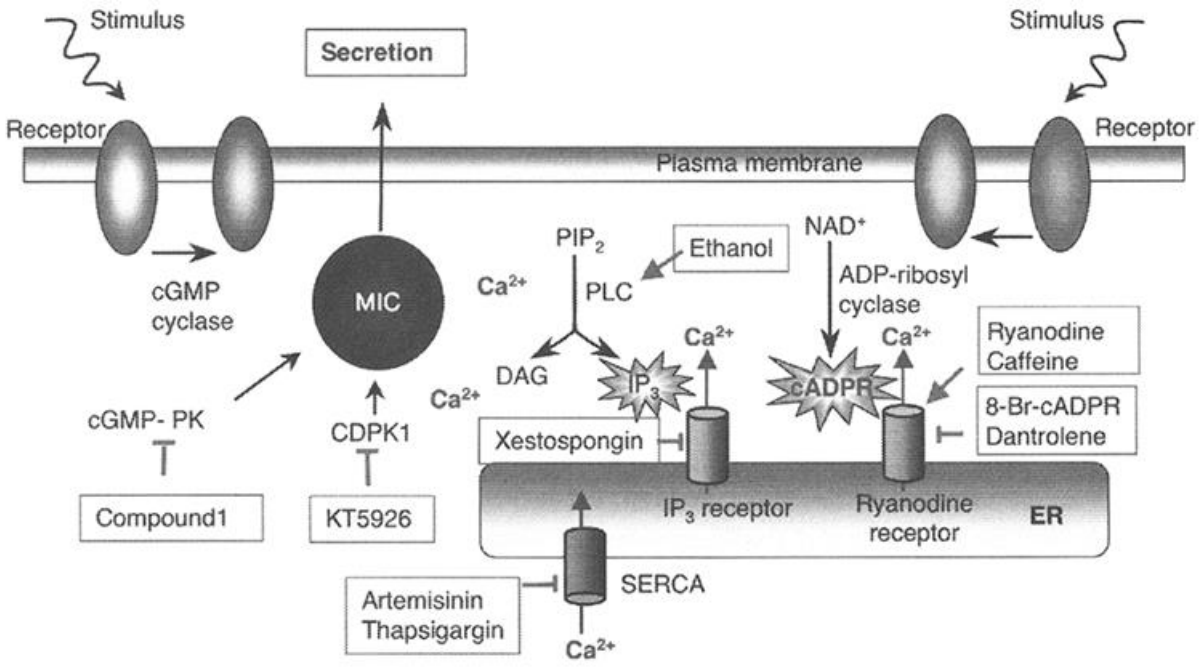

Fig 4. *Microneme secretion and calcium-mediated signaling pathways in T. gondii*. Chemical agonists (➔) or inhibitors (⊤) are also shown. MIC, micronemal proteins; cGMP-PK, cGMP-dependent protein-kinase; CDPK1, calcium-dependent protein-kinase 1; PIP_2, Phosphatidylinositol 4,5-bisphosphate; PLC, Phospholipase C; DAG, Diacylglycerol; cADPR, Cyclic ADP-ribose; SERCA, Sarcoplasmic reticulum calcium ATPase. Taken from (Nagamune et al., 2008a).

1.2. Genetic manipulation of *T. gondii*

T. gondii is the most experimentally-tractable Apicomplexan parasite due mainly to its promiscuous choice of host cells and its ability to be maintained in asexual cycle indefinitely in cell culture or murine systems. Initial forward genetic studies were performed by chemical mutagenesis and were fundamental for the establishment of basic cell culture protocols leading to the selection of clonal lines (Pfefferkorn and Pfefferkorn, 1976). Classical crossing experiments between different strains and analysis of the progeny have since then been made and allowed to tract loci controlling complex genetic traits, like virulence between different *T. gondii* lineages and to analyze populations structure (Pfefferkorn and Kasper, 1983; Su et al., 2002). However, this approach is highly expensive and laborious, and also requires the definitive feline host.

It was not until the establishment of an efficient transfection protocol by electroporation that modern reverse genetic studies were feasible (Soldati and Boothroyd, 1993). Since then, vectors have been developed either for random integration or targeting of foreign genes to specific loci by homologous recombination. Initially, however, gene replacement was hampered by a high frequency of non-homologous recombination in *T. gondii*. To address this issue, Fox et al. (2009) developed a type I strain of *T. gondii* deficient in non-homologous end-joining (NHEJ) DNA repair pathway by deleting the parasite KU80 protein. The resulting mutant maintained most of the phenotypic features of the wild-type parasites, including virulence but had a high efficient rate of homologous recombination. Since then, the *Δku80* strain has become the power horse to analyze the function of putative genes in *T. gondii* by targeted gene replacement with different selection markers. More recently, the same achievement was accomplished in a type II strain, which would facilitate studies on the genetic basis of bradyzoite differentiation (Fox et al., 2011).

Another breakthrough, especially for the analysis of essential genes in *T. gondii* was the tetracycline-inducible knockdown system (Meissner et al., 2002). This system utilizes a parasite line expressing a transactivator (TATi-1), which specifically activates a *pTetO7* promoter to induce the expression of the gene of interest (G.O.I.). However, in presence of anhydrotetracycline (aTC), TATi-1 is blocked, silencing the *pTetO7*-driven expression. Once the inducible copy of the G.O.I. is introduced in *T. gondii* genome, the endogenous gene is deleted by double homologous recombination of its 5' and 3'-UTRs, and replaced by a

resistance selection marker. This system is very useful in the analysis of genes thought to be essential and which remain refractory to direct deletion.

Other conditional systems include the targeting of the protein of interest to the proteasome where it is rapidly degraded, by adding a FKBP-derived destabilization-domain (DD) epitope. The degradation of the chimeric protein, however can be overcome by a cell-permeable ligand (Shield1) in a dose- and time-dependent fashion (Banaszynski et al., 2006; Herm-Götz et al., 2007). This system has been successfully applied in other relevant human pathogens like *Plasmodium falciparum* (Armstrong and Goldberg, 2007) and *Entamoeba histolytica* (Liu and Singh, 2014).

More recently, a novel method to conditionally delete genes by a rapamycin-regulatable Cre-recombinase has been established (Andenmatten et al., 2013). The advantages of this system include a rapid generation of gene knockouts (including essential genes) by addition of the drug for their prompt analysis. In a first application of the technique, the authors have shown that genes encoding proteins considered to be essential for parasite invasion, e.g. myosin A and MIC2, are in fact dispensable. The disadvantages of the Cre-system, however are that the Cre-mediated recombination does not occur in 100% of parasites and therefore makes difficult the analysis of the knockout phenotype (Jiménez-Ruiz et al., 2014).

1.3. Membrane and lipid biology of eukaryotes

Lipids are the main components of biological membranes, which separate living cells from the surrounding medium. They also define the subcellular organelles and the vesicle trafficking of proteins between different cellular compartments (van Meer et al., 2008). The main organization of biological membranes was described by Singer and Nicolson (1972) as a fluid mosaic, or a two-dimensional oriented solution of integral proteins embedded in the viscous phospholipid bilayer solvent, where cholesterol (or ergosterol in fungi) intercalates and regulates the membrane fluidity (Fig. 5).

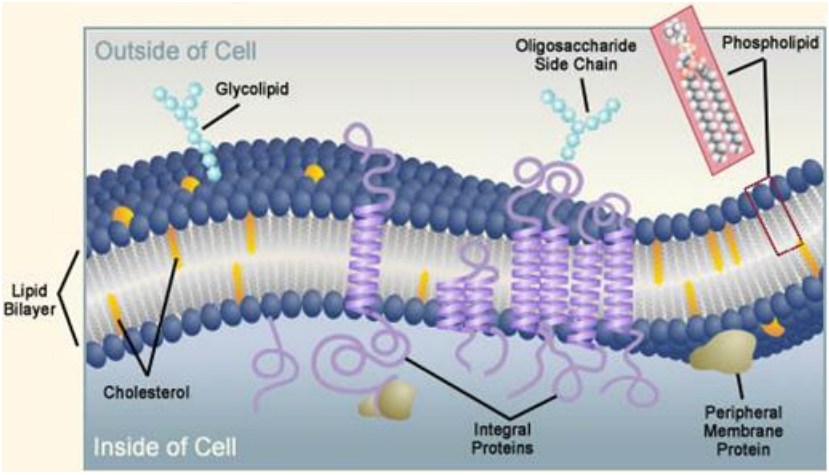

Fig 5. *Scheme depicting the fluid mosaic model of the plasma membrane*. Modified from http://www.biology.arizona.edu/cell_bio/problem_sets/membranes.

Phospholipids are divided in two major groups, glycerophospholipids, which are composed of a glycerol moiety attached to two fatty acyl chains and a hydrophilic polar head group linked by a phosphate group. On the other hand, sphingolipids consisting of head groups linked via phosphate to ceramide (Fig 6)

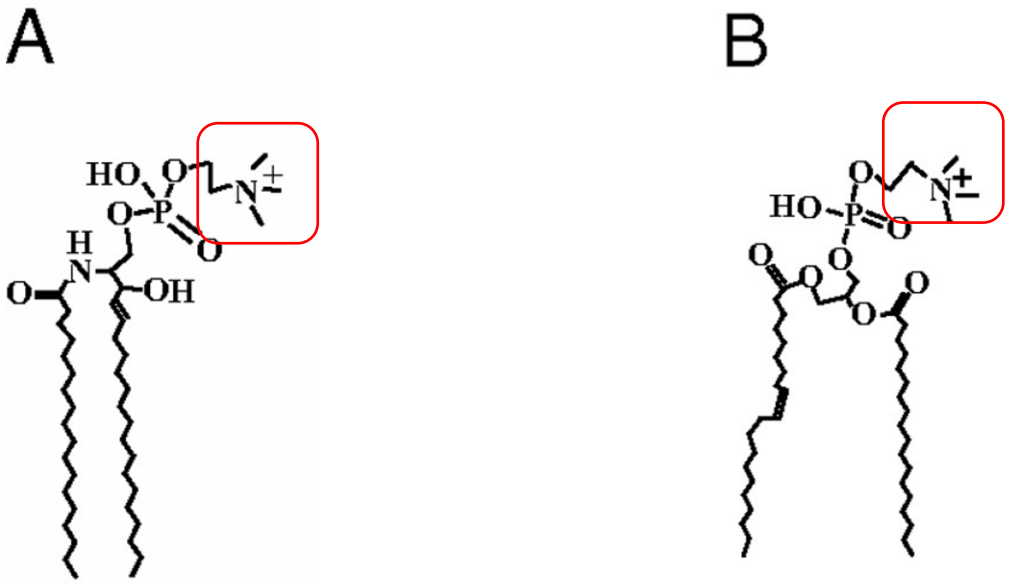

Fig 6. *Scheme showing the structure of the two major phospholipid groups*, sphingolipids (A) and glycerophospholipids (B), in particular, sphingomyeline and phosphatidylcholine, respectively. Polar head groups (red rectangle) may vary, including choline, serine, ethanolamine and inositol. Modified from (An et al., 2011).

The distribution and variety of phospholipids is responsible for the biophysical properties of biological membranes. For example, the length and degree of saturation of the fatty acyl chains is responsible for the thickness and ordering of the hydrophobic region of the membrane; while the electrostatic charge of their polar headgroups mediates interactions with charged proteins (Janmey and Kinnunen, 2006).

Each major phospholipid has intrinsical biophysical properties, which contribute to the stability and functions of biological membranes. For example, lysophospholipids and phosphoinositides have an inverted conical shape due to their relative bulky headgroups compared to their hydrophobic tails (Fig 7a), and tend to form structures with a positive membrane curvature like micelles. Cylindrical-shape phospholipids like PtdCho and sphyngomyelin, on the other hand, readily form flat bilayers and are responsible for the basic structure of the cell membranes (Fig. 7b). However, conical-shape lipids like PtdEtn, with small polar head group, tend to form structures with a negative curvature such as inverted hexagonal tubes with headgroups inside and hydrophobic tails facing out. (Fig 7c). Overall, the relative abundance and distribution of lipids will determine the shape and curvature of the membranes (Janmey and Kinnunen, 2006).

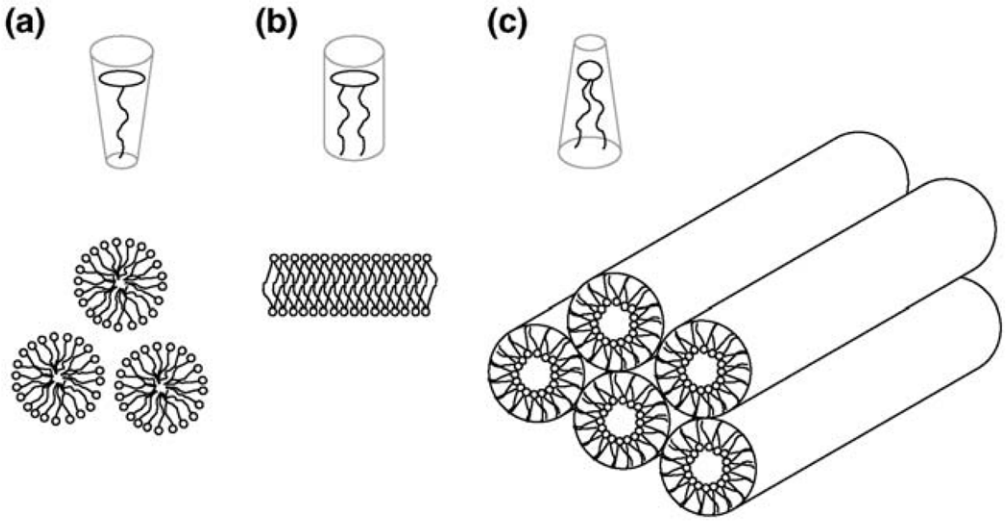

Fig 7. *Typical structures formed by phospholipids* (A) Conical lipids, like polyphosphoinositides and lysophospholipids usually self aggregate in micelles. (B) Cylindrical lipids like PtdCho and sphyngomyelin tend to form flat bilayers. (C) Inverted conical lipids, like PtdEtn forming inverted hexagonal tubes. Taken from (Janmey and Kinnunen, 2006).

1.3.1. Mammalian cells

In mammalian cells, the main phospholipid classes are phosphatidylcholine (PtdCho), phosphatidylethanolamine (PtdEtn), Phosphatidylserine (PtdSer) and Phosphatidylinositol (PtdIns) (van Meer and de Kroon, 2011; van Meer et al., 2008). The relative distribution of these and other lipids however, varies according to the subcellular organelle. In particular the plasma membrane is enriched in cholesterol to give more rigidity, compared to the endoplasmic reticulum or the Golgi complex, which have more PtdCho to give more fluidity (van Meer and de Kroon, 2011). Mitochondria, in accordance to their bacterial origin are enriched in PtdEtn, phosphatidylglycerol and cardiolipin, a tipical bacterial lipid (Daum, 1985). On the other hand, the endosomes on their way to maturation are enriched in bis(monoacylglycero)phosphate (Kobayashi et al., 2002), which participates in multivesicular body generation, fusion processes and sphingolipid hydrolysis (Kolter and Sandhoff, 2005; Matsuo et al., 2004). The main pathways for phospholipid synthesis in mammals, including humans, are shown in Figure 8.

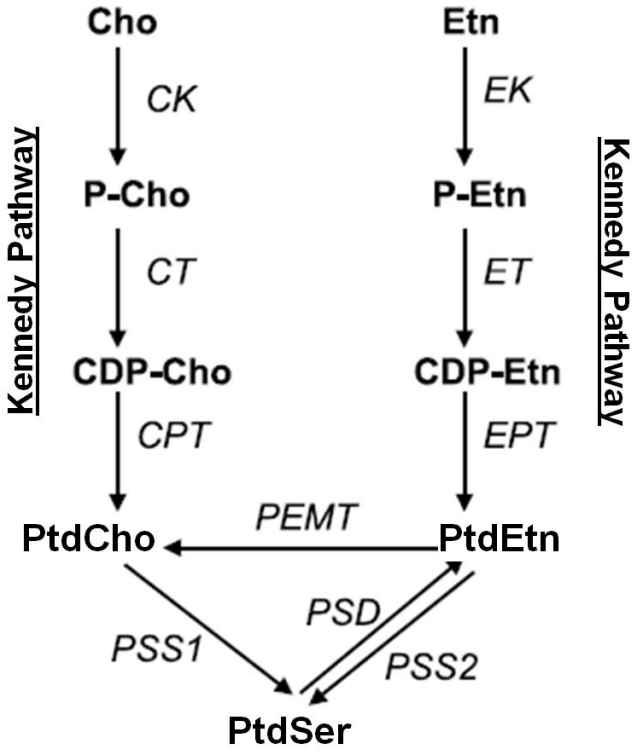

Fig 8. *Inter-relationships among phospholipid biosynthetic pathways in mammalian cells*. Cho: choline; CK: choline kinase; CPT: CDP-choline:1,2-diacylglycerol cholinephosphotransferase; CT: CTP:phosphocholine citidytransferase; Etn: ethanolamine; EK: ethanolamine kinase; ET:

CTP:phosphoethanolamine cytidil-transferase; EPT: CDP-ethanolamine:1,2-diacylglycerol ethanolamine-phosphotransferase; PtdCho: phosphatidylcholine; PtdEtn: phosphatidylethanolamine; PEMT: phosphatidylethanolamine *N*-methyltransferase; PtdSer: phosphatidylserine; PSD: phosphatidylserine decarboxylase; PSS: phosphatidylserine synthase. Modified from (Vance and Vance, 2004).

Based on their charge, phospholipids are also actively segregated between the outer and inner leaflet of the plasma membrane of eukaryotes, with anionic phospholipids (PtdSer and PtdIns) at the inner leaflet, and cationic phospholipids like PtdCho and sphingomyelin predominantly at the outer/luminal face (Ikeda et al., 2006; Yamaji-Hasegawa and Tsujimoto, 2006). Among these, PtdSer is one of the most abundant an its roles extend far beyond the membrane biogenesis including apoptosis (Fadok et al. 1992, Li et al. 2003), membrane potential (Levenstein and Grinstein 2010), protein sorting and secretion (Uchida et al. 2011) and as a precursor of other phospholipids (Gupta et al., 2005, 2012; Vance, 2008; Voelker, 1984). Many of the PtdSer functions depend on the acidic nature and negative charge of this phospholipid, which allows it to associate with calcium ions and cationic proteins, and to help in the maintenance of the membrane potential at the inner leaflet of the plasma membrane (Levenstein and Grinstein 2010). PtdSer has been shown to be essential in mammals (Kuge et al. 1997) and plants (Yamaoka et al. 2011), but not in yeast, for which it is dispensable but necessary for its optimal growth (Hikiji et al., 1988).

1.3.2. Protozoan parasites

Protozoan parasites are a very heterogeneous group comprising distantly related phyla. There are several specific lipid components and pathways with potential therapeutic applications. Such differences arise not only from their parasitic nature, but also from their divergent phylogenetic origin (Vial et al., 2003). Most of the available research data come from the trypanosomatid and apicomplexan parasites, due to their medical and veterinary importance and also to their relative ease of culture (Ramakrishnan et al., 2013).

Apicomplexan parasites, including *Plasmodium* (Hsiao et al., 1991; Vial and Ancelin, 1992), *Toxoplasma* (Foussard et al., 1991; Gupta et al., 2005; Welti et al., 2007) and *Babesia*

(Florin-Christensen et al., 2000) are characterized by a higher amount of PtdCho and much less PtdSer as well as lower cholesterol/phospholipid ratio (implicating a higher degree of fluidity) in their membranes compared to their host mammalian cells (Ramakrishnan et al., 2013; Vial et al., 2003). In particular *Plasmodium*-infected erythrocytes contain almost no detectable cholesterol and less sphingomyelin (14.6% versus 28.0%), but contain more PtdCho (38.7% versus 31.7%) and PtdIns (2.1% versus 0.8%) (Hsiao et al., 1991).

In the case of *Toxoplasma*, PtdCho is the dominant phosholipid (60-75% of total phosphorus lipid) followed by PtdEtn (25-15%), PtdIns (10%), PtdSer (6%) and PtdOH (1.5%) (Foussard et al., 1991; Gupta et al., 2005; Hartmann et al., 2014). Lipidomic analysis using electrospray ionization mass spectrometry has also revealed small amounts of phosphoethanolamine-ceramide (PEtn-Cer), in addition to the above-mentioned phospholipid classes (Welti et al., 2007). The same report also showed that *T. gondii* phospholipids, particularly PtdCho, are enriched in shorter and saturated fatty acyl chains.

Figure 9 shows the main pathways for phospholipid synthesis documented so far in *T. gondii*, including the Kennedy pathways for PtdCho and PtdEtn synthesis (Gupta et al., 2005; Sampels et al., 2012). As well as the decarboxylation of Ptdser as a source of PtdEtn (Hartmann et al., 2014). *T. gondii* also expresses a functional phosphatidylinositol synthase which catalyzes the synthesis of PtdIns from CDP-DAG and inositol (Séron et al., 2000). PtdSer synthesis on the other hand has been shown to proceed by a base-exchange mechanism, most likely with PtdEtn (Gupta et al., 2005). However, contrary to PtdCho and PtdEtn, the genetic identity of the enzyme(s) responsible for PtdSer synthesis in *T. gondii* has not been described so far, and constitutes one of the main objectives of the present work.

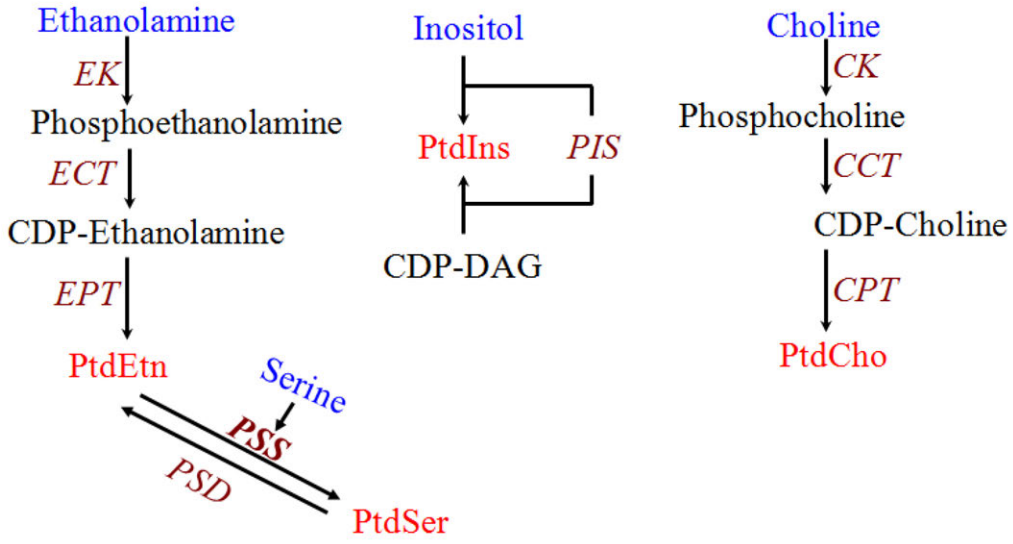

Fig 9. *Biochemical pathways for phospholipid synthesis with experimental evidence in T. gondii*. *C/EK*: choline/ethanolamine kinase; *CCT*: CTP:phosphocholine cytidylyltransferase; CPT: 1,2-diacylglycerol cholinephosphotransferase; *ECT*: CTP:phosphoethanolamine cytidylyltransferase; *EPT*: 1,2-diacylglycerol ethanolaminephosphotransferase; *PIS*: phoshatidylinositol synhthase; CDP-DAG: CDP-diacylglycerol; *PSS*: base-exchange phosphatidylserine synthase; PtdCho: phosphatidylcholine; PtdEtn: phosphatidylethanolamine; PtdIns: phosphatidylinositol; PtdSer: phosphatidylserine.

1.4. Objective of this study

Toxoplasma gondii is an obligate intracellular parasite, which is able to synthesize its major phospholipids to cover the membrane biogenesis needed for its rapid intracellular replication. However, there is evidence that *T. gondii* is also able to scavenge host-derived lipids for their membrane biogenesis (Coppens et al., 2000; Hartmann et al., 2014). The physiological importance of these two mechanisms remains uncertain for most phosphoholipids, including phosphatidylserine. Additionally, other functions of phospholipids for the parasite biology beyond their traditional role as membrane building blocks remain underappreciated. The aim of the present work is to identify and describe the enzymes responsibles for the endogenous synthesis of phosphatidylserine and its novel analog phosphatidylthreonine in *T. gondii*, and to determine the role of both lipids not only for membrane biogenesis but also for the regulation of the parasite lytic cycle and virulence.

2. Materials and Methods

2.1. Materials

2.1.1. Biological resources

Cell line	Source
Human Foreskin Fibroblasts	Carsten Lüder, University of Göttingen, Germany
T. gondii tachyzoites (RH*Δku80-Δhxgprt*-strain)	Vern Carruthers, University of Michigan, Ann Arbor, USA
T. gondii tachyzoites (Δ*ku80*-TaTi strain)	Boris Striepen, University of Georgia, USA
COS-7 cells	Isabelle Coppens, Johns Hopkins University, Baltimore, USA
E.coli (XL-1blue)	Stratagene, Germany
E. coli (M15/pREP4)	Qiagen, Germany
C57BL/6 mice	Janvier Labs, France

2.1.2. Chemical reagents

Product	Manufacturer
1,4-Dithiothreitol (DTT)	Roth, Germany
4',6'-Diamidino-2-phenylindol-dihydrochloride (DAPI)	Merck, Germany
5-Fluoro-2'-deoxyuridine (FudR)	Sigma-Aldrich, Germany
Acetic acid	Roth, Germany

Product	Manufacturer
Adenosintriphosphate (ATP)	Sigma-Aldrich, Germany
Ammonium molybdate	Applichem, Germany
Ammonium persulfate	Sigma-Aldrich, Germany
Ampicillin	Applichem, Germany
Anhydrotetracycline hydrochloride (aTC)	Sigma-Aldrich, Germany
Ascorbic acid	Applichem, Germany
Bovine serum albumin fraction V (BSA)	Applichem, Germany
Bromophenol blue	Merck, Germany
Calcium chloride	Applichem, Germany
Chloramphenicol	Roth, Germany
Chloroform	Roth, Germany
Crystal violet	Sigma-Aldrich, Germany
Cytochalasin D	Sigma-Aldrich, Germany
Deoxynucleotide-triphosphate (dNTPs)	Rapidozym, Germany
Dimethyl sulfoxide (DMSO)	Sigma-Aldrich, Germany
DNA marker (1kb ladder)	Thermo Scientific, Germany
Distilled water (HPLC-purified)	Roth, Germany
Dulbecco's Modified Eagle Medium (DMEM)	Biowest, Germany
Dulbecco's phosphate buffered saline (PBS)	Biowest, Germany

Product	Manufacturer
Ethanol	Roth, Germany
Fluoromount G / DAPI	Southern Biothech, USA
Geneticin	Life Technologies, USA
α-D(+)-Glucose monohydrate	Applichem, Germany
Glycerol	Applichem, Germany
Hank's balanced salt solution (HBSS)	PAA, Austria
Iodine (anhydrous beads)	Sigma-Aldrich, Germany
Isopropanol	Applichem, Germany
Isopropyl-beta-D-thiogalactopyranoside (IPTG)	Applichem, Germany
Kanamycin sulfate	Applichem, Germany
L-glutamine	Biowest, Germany
L-glutathione	Applichem, Germany
Lipofectamine 2000	Life Technologies, USA
Methanol	Roth, Germany
Mycophenolic acid	Applichem, Germany
MEM essential amino acids (50X)	Biowest, Germany
MEM non-essential amino acids (100X)	Biowest, Germany
Ninhydrin Spray solution	Roth, Germany
Paraformaldehyde	Roth, Germany

Product	Manufacturer
Penicillin/Sptreptomycin	Biowest, Germany
Perchloric acid	Applichem Germany
Phenylmethylsulfonyl fluoride (PMSF)	Roth, Germany
Potassium acetate	Roth, Germany
Potassium chloride	Roth, Germany
Potassium hydroxide	Merck, Germany
Rotiphorese gel 30 (Acrylamide)	Roth, Germany

2.1.3. Primers

Primer Name (restriction site)	Nucleotide Sequence (restriction site underlined)	Cloning Vector (research objective)
Annotation of *Tg*PTS and *Tg*PSS		
*Tg*PTS-F	ATGCAACTCCCTTCAAGA	pDrive (T/A-cloning for testing and sequencing *Tg*PTS (TGGT1_273540)
*Tg*PTS-R	TCACTGACTTCGTTCCATTTTCACG	
*Tg*PSS-F	ATGTGTCGGGGACCGCCGCT	pDrive (T/A-cloning for testing and sequencing *Tg*PSS (TGGT1_261480)
*Tg*PSS-R	TCACTCGTCTTTTTGGCCTTC	
Expression and localization of *Tg*PTS and *Tg*PSS in *T. gondii* (*Δku80-TaTi* strain)		
*Tg*PTS-F (*EcoRV*)	CTCATCGATATCATGCAACTCCCTTCAAGA	*pTETO7SAG1-UPKO* (Ectopic expression of *Tg*PTS-HA at the *TgUPRT* locus)
*Tg*PTS-HA-R (*PacI*)	CTCATCTTAATTAATCAAGCGTAATCTGGA ACATCGTATGGGTACTGACTTCGTTCGATT	

*Tg*PSS-F (*EcoRV*)	CTCGATATCATGTGTCGGGGACCGCCGCT	*pTETO7SAG1-UPKO* (Ectopic expression of *Tg*PSS-HA at the *TgUPRT* locus)
*Tg*PSS-HA-R (*PacI*)	CTCTTAATTAATCAAGCGTAATCTGGAACATCGTATGGGTACTCGTCTTTTTGGCCCTTCC	
Making of *Δtgpts* mutant in *T. gondii* (*Δku80-hxgprt*⁻ strain)		
5'COS-*Tg*PTS-F (*NotI*)	CTCATCGCGGCCGCGTTCGCCTCGAGTGCTTG	*pTKO-HXGPRT* (Cloning of the *Tg*PTS 5' crossover sequence)
5'COS-*Tg*PTS-R (*EcoRI*)	CTCATCGAATTCACGAGCCAGTGGAACGAC	
3'COS-*Tg*PTS-F (*HpaI*)	CTCATCGTTAACAGCATCTTTATCGATGCGCT	*pTKO-HXGPRT* (Cloning of the *Tg*PTS 3' crossover sequence)
3'COS-*Tg*PTS-R (*HpaI*)	CTCATCGTTAACTCACTGACTTCGTTCGATTTTC	
Screening for 5' and 3' recombination in the *Δtgts* mutant of *T. gondii*		
5'Scr-*Tg*PTS-KO-F	CGATTCCTTGAGAGCAACTG	*pDrive* (TA-cloning of 5' PCR product for sequencing)
5'Scr-*Tg*PTS-KO-R	GACGCAGATGTGCGTGTATC	
3'Scr-*Tg*PTS-KO-F	ACTGCCGTGTGGTAAAATGAA	*pDrive* (TA-cloning of 3' PCR product for sequencing)
3'Scr-*Tg*PTS-KO-R	GCCATAGAGTTCATTGCGGACTC	

Genetic complementation of the *Δtgts* mutant of *T. gondii*		
*Tg*PTS-F (*NsiI*)	CTCATCATGCATATGCAACTCCCTTCAAGAAAGG	*pTgGRA2-UPKO* (Ectopic expression of *Tg*PTS-HA at the *TgUPRT* locus)
*Tg*PTS-HA-R (*PacI*)	CTCATCTTAATTAATCAAGCGTAATCTGGAACATCGTATGGGTACTGACTTCGTTCGATTTTCACG	

*Tg*PTS$_{(\Delta ECWWD)}$-P1-F (*NsiI*)	CTCATCATGCATATGCAACTCCCTTCAAGAAAGG	*pTgGRA2-UPKO* (Ectopic expression of *Tg*PTS$_{(\Delta ECWWD)}$-myc at the *TgUPRT* locus)
*Tg*PTS$_{(\Delta ECWWD)}$-P1-R (*SbfI*)	CTCATCCCTGCAGGGCGCAGAGTTCGGGGACGAG	
*Tg*PTS$_{(\Delta ECWWD)}$-P2-F (*NsiI*)	CTCATCATGCATAGCATCTTTATCGATGCGCTG	
*Tg*PTS$_{(\Delta ECWWD)}$-P2-myc-R (*PacI*)	CTCATCTTAATTAATCACAGATCTTCTTCAGAAATAAGTTTTTGTTCCTGACTTCGTTCGATTTTCACGT	
Expression of GCamp6s in *T. gondii* (*Δku80-hxgprt*` and *Δtgpts* strains)		
GCamp6s-F (*NsiI*)	CTCATCATGCATTCTCATCATCATCATCATCATGG	*pTgGRA2-UPKO* (Ectopic expression of GCamp6s at the *TgUPRT* locus)
GCamp6s-R (*PacI*)	CTCATCTTAATTAATTACTTCGCTGTCATCATTTGTACA	
Expression of genes flanking the *Tg*PTS locus in *T. gondii* (*Δku80-hxgprt*` , *Δtgpts and Δtgpts/Tg*PTS-HA strains)		
TGGT1_273550-F	ATGCATTGTCAACTAGGAGGC	ORF-specific PCR of TGGT1_273550
TGGT1_273550-R	TTACAGTGTCGAACTGGGGTC	
TGGT1_273530-F	ATGTTGAAGACACCAGTAACGGT	ORF-specific PCR of TGGT1_273530
TGGT1_273530-R	TCAAGCGACAGATAGGTCGTC	

Expression of *Tg*PTS and *Tg*PSS in *E. coli* (M15/pREP4)		
*Tg*PTS-F (*BglII*)	CTCATCAGATCTATGCAACTCCCTTCAAGAAAGG	*pQE60* (expression of *Tg*PTS-6xHis)
*Tg*PTS-His-R (*BglII*)	CTCATCAGATCTCTGACTTCGTTCGATTTTCACG	

*Tg*PSS-F (*BglII*)	CTCATCAGATCTATGTCGGGGACTGCCGCT	*pQE60* (expression of *Tg*PSS-6xHis)
*Tg*PSS-His-R (*BglII*)	CTCATCAGATCTCTCGTCTTTTTGGCCTTCCAACA	
Making of *Δtgss/Tg*PSS-HA$_i$ mutant in *T. gondii* (*Δku80-TaTi* strain)		
*Tg*PSS-F (*EcoRV*)	CTCATCGATATCATGCAACTCCCTTCAAGA	*pTetO7Sag1-UPKO* (Ectopic expression of *Tg*PSS-HA$_i$ at the *TgUPRT* locus)
*Tg*PSS-HA-R (*PacI*)	CTCATCTTAATTAATCAAGCAACTCCCTTCAAGA	
5'UTR-*Tg*PSS-F (*AgeI*)	CTCATCCCACCGGTCACCTGGCTCGGCGACA	*pTKO-DHFR-TS* (Cloning of the *Tg*PSS 5' UTR)
5'UTR-*Tg*PTS-R (*SpeI*)	CTCATCACTAGTCCACTGACCCATACGTTA	
3'UTR-*Tg*PTS-F (*NheI*)	CTCATCGCTAGCACCGTCGAGTCTGGAAAT	*pTKO-DHFR-TS* (Cloning of the *Tg*PSS 3' UTR)
3'UTR-*Tg*PTS-R (*ApaI*)	CTCATCGGGCCCGCATATCTGTACGTAAGC	
Screening for 5' and 3' recombination in the *Δtgpss* mutant of *T. gondii*		
5'Scr-*Tg*PSS-KO-F	CGTGCATGCAGAGGACATC	*pDrive* (TA-cloning of 5' PCR product for sequencing)
5'Scr-*Tg*PSS-KO-R	CACAGTCTCACCTCGCCTTG	
3'Scr-*Tg*PSS-KO-F	CTCGCGGCGTTGAATGTG	*pDrive* (TA-cloning of 3' PCR product for sequencing)
3'Scr-*Tg*PSS-KO-R	GAGAAATCGTGCATGCGACC	
C-terminal 2HA-DD-tagging of *Tg*PSS gene locus of *T. gondii*		
*Tg*PSS-3'IT-2HA-DD-F	TACTTCCAATCCAATTTAATGCGACGGGGAAGTCCTTTGG	*pLIC-2HA-DD-DHFR* (Endogenous C-terminal tagging of *Tg*PSS with 2HA-DD)
*Tg*PSS-3'IT-2HA-DD-R	TCCTCCACTTCCAATTTTAGCCTCGTCTTTTTGGCCTTCC	
Quantification of *T. gondii* infection in mouse brain tissue		
*Tg*B1-F	TCCCCTCTGCTGGCGAAAAGT	Quantification of

*Tg*B1-R	AGCGTTCGTGGTCAACTATCGATTG	parasite load by qRT-PCR
*Mm*ASL-F	TCTTCGTTAGCTGGCAACTCACCT	Quantification of mouse cells by qRT-PCR for normalization of parasite load
*Mm*ASL-R	ATGACCCAGCAGCTAAGCAGATCA	
_Tg_PTS and _Tg_PSS expression in COS-7 cells		
*Tg*PTS-F (*XbaI*)	CTCATCTCTAGAATGCAACTCCCTTCAAGAAAGG	*pcDNA 3.1+* (Expression and localization of *Tg*PTS-v5 in COS-7 cells)
*Tg*PTS-V5-R (*XbaI*)	CTCATCTCTAGACTCACTTCGTTCGATTTTCACG	
*Tg*PSS-F (*HindIII*)	CTCATCAAGCTTATGTCGGGGACTGCCGCT	*pcDNA 3.1+* (Expression and localization of *Tg*PSS-v5 in COS-7 cells)
*Tg*PSS-V5-R (*XbaI*)	CTCATCTCTAGACTCGTCTTTTTGGCCTTC	
Quantitative Real-Time PCR of _Tg_PSS and _Tg_PTS		
*Tg*PTS-qPCR-F	CTCTGCGAATGCTGGTGG	qPCR of *Tg*PTS transcript
*Tg*PTS-qPCR-R	AGAAGCTCCAGTCGGAAGCTT	
*Tg*PSS-qPCR-F	GGTGACTTTGCTGGACCTGA	qPCR of *Tg*PSS transcript
*Tg*PSS-qPCR-R	AGTGCCTCTGTGCTGACGAC	
*Tg*GT1-qPCR-F	GGCTATTTTGGCACCTTTCA	qPCR of *Tg*PSS transcript (housekeeping gene)
*Tg*GT1-qPCR-R	AACGGGAAGACAAACCACAG	

2.1.4. Vectors

Plasmid	**Source**
pcDNA3.1+	Isabelle Coppens, John Hopkins University, Baltimore, USA
pESC-Ura	Stratagene, USA
pQE60	Qiagen, Germany

Plasmid	Source
pNTP3	Isabelle Coppens, John Hopkins University, Baltimore, USA
pNTP3TetO7Sag1	Modified *pNTP3*
pTetO7Sag1-NTP3-UPKO (*pTetUPKO*)	modified *pNTP3*
pTKO	John Boothroyd, Stanford University School of Medicine, USA
pLIC-DHFR-2HA-DD	Boris Striepen, University of Georgia, USA
pTUB8-Der1 -GFP	Boris Striepen, University of Georgia, USA
pS9-GFP	Frank Seeber, Robert Koch Institute, Germany
pGRA2-NTP3-UPKO (pGRA2-UPKO)	Modified *pNTP3*
pGRA2-UPKO-GCamp6s	Modified *pGRA2-UPKO*
pGRA2-UPKO-Lact-C2-GFP	Modified *pGRA2-UPKO*

2.1.5. Antibodies and working dilutions

Antibody and dilution factor	Source
Alexa 594, Alexa 488 (anti-mouse, antirabbit) (1:3000)	Life Technologies, Germany
α-HA (rabbit, mouse) (1:1500)	Life Technologies, Germany
Anti-6xHis-tag mAb IgG1 (mouse)	Dianova, Germany
α-*Tg*Actin (mouse) (1:1000)	Dominique Soldati, University of Geneva, Switzerland

Antibody and dilution factor	Source
α-*Tg*Sag1 (mouse) (1:1000)	(Kim and Boothroyd, 1995)
α-*Tg*Gap45 (rabbit) (1:3000)	(Plattner et al., 2008)
α-*Tg*HSP90 (rabbit) (1:1000)	(Echeverria et al., 2005)
α-*Tg*ROP2 (mouse) (1:1000)	(Sadak et al., 1988)
α-*Tg*MIC2 (mouse) (1:1000)	Dominique Soldati, University of Geneva, Switzerland
α-KDEL (mouse) (1:1000)	(Kaufusi et al., 2014)
α-v5 (mouse) (1:1000)	Abcam

2.1.6. Enzymes

Enzyme	Manufacturer
Antartic phosphatase	NEB, Germany
Dream Taq polymerase	Thermo Scientific, Germany
Pfu Ultra II Fusion HS DNA polymerase	Stratagene, Germany
Proteinase K	Sigma, Germany
Restriction endonucleases, Klenow enzyme	NEB, Germany
T4 ligase	Invitrogen, Germany

2.1.7. Commercial kits

Product	Manufacturer
Avansta western blotting analysis system	Biozym, Germany
DNA purification (plasmid preps)	Analytik Jena, Germany
InnuPREP DOUBLE pure gel DNA extraction kit	Analytik Jena, Germany
pDrive cloning kit	Qiagen, Germany
Platinum SYBR Green qPCR Superscript-UDG	Invitrogen, Germany
Pure Link RNA Mini Kit	Ambion, Germany

2.1.8. Plasticware and disposables

Product	Manufacturer
96, 24, 6-well plates	Costar, USA
Cryo tubes for frozen stocks	Nalgene, Germany
Disposable pipettes (10 ml, 25 ml, 50 ml)	Greiner Bio-One, Austria
Eppendorf tubes (1.5 ml, 2 ml)	Greiner Bio-One, Austria
Electroporation cuvettes (4 mm gap)	Eppendorf, Germany
Falcon tubes (15 ml, 50 ml)	Greiner Bio-One, Austria
Filters (5 µm)	Millipore, Germany
Filter sterilizer (0.22 µm)	Schleicher Schuell, Germany

Product	Manufacturer
Glass beads (0.45 – 0.6 mm)	Sartorius, Germany
Glass Cover slips	Roth, Germany
High performance chemiluminescence film	GE Healthcare, Germany
Microscopy slides	Menzel, Germany
Needles	BD, Germany
Nitrocellulose transfer membrane	Applichem, Germany
Improved Neubauer counting chamber	Neubauer, Germany
Parafilm	Pechiney, USA
PCR tubes	Rapidozym, Germany
Pasteur pipettes	Hartenstein, Germany
Pipette tips	Greiner Bio-One, Austria
Polypropylene tubes (12 ml)	Greiner Bio-One, Austria
RNAase-free barrier tips	Sorenson BioScience, USA
Syringes	BD, Germany
Tissue culture flasks, Petridishes, Multi-well plates	Greiner Bio-One, Austria
Whatman (3 MM)	A. Hartenstein, Germany
X-ray film (FUJI Medical)	A. Hartenstein, Germany

2.1.9. Instruments

Instrument	Manufacturer
AMAXA Nucleofactor	Lonza, Germany
BioPhotometer	Eppendorf, Germany
BTX square wave electroporator (ECM 830)	BTX, USA
ELISA microplate reader	Biotek, Germany
Gel documentation & EASY Enhanced Analysis	Herolab, Germany
Gel electrophoresis chamber and power supply	Gel electrophoresis chamber and power supply Amersham Biosciences, USA
Fluorescence microscope (Apotome Imager.Z2)	Zeiss, Germany
NanoDrop 2000 UV-Vis Spectrophotometer	Thermo Scientific, Germany
PCR Thermocycler (FlexCycler)	JenaAnalytic, Germany
Safety work benches	Heracell, Germany
Scintillation counter (1450 MicroBeta TriLux)	PerkinElmer, USA
TLC developing tank	Roth, Germany
Western Blotting chamber	Peqlab, Germany

2.1.10. Reagent preparations

Solution	Composition
D10 medium	DMEM (high glucose) supplemented with 10% FCS, 2 mM L-Glutamine, 1x NEAA, 1 mM Sodium pyruvate, 100 U/ml Penicillin and 100 μg/ml Streptomycin
Lysogeny Broth (LB) medium	10 g tryptone, 5 g yeast extract and 10 g NaCl in 1 liter deionized H_2O (15 g of agar for plates)
Super Optimal Broth (SOB) medium	20 g tryptone, 5 g Yeast extract, 0.5 g NaCl, 0.186 g KCl and 10mM $MgCl_2$ in 1 liter deionized H_2O
Super Optimal broth with Catabolite repression (SOC) medium	20 g tryptone, 5 g Yeast extract, 0.5 g NaCl, 0.186 g KCl, 10 mM $MgCl_2$ and 20 mM glucose in 1 liter deionized H_2O
10x amino acid mix	Adenine hemisulfate (400 mg), L-Arg (200 mg), L-Asp (1000 mg), L-Gln (1000 mg), L-His (200 mg), L-Leu (600 mg), L-Lys (300 mg), L-Met (200 mg), L-Phe (500 mg), L-Ser (3750 mg), L-Thr (2000 mg), L-Try (400 mg), L-Tyr (300 mg), L-Val (1500 mg) and Uracil (200 mg) in 500 ml deionized H_2O. Uracil was omitted for selective media.
Synthetic drop-out (SD) medium	1.7 g YNB (free of ammonium sulphate and amino acids) and 5 g ammonium sulphate in 500 ml deionized H_2O. The 10x amino acid mix and 40% sugar (final 2 %) stocks were added to obtain synthetic drop-out media

2.2. Methods – Cell culture and transfection

2.2.1. Host cell culture

Human foreskin fibroblasts were cultured in Dulbecco's modified Eagle Medium (DMEM) supplemented with 10% fetal calf serum (FCS), 1mM sodium pyruvate, 2 mM glutamine, 100 µM MEM-non-essential amino acids (glycine, alanine, asparagine, aspartic acid, glutamic acid, proline and serine), 100 units/ml penicillin and 100 µg/ml streptomycin in a humidified incubator (37°C, 5% CO_2, pH 7.4). The cell monolayers were collected after trypsinization and seeded into flasks, plates and dishes as needed.

2.2.2. Parasite culture and selection

Tachyzoites of all *T. gondii* strains were routinely cultured on confluent HFF monolayers at a multiplicity of infection (M.O.I.) of 3 every 2-3 days unless stated otherwise in the same culture conditions as uninfected cells. Selection of transgenic parasites was done in 25 µg/ml mycophenolic acid (MPA) plus 50 µg/ml xanthine (XA), or 1 µM pyrimethamine or 5 µM fluoruracil deoxyribose (FudR) or 20 µM chloramphenicol. In the case of the selections with MPA+XA, pyrimethamine or chloramphenicol, the drug was added 8-24 hrs after transfection with the plasmid encoding the corresponding resistance cassettes. For selection with FudR, parasites were passaged for 2-3 cycles (4-6 days) after transfection under normal conditions before adding D10 medium with the drug. Infected monolayers were then left undisturbed until host cell lysis occurred, usually after 1-2 weeks of selection. Stable resistant parasites were cloned by limiting dilution in all cases.

2.2.3. *T. gondii* transfection

Freshly egressed or syringe-released parasites (10-20 x 10^6 tachyzoites) were pelleted (400xg, 10 min, RT) and resuspended in 700 µl cytomix. Parasite suspension was complemented with 1-50 µg plasmid DNA, 30 µl ATP (sterile 100 mM stock) and 12 µl GSH (sterile 250 mM stock). Electroporation was done by two 1.7 kV pulses at an interval of 100 msec using a BTX square wave electroporator or an AMAXA nuclefactor (program T16). For transfections done using AMAXA nucleofactor, reaction mixture was scaled down to 100 µl.

2.2.4. Stable transfection of COS-7 cells

The cDNAs of *Tg*PTS and *Tg*PSS were amplified from tachyzoite mRNA and cloned at the at *HindIII* and *XbaI* sites in the mammalian expression vector *pcDNA3.1+*. The cloning resulted in expression of C-terminally V5-tagged proteins under the *pCMV* promoter.
For transfection of COS-7 cells the *BglII*-linearized plasmid (4 µg) was diluted in 250 µl of Opti-MEM I (Reduced Serum) Medium. Another batch of 250 µl medium was mixed with 10 µl Lipofectamine 2000 and incubated for 5 min at room temperature. Both solutions (500 µl) were mixed and incubated for 20 min at room temperature. Meanwhile, a 6-well plate containing cultures of COS-7 cells was washed 3 times with PBS and prepared with antibiotic-free medium. The DNA-lipofectamine solution was added to the COS-7 cells and incubated at 37°C for 24 hrs. Cells were harvested by trypsine/EDTA treatment and diluted by at least 10-fold into T150 flasks. Selection of stable transgenic cells was started 48 hrs post-transfection using 800 µg/µl geneticin. Medium with fresh antibiotic was changed twice a week until cells were confluent and stable expression and subcellular localization of V5-tagged proteins was tested by immunofluorescence assay using anti-V5 and anti-KDEL (ER-marker; (Kaufusi et al., 2014)) antibodies.

2.3. Methods – Molecular Cloning

2.3.1. PCR reactions

Template DNA (10-500 ng) was used for PCR. For standard detection PCR, the Dream-Taq polymerase (Thermo Scientific) was utilized. For amplification of open reading frames to be used for expression cloning, the Pfu-Ultra FusionII high fidelity polymerase (Stratagene) was employed. Reaction mixtures and conditions were set according to primer sequences, type of polymerase and the lengths of amplification targets. PCR products were tested by gel electrophoresis in 1% agarose gels with 0.5% ethidium bromide or RotiSafe (Roth, Germany) ran in 1xTAE buffer at 100V. Visualization of DNA product was done under UV light.

2.3.2. DNA ligation

PCR products were purified either by gel extraction after evaluation of their expected size, or directly by column purification kit according to the manufacturer's instructions (Analytic

Jena, Germany). Vector DNA was extracted from overnight *E. coli* cultures according to the kit's instructions, and concentration determined by absorbance readings at 260 nm with a NanoDrop instrument. Both, insert and vector were digested with selected restriction enzymes. For non-directional cloning (using the same restricition site at both ends), the digested plasmid was then dephosphorylated using Antartic Phosphatase (NEB) for 1h at 37°C, and heat inactivated (65°C, 30 min). Digested insert and vector DNAs were mixed at a 1:3 or 1:5 molar ratios, and then ligated with 1 unit of T4 ligase (4°C overnight, or 2 hours at room temperature).

2.3.3. Transformation of *Escherichia coli*

10 µl of the ligation reaction were mixed with 100 µl of freshly thawed competent cells. For regular cloning the Xl1-Blue strain (Stratagene) was used, while the M15/pREP4 strain (Clontech) was employed for expression of recombinant proteins. The samples were incubated on ice for 30 min and then heat-shocked (42°C, 45 sec) followed by 2 min cooling on ice. 700 µl of pre-warmed (37°C) SOC medium were added to each transformation reaction and then shaked at 37°C for 1 hour. Transformed cells were then plated on Ampicillin (100 µg/ml) and/or Kanamycin (50µg/ml) LB-agar plates according to the plasmid or *E. coli* strain. The plates were incubated at 37° overnight, and colonies screened by PCR with insert primers. Plasmid preparations from positive colonies were authenticated by sequencing. *E. coli* frozen stocks were prepared in 25% glycerol and stored at -80°C until further use.

2.3.4. Transformation of *Saccharomyces cerevisiae*

50 ml of YP media containing 2% glucose were inoculated with an overnight-grown pre-culture of *S. cerevisiae* to an OD_{600} of 0.1 and grown at 30°C with shaking (200 rpm) until an OD_{600} of 0.4 was reached. Yeast cells were then pelleted (1000g, 5 min, RT), washed with 25 ml of sterile TE-buffer and then with 10 ml of LiAc/TE buffer. The final pellet was resuspended in N x 100 µl of LiaAc/TE buffer (N equals the number of transformations) and incubated at room teperature for 30 min. 100-200 ng of each plasmid were mixed with 100 µg of salmon sperm DNA and added to 100 µl of competent yeast suspension and mixed by finger tapping.

0.6ml of a PEG4000/LiAc/TE (8:1:1) solution were added to the transformation mix followed

by vortexing for 10 seconds and horizontal incubation for 30 min (200 rpm, 30°C). DMSO (70 µl) was then added to each reaction and mixed by inverting the tube. Samples were heat-shocked for 15 min at 42°C in water bath and immediately chilled on ice for 2 min. Cells were then pelleted at 14000 g for 15 sec and washed with 1x TE buffer prior to suspension in 100 µl of TE buffer. Finally, cells were plated on selective SD plates (-uracil) with 2 % glucose and incubated at 30°C for three to four days. One colony was picked from each plate and streaked onto a master plate for subsequent experiments. Plasmid transformation was verified by plasmid-specific PCR. Frozen stocks were made in 25% glycerol by freezing in liquid nitrogen and stored at -80°C.

2.3.5. Expression of recombinant proteins in *E. coli*

The full-lengths cDNAs of Arabidopsis thaliana (*At*PSS) and *T. gondii* phosphatidylserine synthases (*Tg*PSS) and *T. gondii* phosphatidylthreonine synthase (*Tg*PTS) with a C-terminal 6x his tag were cloned into the pQE60 plasmid, and expressed in the E. coli M15/pREP4 strain. The cultures were grown until OD600 of 0.4-0.6 was reached, and protein expression was induced with 1 mM IPTG overnight at 25 °C. A further 2 h incubation at 37°C was performed to stimulate the activity of *T. gondii* enzymes. Cells were then OD600-normalized and centrifuged (5000xg, 15 min, 4°C). Pellets were then stored at -20°C or processed directly for lipid extraction.

2.3.6. Nucleic acid preparation

Genomic DNA was prepared from *T. gondii* tachyzoites (>1x10^6 cells) according to (Rotureau et al., 2005). Briefly, cells were pelleted and incubated in 200 µl of lysis buffer supplied with 1µl Proteinase K (50 mg/ml) at 55°C for 30 min. For gDNA precipitation, 300 µl isopropanol were added to each sample and then centrifuged at 15.000 rpm for 30-45 min (4°C). gDNA pellets were air-dried and resuspended in 20-50 µl DNase- RNase- free water. DNA concentration was determined by NanoDrop Instrument and samples stored at -20°C.

To prepare total RNA, RNase-free plasticware and DEPC-treated water were used throughout the procedure. Briefly, 5-20x10^6 freshly-egressed parasites were lysed in 1ml TRIzol, by repeated pipetting and left at room temperature for 5 min. At this point samples were either stored at -80°C or processed for RNA isolation using a PureLinkTm RNA MiniKit. Briefly,

200 µl chloroform were added to each sample, mixed by inversion and upper aqueous phase containing the RNA was transferred to a spin cartridge. Samples were then centrifuged (12.000 x g for 15 sec at room temperature) and subjected to an on-column DNase I treatment for 15 min prior to two washings steps. Purified RNA was then eluted with 30 µl RNase free water and stored at -80°C. The RNA preparation was used for isolation of cDNA for quantitative real-time PCR (qRT-PCR) or expression cloning. The cDNA was synthesized with the SuperScript III, First-strand synthesis kit (Life Technologies) using oligo-dT and random primers and stored at -20°C.

2.4. Methods –Assays

2.4.1. Invasion and Egress assays

Invasion and egress assays were performed as previously described (Heaslip et al., 2011). Briefly, freshly syringe-released parasites (M.O.I. of 10 for invasion assays and M.O.I. of 1 for egress assays) were left to infect HFF monolayers on glass coverslips for 1 hour for invasion assays or 40-72 hours for egress assays. Afterwards, coverslips were fixed in 4% paraformaldehyde/0.05% glutaraldehyde for 2 min, followed by neutralization with PBS/Glycine 0.1M for 5 min. Cells were then blocked in PBS/BSA 3% for 30 min. Egressed vacuoles or non-invaded (attached) parasites were then stained with mouse anti-*Tg*Sag1 (1:1500) for 1 h. Samples were then washed three times with PBS (5 min each), permeabilized with 0.2% Triton X-100/PBS (20 min), and stained with anti-*Tg*Gap45 (1:3000, 1 h). Samples were next washed three times with 0.2% Triton X-100/PBS (5 min each) and incubated with Alexa488-/Alexa594-conjugated antibodies (1:3000, 45 min). The fraction of invaded parasites was determined by counting the parasites labeled with anti-*Tg*Gap45/Alexa594 (red) but not with anti-*Tg*Sag1/Alexa488 (green) antibodies, while the fraction of egressed vacuoles was determined directly from the number of vacuoles with anti-*Tg*Sag1-stained parasites.

2.4.2. Motility assays

Motility assays were performed with 4 x 10^5 freshly syringe-released parasites in HBSS buffer and left to glide on BSA (0.01%)-coated glass coverslips for 15 min at 37°C. Parasites

were then fixed in paraformaldehyde 4%/glutaraldehyde 0.05% for 10 min. Sag1-trails were stained with mouse anti-*Tg*Sag1 (1:1500)/Alexa488 antibodies. The fraction of parasites with a trail and the trail length were quantified with the ImageJ software (NIH, USA).

2.4.3. Evacuole assays

Evacuole assays were performed according to Mital et al. (2005). Fresh syringe-released parasites were harvested 40 hrs post-infection and centrifuged (100xg, 4 min 4°C). Parasite pellet was resuspended (10^7 tachyzoites/ml) in Endo buffer (44.7 mM K2SO4, 10mM Mg_2SO_4, 106 mM sucrose, 5 mM glucose, 20 mM Tris, 0.35% w/v BSA, pH 8.2; (Endo and Yagita; Kafsack et al., 2004) containing 1 μM cytochalasin D (CytD).

After 10 min of incubation at room temperature, 3 x 106 pre-treated parasites were added to confluent monolayers grown on glass coverslips and incubated for 20 min at 37°C. the buffer was then replaced with pre-warmed HHFCS (Hanks' balnced salt solution containing 10mM HEPES, pH 7.0 supplemented with 1% (v/v) fetal calf serum) containing 1 μM CytD, and the samples incubated at 37°C for another 15 min. Monolayers were then gently washed three times with PBS, fixed in 100% methanol on ice for 10 min, and labeld with mouse anti-ROP1 (mAb Tg49, a generous gift from Dr. J. Schwartzman, Darmouth college) or mouse anti-ROP2,3,4 (Mab T3 4A7; a generous gift from D. Jean-Francois Dubremetz, Université Montpellier) followed by Alexa 488-conjugated goat anti-mouse IgG. For each set of parasites, the number of evacuoles associated with at least 100 parasites was counted. The mean evacuole length was also determined, using the ImageJ software (NIH, U.S.A.).

2.4.4. Plaque and replication assays

Plaque assays encompass all events of the parasite's lytic cycle including host cell invasion, intracellular replication, and egress from nutrient-depleted infected host cells. HFF cell monolayers grown on 6-well plates were infected with 200-500 tachyzoites and cultured for 7 days without perturbation. Infected monolayers were then fixed with cold methanol (-80°C, 5 min) and stained with crystal violet for 10 min followed by 2x washing with PBS. The images were documented at 4x magnification using an inverted Leica microscope. The mean area of the plaque images from three independent biological replicates (at least 50 plaques each) was calculated for evaluating the parasite growth.

For intracellular replication assays, HFFs grown on glass coverslips were infected with parasites (MOI=1) and subjected to IFA using anti-*Tg*Gap45 (1:3000) antibody every 12 h. The parasite replication was deduced from the number of parasites in their vacuoles. At least three independent experiments each with 50-100 vacuoles at each defined time point were performed and the mean number of parasites per vacuole was calculated.

2.4.5. Lipid Extraction

Heavily infected monolayers (40-48h p.i.) were scrapped and parasites syringe-released by passing twice through a 23G and once through a 27G needle. Host cell debris was removed by passing the parasite suspension through a 5µm filter (Merck Millipore, Germany). An uninfected host-cell control was also included. Cell pellets were resuspended in 0.4 ml of PBS and lipids were extracted by a Bligh and Dyer method (Bligh and Dyer, 1959). Briefly, 0.5 ml chloroform and 1 ml methanol were added. The sample was vortexed and after 20 min it was centrifuged at 2000g for 5 min to precipitate protein. Supernatant was transferred to a new glass tube and 1 ml water and 1 ml chloroform were added. After votexing and centrifuging (2000 g, 5 min) the lower chloroform phase was transferred to a conical glass tube. 1 ml of chloroform was added to the upper phase, the mixture was shaken and centrifuged (2000 g, 5 min) and the lower phase was removed again and combined with the previous one. The solvent was evaporated under nitrogen at 37°C.

2.4.6. Thin-Layer Chromatography

Lipids were resolved by two-dimensional TLC in chloroform/methanol/ammonium hydroxide (65/35/5, v/v) and chloroform/acetic acid/methanol/water (75/25/5/2.2, v/v) (Gupta et al., 2005); or by one-dimensional TLC in chloroform/ethanol/water/triethylamine (30/35/7/35, v/v) (Vaden et al., 2005) using silica 60 plates (Merck, Germany). They were visualized by staining with iodine vapors and/or ninhydrin spray, and were identified based on their co-migration with authentic standards (Avanti Lipids).

2.4.7. Lipid phosphorus quantification

The major iodine-stained phospholipid bands were scraped off the TLC plate, and quantified by phosphorus assay as already described (Rouser et al., 1970). Briefly, Scrapped lipid bands

are transferred into clean glass tubes and 0.180 ml perchloric acid were added and the tubes placed in a heated block (160-180°C) for about 30 min or until the yellow color disappeared.

When cool, 1.2 ml water were added to the tubes, followed by 0.2 ml of ammonium molybdate solution (2.5% w/v) and then 0.2 ml of ascorbic acid solution (10% w/v). Samples were vortexed after each addition. The tubes were then placed in a water bath (50°C) for 15 min. The absorbances of cool samples (including the standards) are read at 820 nm. Standards (0 to 120 nmol phosphorus/tube) were prepared in a 1.2 ml volume with water. Heating for standards is not necessary before adding reagents.

In the presence of silica gel (scraped bands from TLC plates), the tubes are left to decant and the colored solution is removed carefully before measuring its absorbance. The amount of phospholipids is calculated directly on a molar basis from the amount of phosphorus according to linear regression equation obtained from standards readings.

2.4.8. Lipidomics - Lipid extract fractionation

Total lipid extract was run through a silica 60 column embedded in chloroform. Neutral lipid fraction was eluted by washing 4 times with 1 column-volume of acetone. Afterwards, the phospholipid fraction was eluted by washing 5 times with 1 column-volume of chloroform/methanol/water (1/9/1). Each fraction was collected and evaporated under nitrogen at 37°C and kept at -20°C until analysis.

2.4.9. Lipidomics - HPLC and tandem mass spectrometry (MS/MS) analysis

An automated HPLC-electrospray (ESI) or atmospheric pressure ionization (APCI)-tandem mass spectrometry approach was used. An aliquot of 10-20 µl of the fractionated phospholipid extracts dissolved in chloroform/methanol (1/1) was introduced into a Kinetex 2.6µ HILIC column at a max flow rate of 1ml/min to separate phospholipid classes. Injection of samples was performed by an HTC PAL Autosampler (Plate code:VT98, CTC Analytics). Afterwards, samples were pumped into a 4000 Q-TRAP mass spectrometer (AB Sciex instruments) by a Flexar FX-15 pump (Perkin Elmer) at a defined flow rate of 1000 µl/min and pressure of 650 psi. An external standard mixture was also run to quantify the response factor of the major

phospholipid classes and to determine their retention time. This mixture consisted of: PtdEtn (3 pmol/µl), Sphingomyelin (1.25 pmol/µl), PtdCho 34:1 (4.82 pmol/µl), PtdSer 34:1 (1.25 pmol/µl). Data were analyzed using custom scripts on the acquisition software (Analyst v1.6.1; Sciex).

2.4.10. Metabolic labeling with radioactive precursors

Freshly-egressed parasite preparation was performed as described for lipid extraction on ice. Thereafter, 5 x 10^7 tachyzoites of each strain were incubated in 1ml medium with ^{14}C-Threonine (2µCi, 40µM) or ^{14}C-Serine (2µCi, 100µM). The medium contained 20 mM HEPES, 140 mM KCl, 10 mM NaCl, 2.5 mM $MgCl_2$, 5 mM glucose, 1mM $CaCl_2$, 1 mM sodium pyruvate, MEM vitamin solution, 1X essential and non-essential MEM amino acids (PAA, Germany), pH 7.4. After 2-4 hrs at 37°C, reaction was stopped by addition of each 2.2 ml methanol and chloroform, followed by 1 ml 0.2M KCl. Resulting lower chloroform phase was used to recover phospholipids for TLC analysis and phosphorimaging.

2.4.11. Intracellular labeling with stable isotope precursors

Uninfected host cells were cultured in DMEM wo/ threonine (BioConcept, Switzerland) medium supplemented with 10% dyalized FCS and 0.4 mM (U-13C)-Thr for 2 days prior to infection. At the day of infection, fresh ^{13}C-Thr$_{(1-4)}$ D10 medium was added to host cells, which were then infected with freshly syringed-released parasites (M.O.I.: 3). Two days after infection, parasites grown in ^{13}C-Thr –loaded HFF cells were syringe-released and filtered through 5 µm filters to remove host-cell debris. Parasites were then washed twice in PBS and counted. Parasite pellets were frozen at -80°C until further analysis.

Lipid extraction proceeded as already explained, and phospholipid fractions were then subjected to HPLC and MS/MS analysis. Fractionation profile revealed neutral losses of 101 Da for unlabeled PtdThr (^{12}C-Thr$_{(1-4)}$) and 105 Da for ^{13}Thr$_{(1-4)}$-labeled-PtdThr.

2.4.12. Measurements of cytosolic calcium in intracellular parasites

Genetically-encoded calcium indicator, GCamP6s, is composed of a myosin light chain kinase domain (M13) fused to a circularly permutated GFP (CpEGFP) and a calmodulin (Ca^{2+}-binding) domain (Chen et al., 2013). When Ca^{2+} levels are low, CpEGFP fluorescence is

quenched, however when Ca^{2+} is suddenly increased (as during parasite egress or invasion (Arrizabalaga and Boothroyd, 2004; Lovett and Sibley, 2003)), GFP signal is greatly increased (Fig. 10). GCamP6s was cloned into *pTgGRA2-UPKO* plasmid at the *Nsi*I/*Pac*I sites for targeted expression under the control of the *TgGRA2* promoter at the *UPRT* locus. Transgenic parasite lines (parental, *Δtgpts*) stably expressing GCamP6s were generated by FUDR selection (Donald and Roos, 1995). HFF monolayers cultured in 24-well plates were infected with GCamP6s-expressing parasites (24-50 hrs), and calcium-induced GFP fluorescence was quantified by a microplate reader (BioTek Instruments; excitation, 485 nm; emission, 528 nm; area scan mode; 37ºC). The negative (uninfected cells) and positive (infected cells exposed to 5 μM A23187) controls were also included with each assay. All experiments were executed in colorless DMEM (without red phenol) supplemented with 10% fetal bovine serum.

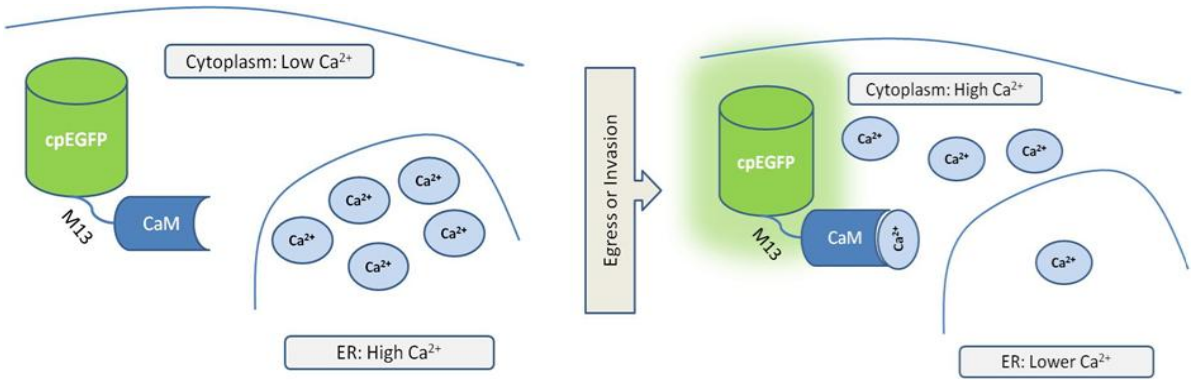

Fig. 10. *Cartoon depicting the GCamp6s calcium measurement in T. gondii.* During resting state (left), the cytoplasmic Ca^{2+} levels are too low to activate the indicator, however during egress or invasion signaling (right), the ER releases Ca^{2+} which in turn binds to the calmodulin (CaM) domain of the indicator and enhances the cpEGP fluorescence.

2.4.13. Quantification of cerebral toxoplasmosis by PCR

Immunized mice received 4 weeks before the infection with the type II ME49 infection *Δtgpts* parasites. The *T. gondii* DNA loads were determined 4 weeks after the ME49 infection in brain homogenates. As described previously (Bereswill et al., 2014), perfused brain tissue samples were snap-frozen and kept at -80°C. 30 mg of brain tissue were used for nucleic acid

purification using the spin column based AllPrep DNA/RNA/Protein Mini Kit (QIAgen, Hilden, Germany) and following the manufacturer's instructions. On-membrane DNase I digestion (peqGOLD, Erlangen, Germany) was performed during RNA purification. RNA and DNA purity and concentration were determined by absorbance at 230, 260 and 280 nm in a NanoDrop spectrophotometer (Fisher Scientific, Germany). Semi-quantitative real time-PCR analyses were performed to determine parasite loads in brains. FastStart Essential DNA Green Master (Roche, Grenzach-Wyhlen, Germany) was used with 90 ng genomic DNA in a reaction volume of 20 µL. Triplicate reactions were developed in a LightCycler® 480 Instrument II (Roche, Grenzach-Wyhlen, Germany). After an initial activation step (95°C for 10 min), 45 amplification cycles were run, comprising of denaturation at 95°C for 15 sec, annealing at 60°C for 15 sec and elongation at 72°C for 15 sec. The following primers were manufactured by Tib MolBiol (Berlin, Germany) and used at a final concentration of 0.3 µM: *Toxoplasma gondii* B1: (Forward) 5'- TCCCCTCTgCTggCgAAAAgT-3' and (Reverse) 5'-AgCgTTCgTggTCAACTATCgATTg-3' . *Mus musculus* argininosuccinate lyase (ASL) gene: (Forward) 5'-TCTTCgTTAgCTggCAACTCACCT-3' and (Reverse) 5'-ATgACCCAgCAgCTAAgCAgATCA-3'. Parasite loads (target: *Toxoplasma gondii*, B1 gene) were measured relative to mouse cell number (reference: *Mus musculus*, argininosuccinate lyase (ASL) gene), that is the target/reference ratio calculated with the LightCycler® 480 Software release 1.5.0 (Roche, Grenzach-Wyhlen, Germany).

2.4.14. Cerebral histopathology

As described previously (Möhle et al., 2014), brains and spinal cords were removed and immersed in 4% paraformaldehyde (PFA) for several days. Spinal cords cylinders were cut at different heights and manually arranged in a paraffin tissue microarray (TMA) of 5 x 7 cylinders per block for parallel processing as previously described (Vogler et al., 2006). Paraffin-embedded, 4-µm thick sections were deparaffinized and conventionally stained with hematoxylin-eosin (H&E) stain. Immunohistochemical analysis was performed according to previous work (Krohn et al., 2011) using a BOND-MAX (Leica Microsystems GmbH/Menarini, Germany) with antibodies against ionized calcium-binding adapter molecule 1 (IBA1, 1:2,000, Wako 019-19741, Germany) to label microglia, glial-fibrillary acid protein (GFAP, 1:1,000, DAKO Z033401, Germany) to label astrocytes, myelin basic protein (MBP, 1:1,600, DAKO A062301, Germany) to label myelin sheets, neurofilament (NF200; 1:160, Sigma-Aldrich N4142-.5ML, Germany) to label axons, NeuN (1:1,000, Millipore MAB377,

Germany) to label neurons, and anti-Toxo (1:200, Dianova DLN-16734, Germany) to label *T. gondii*. Slides were developed using the Bond^{TM} Polymer Refine Detection kit (Menarini/Leica, Germany). For the evaluation whole tissue sections and TMAs were digitized at 230 nm resolution using a MiraxMidi Slide Scanner (ZeissMicroImaging GmbH, Germany).

2.4.15. Quantification of *Toxoplasma* cysts in the brain

T. gondii cysts of the ME49 type II strain were harvested from the brains of female NMRI mice strain infected intraperitoneally with *T. gondii* cysts 5 months earlier, as already described (Parlog et al., 2014). Brains obtained from infected mice were mechanically homogenized in 1 mL sterile phosphate-buffered saline (PBS) and the cysts were counted using a light microscope. Immunized mice received *Δtgpts* parasites (500 tachyzoites) 4 weeks before the infection with the type II ME49 strain. A control group of naïve animals was also included. Three cysts were administered intraperitoneally into each mouse in a total volume of 200µL. All cysts employed proceded brom the same bank of the ME49 strain to minimize their variability across different infections. *T. gondii* total cysts numbers were determined 4 weeks after the ME49 infection in brain homogenates as described above.

3. Results

3.1. The Lytic cycle and virulence of *Toxoplasma gondii* are regulated by a novel phosphatidylthreonine synthase

3.1.1. Phosphatidylthreonine is a natural-occurring major phospholipid in *T. gondii*

The phospholipid profile of *Toxoplasma* is dominated by phosphatidylcholine (PtdCho), followed by phosphatidylethanolamine (PtdEtn), phosphatidylinositol (PtdIns), phosphatidylserine (PtdSer) and phosphatidic acid (Gupta et al., 2005). Total lipids of *Toxoplasma* were separated by 2-dimensional thin layer chromatography (2D-TLC) and corroborated most of these results, however an additional lipid band, X1, which migrated very close to PtdSer was observed (Fig 11a).

To characterize the lipid species of the main phospholipid classes, we recurred to an HPLC/MS/MS approach, in which main phospholipids are separated initially by their elution time on HPLC, detected by their ionization energies and identified by their mass/charge ratio (m/z) in MS/MS. This work was done and analyzed as a part of my research stay at the Institute of Biomembranes of Utrecht University (Netherlands) headed by Prof. Bernd Helms, under supervision of Prof. Jos Brouwers. Fig 1a shows a typical chromatogram of *T. gondii* lipids, which reflects the same lipid distribution observed on TLC, including the unidentified peak, X1, almost co-eluting with the PtdSer fraction. Additionally, we also identified a peak corresponding to the previously reported PEtn-Cer (Welti et al., 2007). PEtn-Cer was identified as a major 16:1 species (m/z 659.1). Mass spectrometry analysis of the lipids within the range of 3.5 to 3.8 min of elution time, identified some PEtn-Cer and PtdSer species. However, the major peak in this fraction with an m/z of 850 did not match any known PtdSer or PEtn-Cer species (Fig 11b). Deeper fragmentation analysis of the unidentified peak of m/z 850 indicated a neutral loss of 101 atomic mass units instead of the expected 87 for serine or 196 for ethanolamine in the negative mode. This mass and the similar elution time to PtdSer would match threonine as the polar head group of this particular lipid species, as has been previously identified by a similar HPLC/MS/MS approach in mouse macrophages (Ivanova et al., 2010). The fatty acyl chains of this species were identified as 20:4 and 20:1 (Fig 11c).

Other minor PtdThr species were identified by a neutral loss of m/z 101, and are also characterized by very long polyunsaturated fatty acyl chains (Fib 11b).

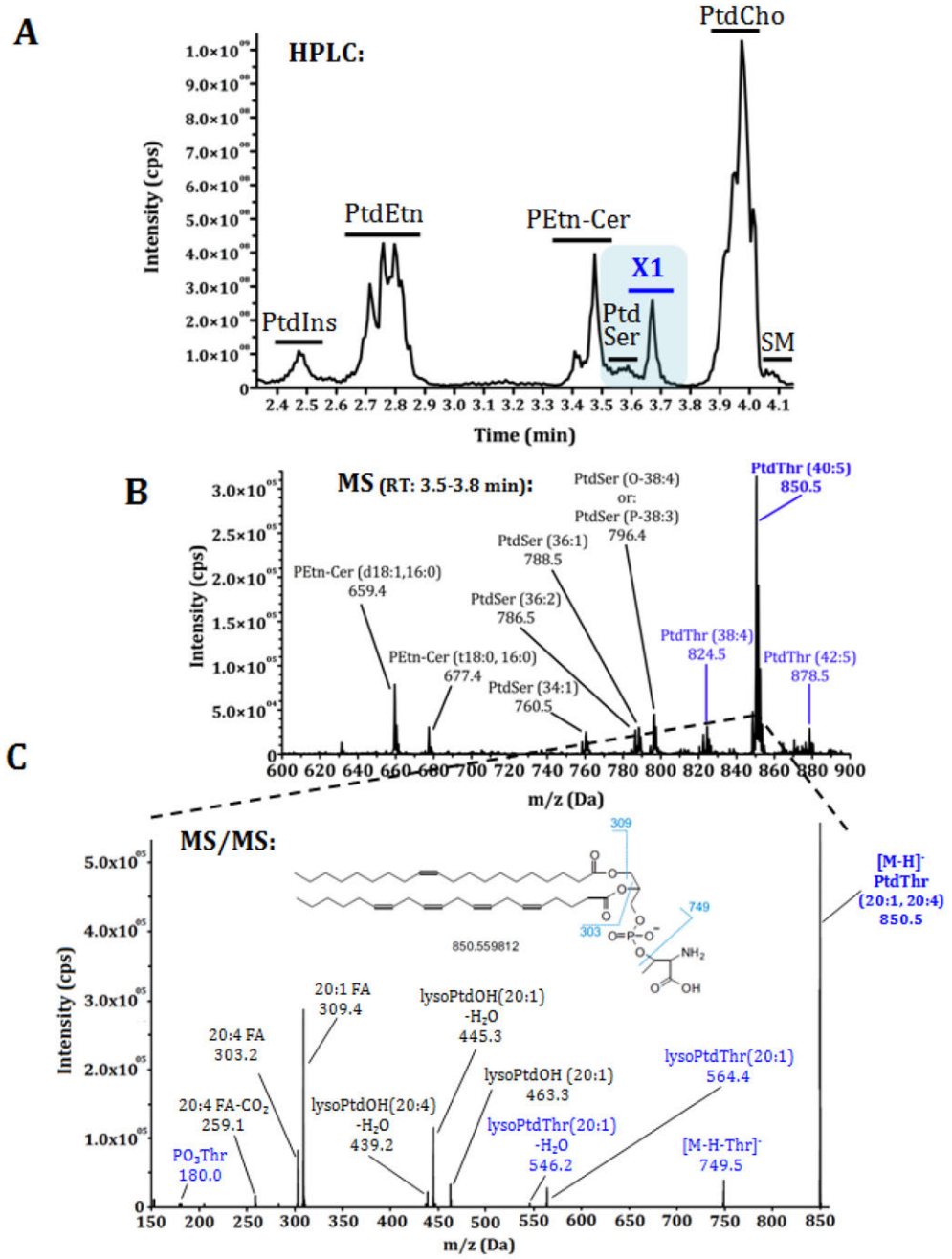

Fig. 11. *Lipidomics of T. gondii tachyzoites identifies a novel parasite lipid, Phosphatidylthreonine.* **(A)** HPLC elution profile showing the retention times and peak intensities of phospholipids isolated from extracellular parasites (10^7). X1, eluting between 3.5-3.8 min, represents a previously unknown lipid. **(B)** MS analysis of X1 fraction revealing PtdThr, PtdSer and PEtn-Cer species. Individual lipids were identified by their fragmentation patterns and *m/z* ratios in the negative ionization mode. **(C)** MS/MS spectrum of X1-derived major peak (*m/z* 850) from *panel B*. Note the neutral loss of 101 Da (850.5-749.5 transition). Acyl chains (*sn*-1, 20:1; *sn*-2, 20:4) were identified by their masses.

3.1.2. Phosphatidylthreonine is a parasite-exclusive phospholipid

Given that phosphatidylthreonine has been previously reported as a minor lipid component of mammalian cells, mainly under serine-deprived conditions and upon some viral infections (Mark-Malchoff et al., 1978; Mitoma et al., 1998), we analyzed the lipid composition of uninfected host human fibroblasts and searched for the presence of PtdThr. Figure 12 shows that MS analysis of the HPLC time window from 3.5 to 3.8 min where PtdThr is expected to elute, only shows peaks for PtdSer species and none for PtdThr or PEtn-Cer, another parasite-specific phospholipid (Welti et al., 2007). These results were also validated by ESI-MS in the negative ionization mode (Appendix 1). These data indicate the *de novo* synthesis of PtdThr in *T. gondii*.

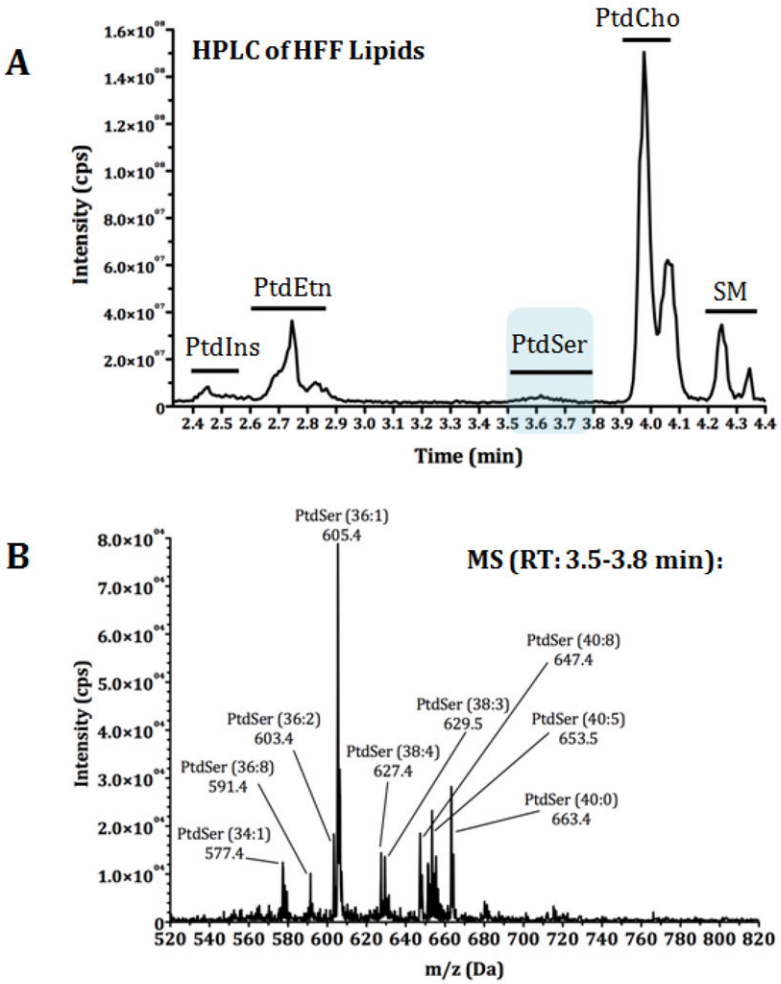

Fig. 12. *Human foreskin fibroblast cells do not contain detectable amounts of phosphatidylthreonine*. **(A)** HPLC elution profile showing the retention times and peak intensities of phospholipids isolated from host fibroblasts. **(B)** APCI-MS analysis of the indicated HPLC fraction revealing predominantly PtdSer species and lack of detectable PtdThr-derived lipid species.

3.1.3. Intracellular *T. gondii* can synthesize phosphatidylthreonine *de novo* from free threonine precursor

Intracellular labeling of tachyzoites grown on HFF cells culutured with stable threonine isotope (^{13}C-Thr$_{(1-4)}$) was evaluated by tandem mass spectrometry of the main PtdThr species (40:5, Fig. 13). As seen in Fig. 13A, the distribution of the resulting peaks after the neutral loss of the threonine moiety of the 854 Da species in an unlabeled sample showed only a major 753 Da peak expected for the loss of "normal" (^{12}C-Thr$_{(1-4)}$ and minor 752, 751 and 750 Da peaks in the predicted decreasing abundancies of natural carbon isotopes (Smith, 1972). On the other hand, a ^{13}C-Thr$_{(1-4)}$ labeled sample showed an additional 749 Da peak, which is expected for the neutral loss of the 105 Da of ^{13}C-Thr$_{(1-4)}$ included in the growth medium as sole threonine source. Unexpectedly however, the magnitude of this peak was only about 5% of the total PtdThr (40:5). Nevertheless, this result undoubtedly confirms the identity and the synthesis of PtdThr from free threonine precursor in *T. gondii*. The low magnitude of the labeling however, also indicates a very poor threonine transport into the parasite, and suggests that it must be able to synthesize most of its threonine pool by itself rather than scavenging from the host cell, for which it is an essential amino acid (McCoy et al., 1974). The intracellular labeling with ^{13}C-Thr$_{(1-4)}$ was performed at the Department of Molecular Parasitology and samples were shipped and analyzed by our collaborators at the Institute of Biomembranes of Utrecht University.

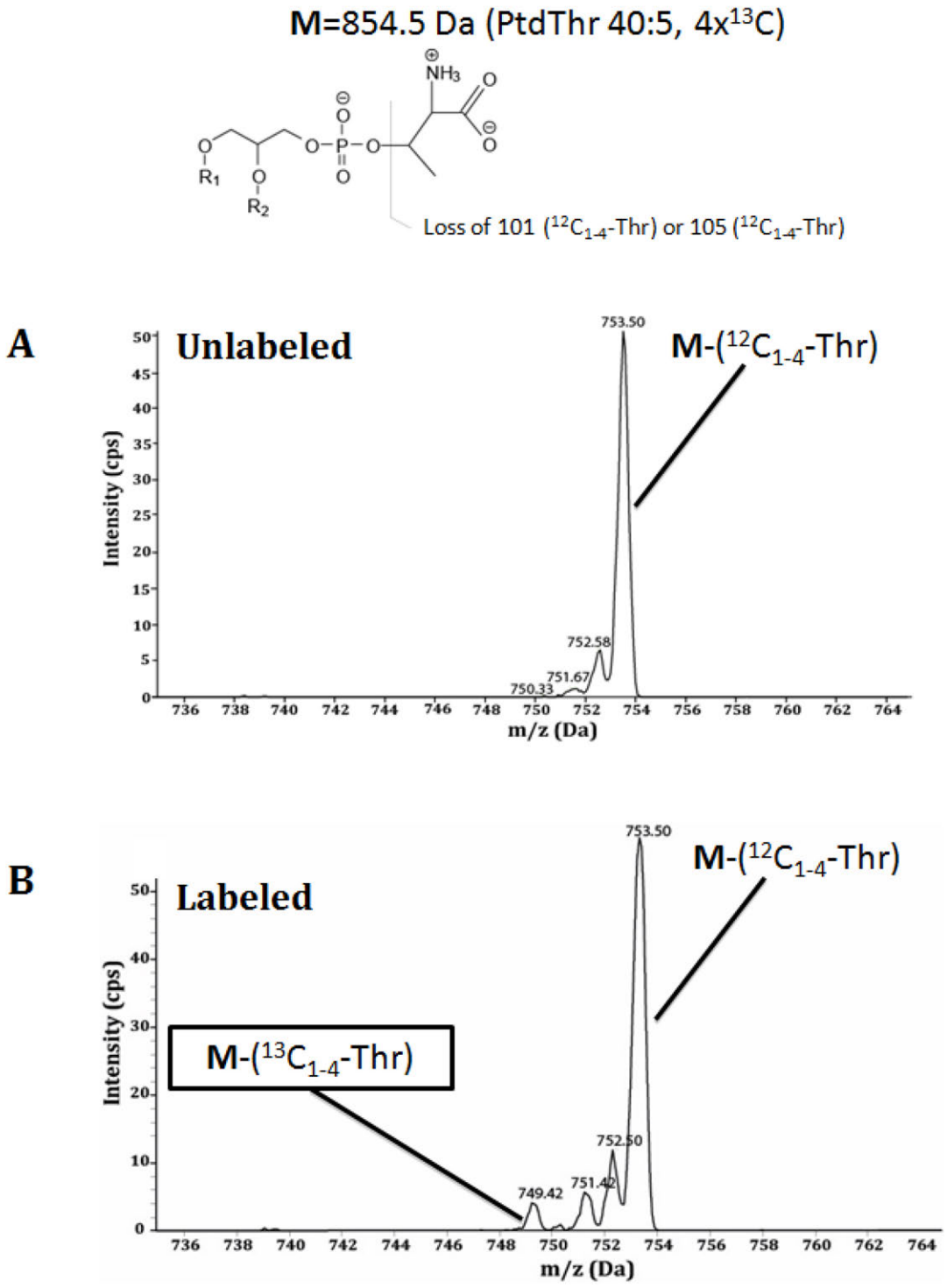

Fig. 13. *Toxoplasma can incorporate free threonine into PtdThr during its intracellular replication*. Wild-type parasites were grown in HFF monolayers supplied with $^{13}C_{1-4}$-threonine for 2 days. Lipids from syringe-released purified parasites were subjected to MS/MS analyses. Unlabeled control samples were also analyzed. The transitions 854.5-753.5 and 854.5-749.5 indicate the neutral losses of $^{12}C_{1-4}$-Thr (nl101) and $^{13}C_{1-4}$-Thr (nl105), respectively, from the PtdThr (40:5, 4x^{13}C) peak.

3.1.4. *Toxoplasma* genome encodes 2 putative enzymes for the base-exchange synthesis of phosphatidylserine and phosphatidylthreonine

To study the synthetic pathways of phosphatidyldserine and its close analog, phosphatidylthreonine, we searched the *Toxoplasma* database (ToxoDB.org) for orthologs of yeast, *E. coli* (CDP-DAG dependent), human and Chinese hamster (base-exchange) phosphatidylserine synthases. No orthologs for the CDP-DAG dependent enzymes from yeast or *E. coli* were found in *Toxoplasma* genome. However, 2 putative orthologs of mammalian base-exchange phosphatidylserine synthases were found in *Toxoplasma gondii* GT1 strain (type I). The accesion numbers of these orthologs in ToxoDB (version 9.0) are TGGT1_261480 and TGGT1_273540. The open reading frames of TGGT1_261480 and TGGT1_273540 were cloned from cDNA prepared from the tachyzoite mRNA, which encoded proteins with 540 and 614 amino acid residues, respectively. Both ORFs contain a PSS domain (PF03034), including the highly conserved catalytical motif ECWWD (Ohsawa et al. 2004). However, TGGT1_273540 contained a glutamate instead of the highly conserved asparagine residue at a position known to be essential for serine binding as a substrate (Ohsawa et al. 2004). Other remarkable substitutions in the substrate-binding pocket included tryptophan and serine residues instead of histidine and cysteine at the equivalent positions in most eukaryotic PSS orthologs, including TGGT1_261480 (Fig. 14). Interestingly, these substitutions correlated with a different phylogenetic grouping of TGGT1_273540 with only selected free-living and parasitic chromalveolates, while TGGT1_261480 grouped as expected with the mainstream PSS clade including orthologs from other apicomplexan and protozoan parasites as well as from plants, fungi and mammalian organisms (Fig 15). Based on these assumptions and on following results, the acronyms *Tg*PTS (PtdThr synthase) and *Tg*PSS (PtdSer synthase) were accrued for TGGT1_273540 and TGGT1_261480, respectively.

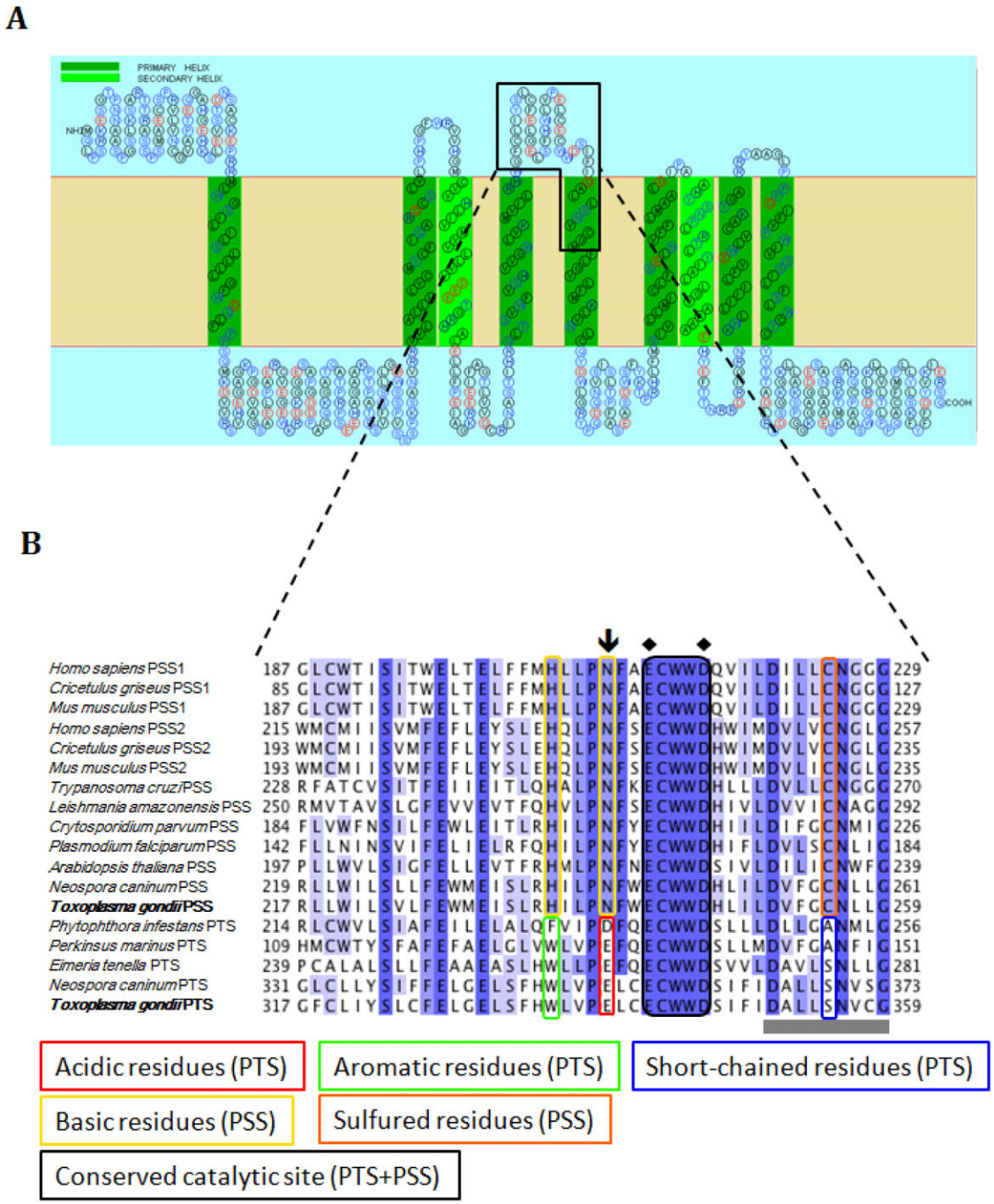

Fig. 14 *PtdThr synthase from T. gondii harbors multiple substitutions in the conserved catalytic domain of an otherwise base-exchange PtdSer synthase*. **(A)** Secondary structure and membrane topology of TGGT1_273540 (*Tg*PTS) predicted by SOSUI (http://bp.nuap.nagoya-u.ac.jp/sosui). **(B)** Amino acid sequence alignment of PtdSer synthases (PSS) with PtdThr synthases (PTS) from *T. gondii* and its orthologs. The diamond and arrow signs indicate the residues known to be critical for PSS activity and for substrate binding, respectively. Note that some strictly-conserved residues in PSS enzymes show distinct substitutions in PTS orthologs (colored boxes). The gray bar under the alignment denotes the predicted transmembrane domain.

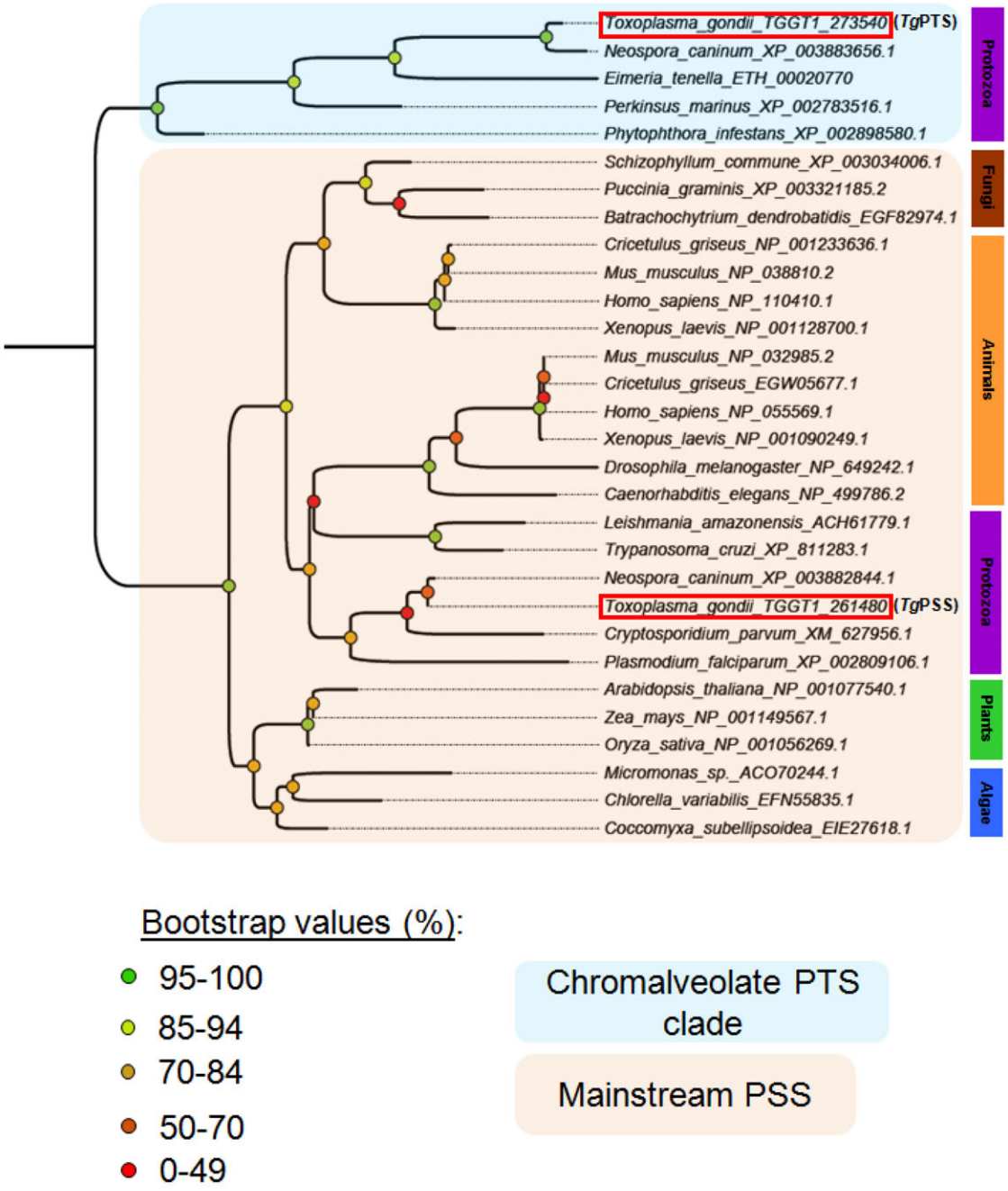

Fig. 15 *Orthologs of PtdThr synthase are present in selected free-living and parasitic protists, but absent in most other organisms*. Phylogenetic analysis of the orthologs of PtdThr synthase (PTS) and PtdSer synthase (PSS) from distinct organisms shows an early divergence of the two enzymes. *Tg*PSS (TGGT1_261480) clusters with the mainstream PSS clade that also includes other parasite orthologs. By contrast, *Tg*PTS (TGGT1_273540) segregates with selected parasitic (*Eimeria*, *Neospora, Phytophtora*) and free-living (*Perkinsus*) chromalveolates. The colored circles signify the bootstrap values generated by the maximum-likelihood estimation program PhyML of the online suite www.phylogeny.fr. Sequences for the phylogenetic analysis were obtained from the databases (NCBI, ToxoDB). The NCBI accession numbers: *Tg*PTS, KJ026547; *Tg*PSS, KJ026548.

3.1.5. Phosphatidylthreonine and phosphatidylserine syntheses occur in the parasite endoplasmic-reticulum

The ORFs of *Tg*PTS and *Tg*PSS were amplified from cDNA of Δ*ku80* type I tachyzoites, sequenced and cloned with a C-terminal hemaglutinin (HA) tag into *T. gondii*. Consistent with their phylogenetic relationship, immunofluorescent imaging of the epitope-tagged *Tg*PTS-HA and *Tg*PSS-HA enzymes showed a predominant distribution in the endoplasmic reticulum, as evidenced by their similar distribution to the ER marker, Der1-GFP (Agrawal et al., 2009) (Fig. 16). These results also suggested ER as being the major site for syntheses of PtdThr and PtdSer in *T. gondii*.

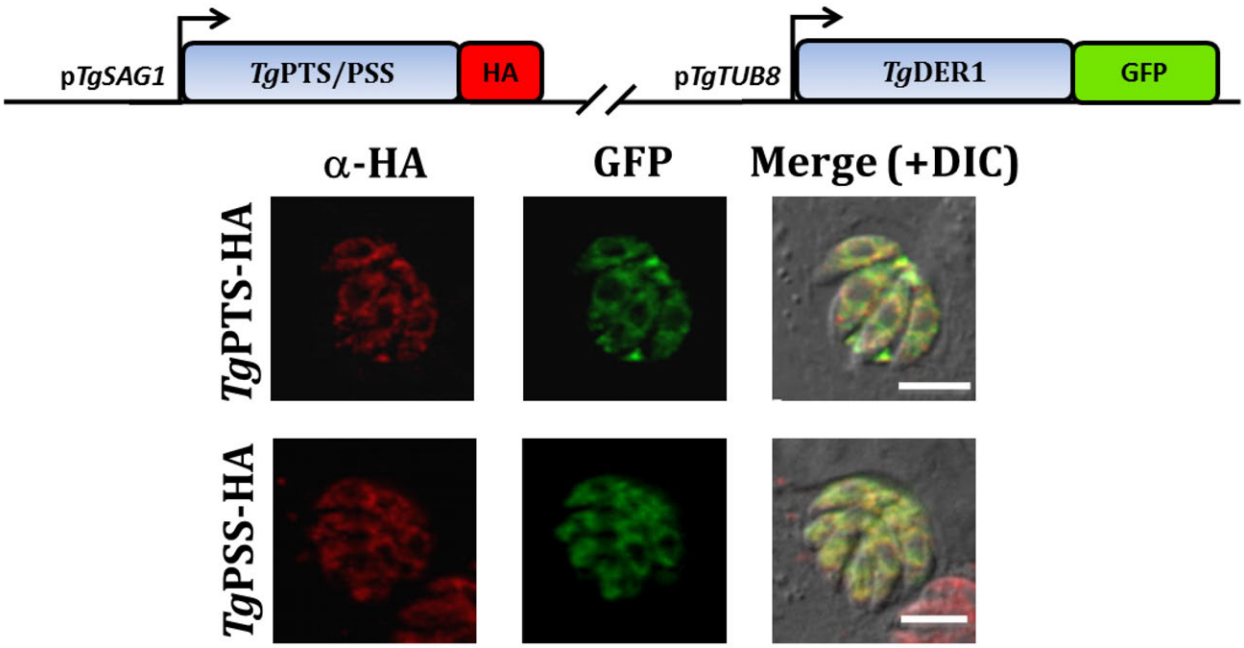

Fig. 16. *PtdThr and PtdSer are synthesized in the endoplasmic reticulum of T. gondii.* Immunostained images of the HA-tagged PtdThr synthase (*Tg*PTS) and PtdSer synthase (*Tg*PSS) expressed at the UPRT locus in stable transgenic parasites under the control of the *TgSAG1* promoter. Co-localization was performed with *Tg*Der1-GFP (ER marker). Yellow fluorescence in the merge channel indicates the expression of *Tg*PTS and *Tg*PSS in the parasite ER (Size bars, 5 µm).

3.1.6. *Tg*PTS and *Tg*PSS are expressed in the ER of transgenic COS-7 cells

A C-terminally V5-tagged *Tg*PTs ORF was cloned into the pcDNA 3.1+ vector under the *pCMV* promoter and transfected into COS-7 cells. Stable transgenic cells were selected by geneticin, and expression was confirmed by immunofluorescence imaging against the V5 epitope. As shown in Figure 17, the endoplasmic reticulum localization of *Tg*PTS as well of *Tg*PSS, which worked as a control, was confirmed by their similar fluorescence pattern to the –KDEL motif, an ER targeting signal in mammalian cells (Raykhel et al., 2007).

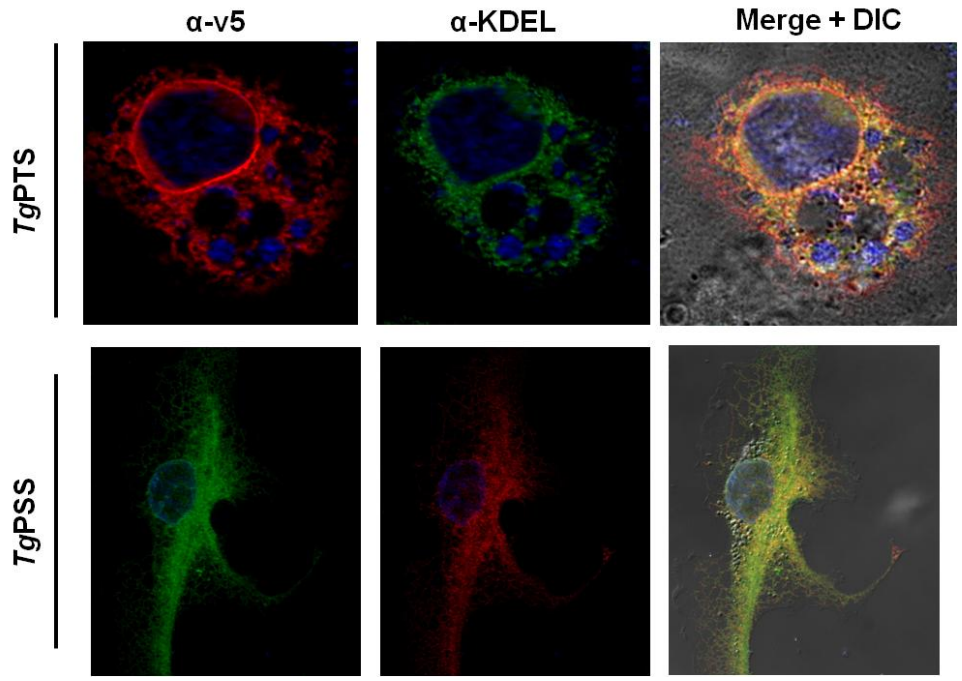

Fig. 17. *TgPTS and TgPSS are expressed in the ER in COS-7 cells.* Immunofluorescence images showing localization of transgenic *Tg*PTS-v5 and *Tg*PSS-v5 similar to an ER-marker (α-KDEL) in COS-7 cells.

3.1.7. The *Δtgpts* mutant lacks autonomous synthesis of PtdThr

To determine the function of *Tg*PTS, we disrupted the gene in *T. gondii* (Fig 18A). The *Δtgpts* mutant was isolated by recombination- and ORF-specific PCR screening, which confirmed a successful disruption of the PTS gene locus (Fig 18B). Consistently, the ORF-specific primers amplified a band of 4.2 kb in the *Δtgpts* strain in lieu of the expected 1.8 kb in the parental parasites (Fig. 18C), which corroborated the targeted insertion of the selection marker and deletion of the predicted catalytic site (342ECWWD346; (Ohsawa et al., 2004)).

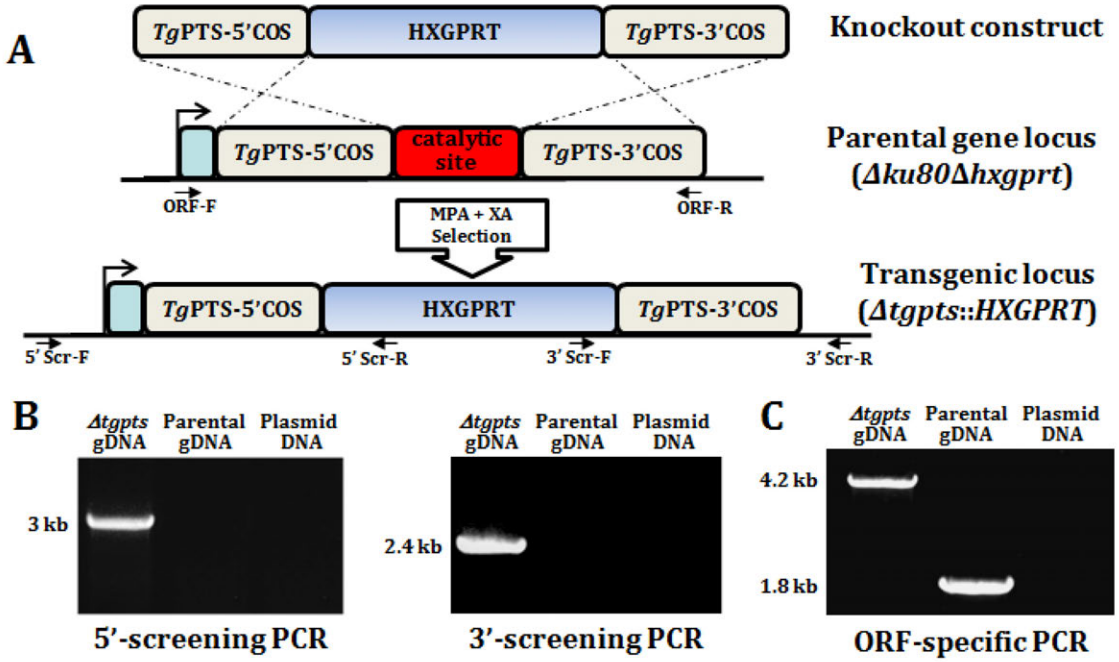

Fig. 18. *Targeted gene disruption of TgPTS in T. gondii.* **(A)** Scheme for the targeted disruption of the *TgPTS* gene by double homologous crossover. The knockout plasmid contained 5' and 3' crossover sequence (COS) of *Tg*PTS flanking the hypoxanthine xanthine guanine phosphoribosyltransferase (HXGPRT) marker, which allows transgenic selection by mycophenolic acid (MPA) and xanthine (XA). The PTS gene-disrupted parasites lacking the conserved catalytic (ECWWD) site were screened by 5' and 3' screening primers (5'Scr-F/R, 3'Scr-F/R; Table S1). The conserved ECWWD domain is known to be critical for base-exchange activity of the mammalian PSS proteins (Ohsawa et al., 2004). **(B)** PCR images of a representative clonal *Δtgpts* strain showing specific amplification of a 3 kb or 2.4 kb DNA band by 5' and 3' genomic screening, respectively. The parental gDNA and knockout plasmid were included as negative controls. **(C)** ORF-specific PCR confirming a successful insertion of the selection marker at the *TgPTS* locus. PCR shows amplification of an expected 4.2 kb band in the *Δtgpts* strain as opposed to the expected 1.8 kb in the parental parasites, and none in the plasmid DNA (negative control). Identity of all PCR amplicons was confirmed by sequencing.

The expression of adjacent transcripts flanking the *Tg*PTS gene was unaffected further confirming the specificity of transgenic manipulation (Appendix 2). Synthesis of PtdThr was abrogated in the *Δtgpts* strain, as shown by TLC and lipid phosphorus assays (Fig. 19D, E). Concurrently, we observed a three-fold gain in PtdSer, which was proportionate to PtdThr level in the parental strain (Fig. 19A). Genetic complementation of the mutant with a functional *Tg*PTS recovered PtdThr, as well as restored a normal PtdSer content (Fig. 19A).

We also determined a significant and reversible increase in PtdCho (20%) of the mutant, which may serve as a co-substrate for the base-exchange reaction catalyzed by *Tg*PTS. No significant changes were observed in PtdEtn or PtdIns amounts in the mutant. The HPLC/MS analyses confirmed the absence of all PtdThr-derived and a parallel increase in PtdSer species in the mutant (Fig. 20A). Interestingly, certain minor PtdSer species (acyl or alkyl ether-linked PtdSer, 796.4 *m/z*) were also absent in the mutant, which implied a secondary affinity of *Tg*PTS towards serine (Fig. 20A). HPLC and TLC analysis of amino acid derived by lipid hydrolysis also validated the loss of lipid-conjugated threonine (Fig. 20B-C). Regarding the fatty acyl distribution of other major phospholipids, besides PtdSer and PtdThr, a significant increase of PtdCho (40:5) and a reduction in short-chained PtdIns species were observed between the parental and *Δtgpts* strains (Appendix 3).

Consistent with above results, expression of a mutagenized isoform lacking the strictly conserved ECWWD residues (*Tg*PTS$_{(\Delta ECWWD)}$) was unable to produce PtdThr in the *Δtgpts* strain (Fig 20D), which confirmed the catalytic importance of these residues and the specificity of our knockout line. Taken together, these results show an autonomous synthesis of PtdThr in *T. gondii*, and its abolition in the mutant lacking PTS expression.

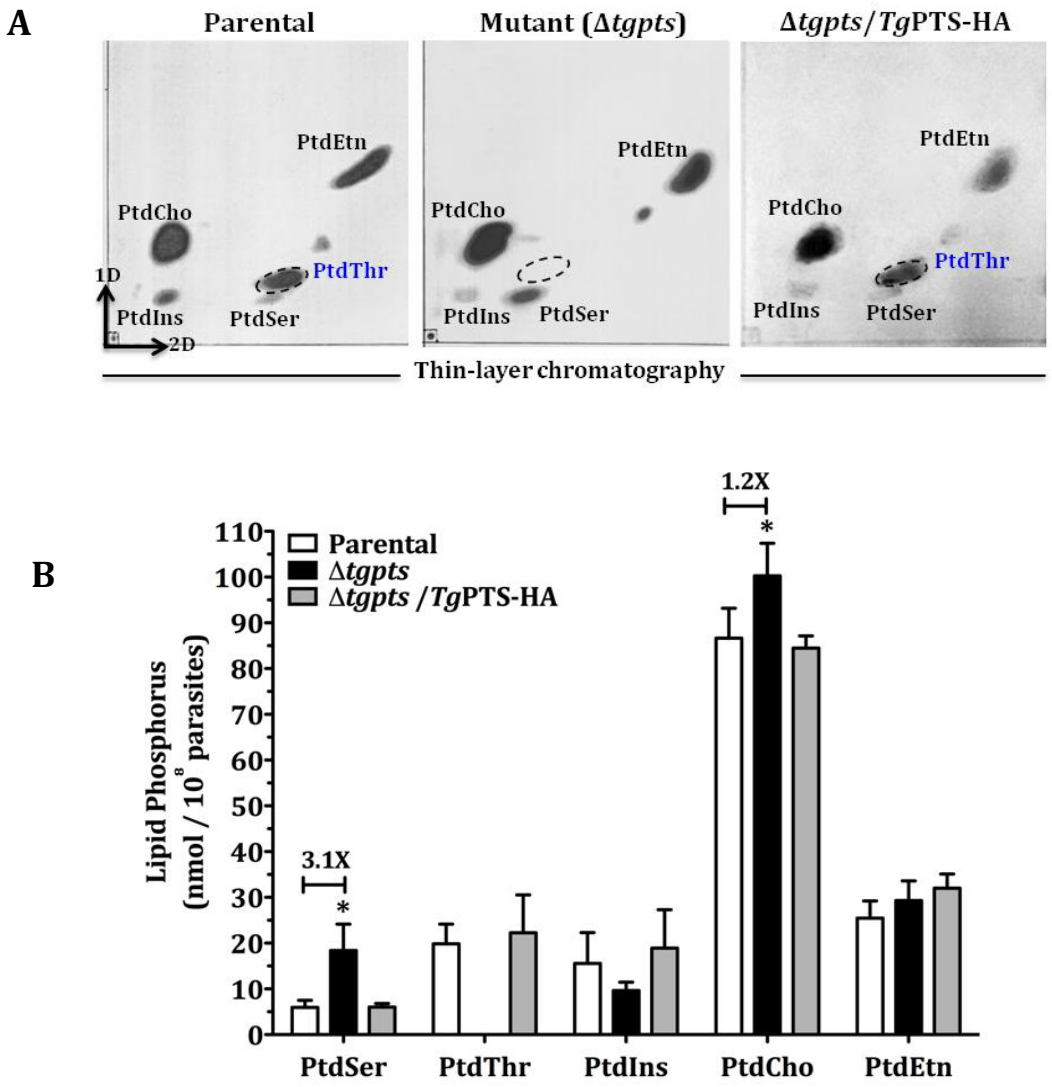

Fig 19: *The Δtgpts strain is devoid of autonomous PtdThr synthesis*. **(D)** Lipid profiles of the indicated strains by two-dimensional thin layer chromatography. Total lipids (0.8-1x10^8 parasites) were resolved and detected by iodine vapor staining. Note the absence of PtdThr band and increased production of PtdSer in the *Δtgpts* mutant. **(E)** The *Δtgpts* mutant contains an increased content of PtdSer and PtdCho. Total lipids (0.8-1x10^8 parasites) were resolved by two-dimensional thin layer chromatography, visualized by iodine vapor staining, and then subjected to phosphorus measurements of lipid bands (n=4, *$p<0.05$).

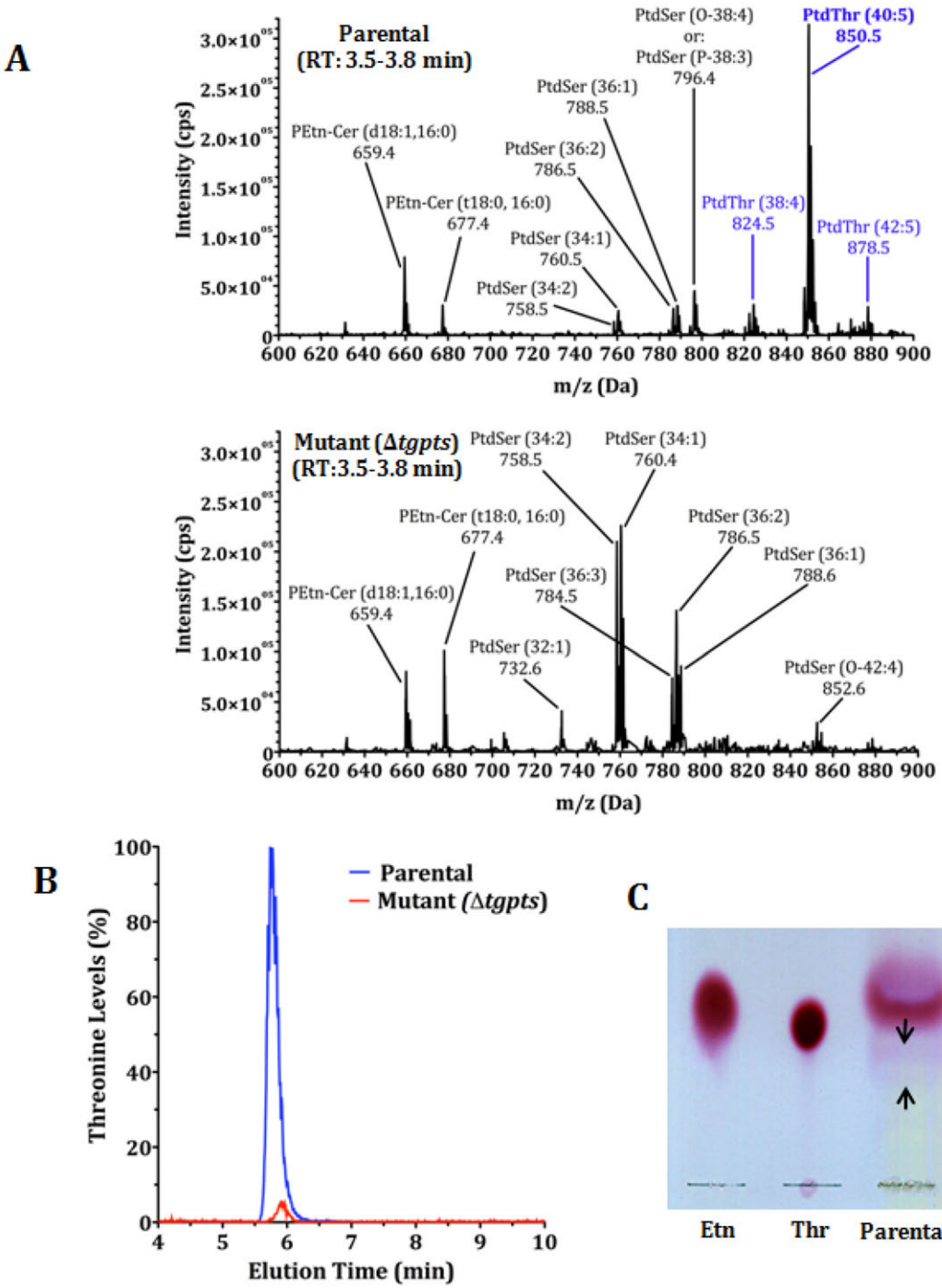
A
Parental
(RT: 3.5-3.8 min)
Intensity (cps)
m/z (Da)
PEtn-Cer (d18:1,16:0)
659.4
PEtn-Cer (t18:0, 16:0)
677.4
PtdSer (34:2)
758.5
PtdSer (34:1)
760.5
PtdSer (36:1)
788.5
PtdSer (36:2)
786.5
PtdSer (O-38:4)
or:
PtdSer (P-38:3)
796.4
PtdThr (38:4)
824.5
PtdThr (40:5)
850.5
PtdThr (42:5)
878.5
Mutant (Δtgpts)
(RT:3.5-3.8 min)
PtdSer (34:2)
758.5
PtdSer (34:1)
760.4
PEtn-Cer (t18:0, 16:0)
677.4
PtdSer (36:2)
786.5
PtdSer (36:1)
788.6
PtdSer (36:3)
784.5
PEtn-Cer (d18:1,16:0)
659.4
PtdSer (32:1)
732.6
PtdSer (O-42:4)
852.6
B
Parental
Mutant (Δtgpts)
Threonine Levels (%)
Elution Time (min)
C
Etn
Thr
Parental
Mutant
(Δtgpts)
Ser
D
Δtgpts/TgPTS
(ΔECWWD)-myc
PtdEtn
PtdCho
PtdIns
PtdSer

Fig. 20. *The Δtgpts strain is deficient in PtdThr, and in lipid-derived threonine*. **(A)** Representative MS profiles of the HPLC-resolved lipid (retention time (RT), 3.5 – 3.8 min) from the parental and *Δtgpts* strains (~10^7 parasites each) confirming the presence of a major (*m/z* 850.5, 40:5) and two minor (*m/z* 824.5, 38:4; *m/z* 878.5, 42:5) PtdThr species in the parental parasites, which are completely absent in the mutant. Note that PtdSer peaks are more intense in the *Δtgpts* sample, which is in agreement with lipid analysis by TLC and chemical phosphorus assays (Fig 3). **(B)** HPLC profiles of the amino acid (threonine) obtained by hydrolysis of the parental and mutant lipids (10^7 parasites each). Unlike parental, the *Δtgpts* strain shows a negligible amount of lipid-derived threonine. Detection and quantification was performed by multiple-reaction-monitoring (MRM) MS of threonine decarboxylation (transition, 120/74 Da). **(C)** TLC profile of amino acid lipid hydrolysates of parental and mutant parasites. Amino acid bands were visualized by ninhydrin staining. Note threonine (downward arrow) and serine (upward arrow) bands in parental but only serine band in *Δtgpts* train **(D)** Lipid profile of total lipids ($0.8x10^8$ parasites) of the *Δtgpts* strain complemented with a mutagenized *Tg*PTS isoform with deleted base-exchange domain (ΔECWWD) shows no PtdThr, and confirms the requirement of *Tg*PTS catalytic activity for PtdThr synthesis in *T. gondii*.

3.1.8. Parasite Egress and Invasion but not intracellular replication are impaired by genetic disruption of phoshatidylthreonine synthase

We next assessed the physiological impact of genetic ablation on the parasite growth by plaque assays, which recapitulate all the steps (invasion, replication and egress) of the lytic cycle of *T. gondii*. The *Δtgpts* strain formed significantly smaller (-70%) and considerably fewer (-80%) plaques when compared to the parental strain (Fig 21). Ectopic expression of wild-type *Tg*PTS, but not of a mutagenized isoform (*Tg*$PTS_{(\Delta ECWWD)}$) without catalytic activity (Fig. 20D, Appendix 4), largely rescued the parasite growth. These assays demonstrate the mandatory requirement of PTS activity for an effective functioning of the lytic cycle in *T. gondii*.

In depth phenotypic characterization was performed to determine which steps of the lytic cycle were compromised in the Δ*tgpts* parasites. Surprisingly, the intracellular replication rate of the mutant strain remained normal (Fig. 22A). On the other hand, a slower egress was observed for Δ*tgpts* parasites. While more than 67% and 94% of the wild-type parasite

vacuoles were already egressing 60 and 72 hours after infection, respectively, only about 27% and 46% of the Δ*tgpts* vacuoles showed signs of egress at the same time points (Fig. 22B).

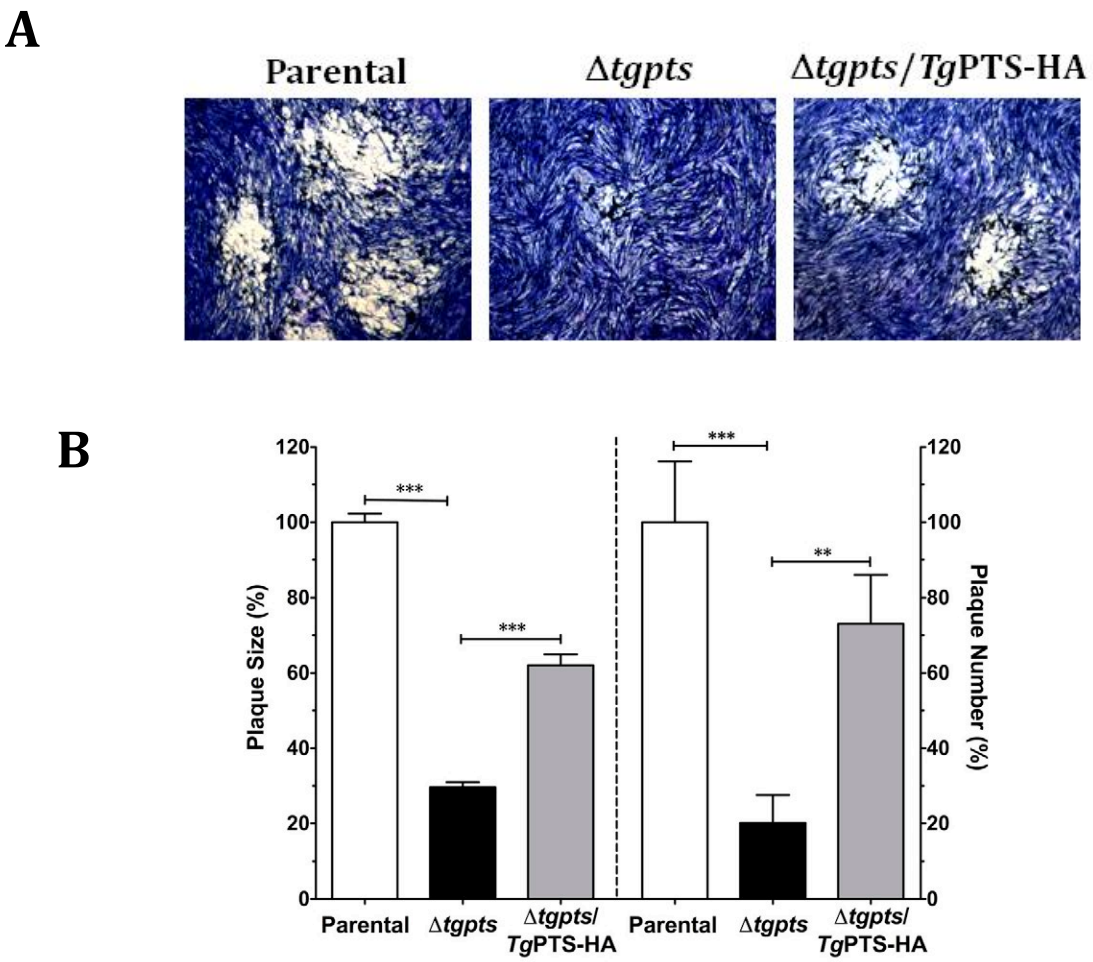

Fig. 21. *In vitro growth fitness defect of the Δtgpts mutant.* **(A)** Representative pictures of plaque assays, which recapitulate successive lytic cycles of tachyzoites in host cells. The mutant was generated as described in *methods* and shown in Fig S4. Complemented strain expressed wild-type *Tg*PTS-HA inserted at the UPRT gene locus, and regulated by *TgGRA2* promoter. **(B)** Quantification of plaque area (left Y axis) and numbers (right Y axis) was performed by scoring 120-300 plaques from each strain (n=3).

Complete host monolayer lysis for the mutant was not observed until 96 hours post-infection at the established multiplicity of infection (MOI=1) (Fig. 22A). Again, the egress delay was also restored in the complemented strain (Fig 22B). Interestingly, *Tg*PTS gene disruption also caused a significant ~2-fold decrease on the invasion ability when compared to the parental

RH*Δku80* strain. This defect was also recovered upon complementation with functional *Tg*PTS (Fig 22C).

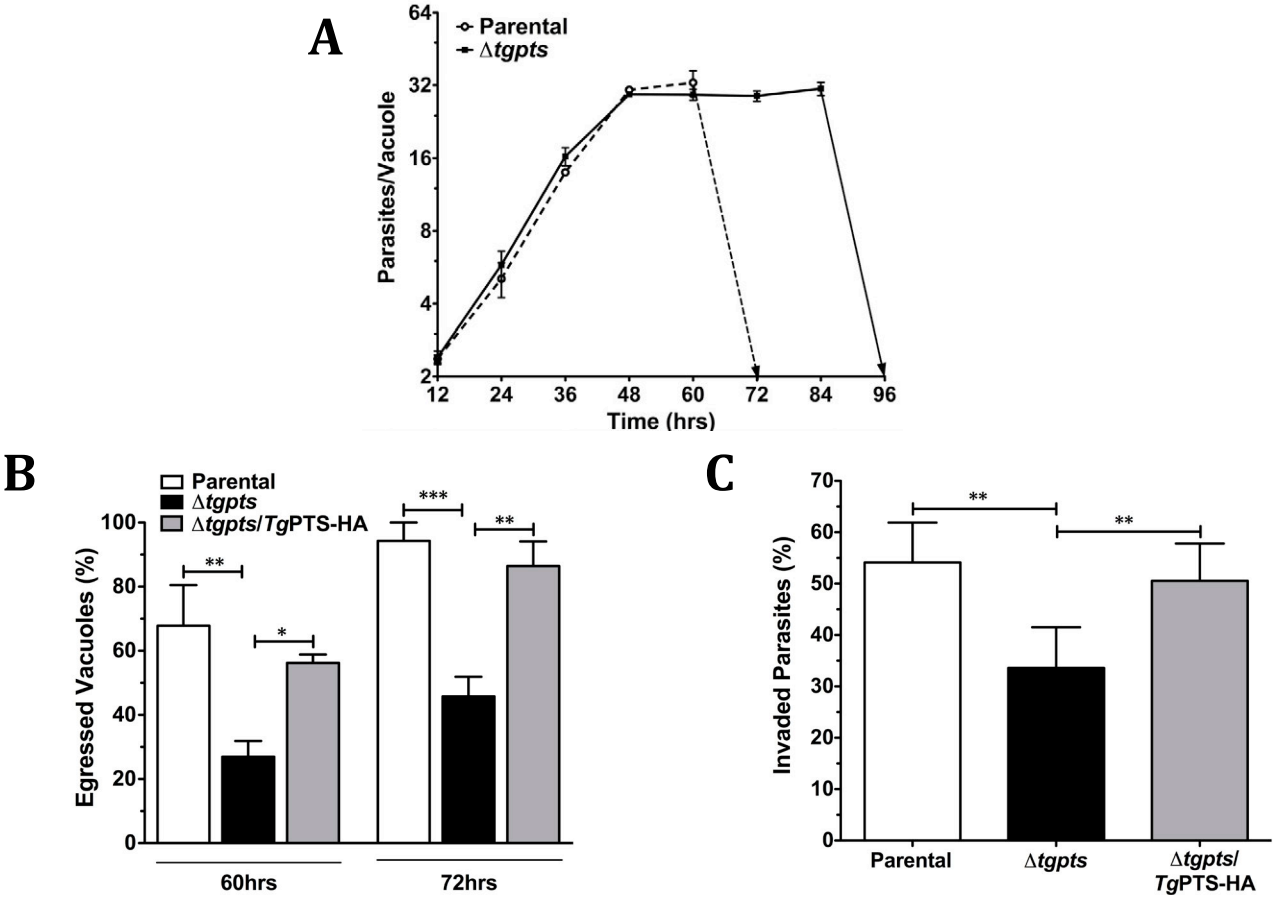

Fig. 22. *Δtgpts parasites have a defective exit and entrance into their host cells*. **(A)** Intracellular replication rates of the parental and *Δtgpts* strains deduced by mean number of parasites per vacuole at different periods. A total of 100-200 vacuoles were analyzed (n=4). **(B)** The natural egress of the indicated parasite strains at 60 and 72 hrs following infection (MOI, 1; 200-300 vacuoles from n=4). **(C)** Invasion efficiency of the parental, mutant and complemented parasites (700-1000 parasites of each strain from n=5). The numbers of egressed vacuoles and invaded parasites were estimated by dual-color staining. Error bars indicate the mean ± SEM (*p<0.05, **p<0.01, ***p<0.001).

3.1.9. Evacuole formation is not affected by PtdThr depletion

To assess which stage of invasion was impaired in *Δtgpts* parasites, evacuole assays were performed in presence of cytochalasin D, an actin depolimerization agent which paralyzes and blocks parasite entrance to the host cell, but not the initial attachment and formation of rhoptry-derived evacuoles, which will contribute to the formation of the parasitophorous

vacuole (Håkansson et al., 2001; Meissner et al., 2002). Under these conditions parasites of both, parental and mutant strains were able to form evacuoles at a similar proportion and length, as detected by ROP2 staining (Fig. 23). These results indicate that PtdThr is dispensable for the initial attachment and subsequent evacuole formation of the invasion process, but not for the efficient penetration into the host cell by the *Δtgpts* parasites (Fig. 22C).

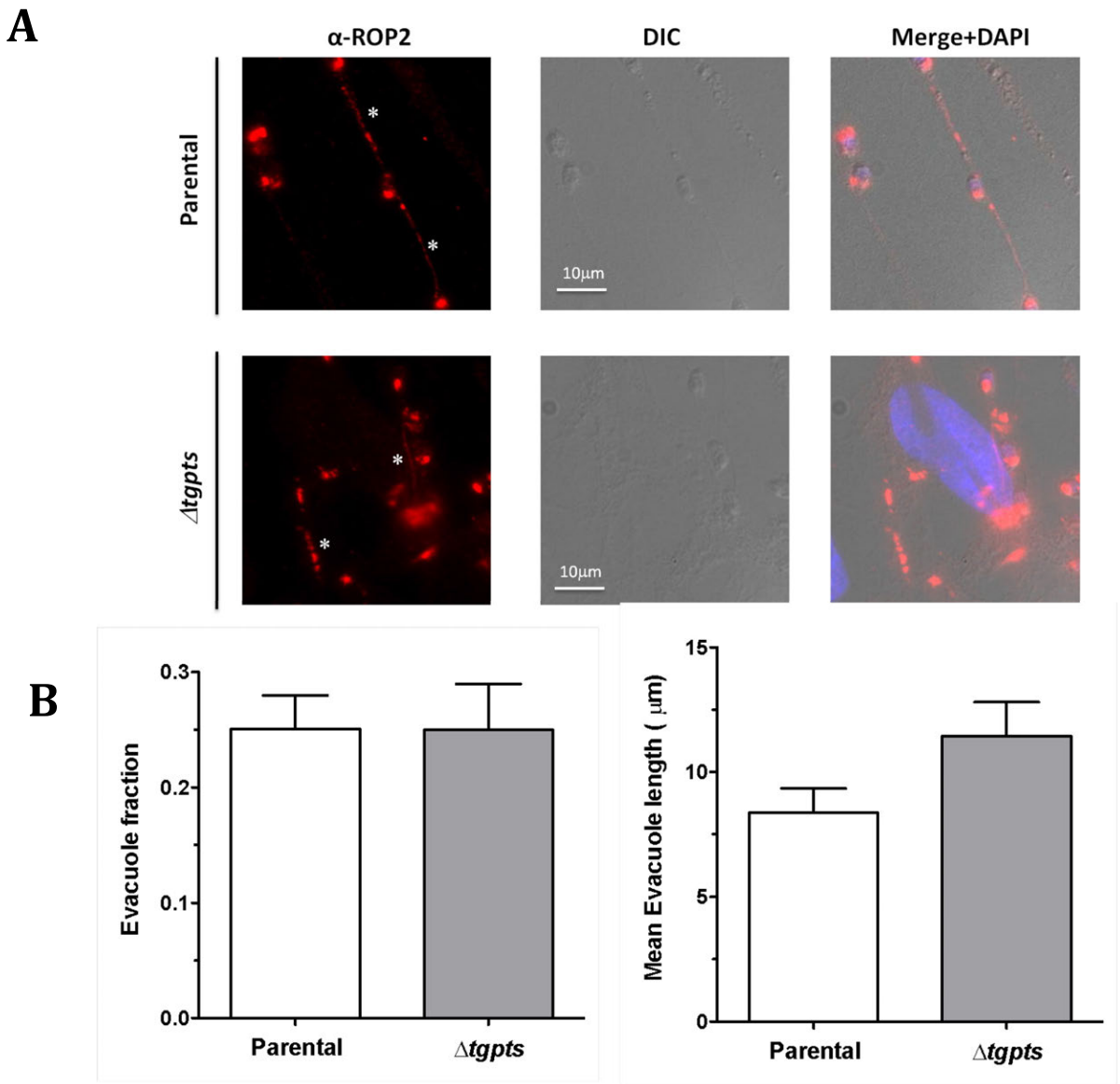

Fig 23. *Evacuole formation is not altered upon PtdThr depletion*. **A**. Representative images showing the evacuoles (*) formed by the parental and *Δtgpts* parasites as detected by anti-ROP2 immunofluorescence. **B**. Quantification of the fraction of parasites forming ROP2-evacuoles (left) and their length (right). Error bars indicate the mean ± SEM (n= 10 random fields).

3.1.10. A reduced parasite motility explains impaired lytic cycle of *Δtgpts* parasites

Gliding motility in *T. gondii* drives parasite egress from dilapidated host cells and ensues active invasion of neighboring cells (Meissner et al., 2002), all of which eventually underlie the parasite virulence. On the other hand, intracellular replication, which remained unaffected in the *Δtgpts* strain, does not require motile parasites. Hence, we performed *in vitro* motility assays to investigate if parasite motility was impaired upon PtdThr depletion. As shown (Fig. 24A-B), the *Δtgpts* strain showed a distinguished reduction in the fraction of motile parasites and their trail length when compared to the parental and complemented strains.

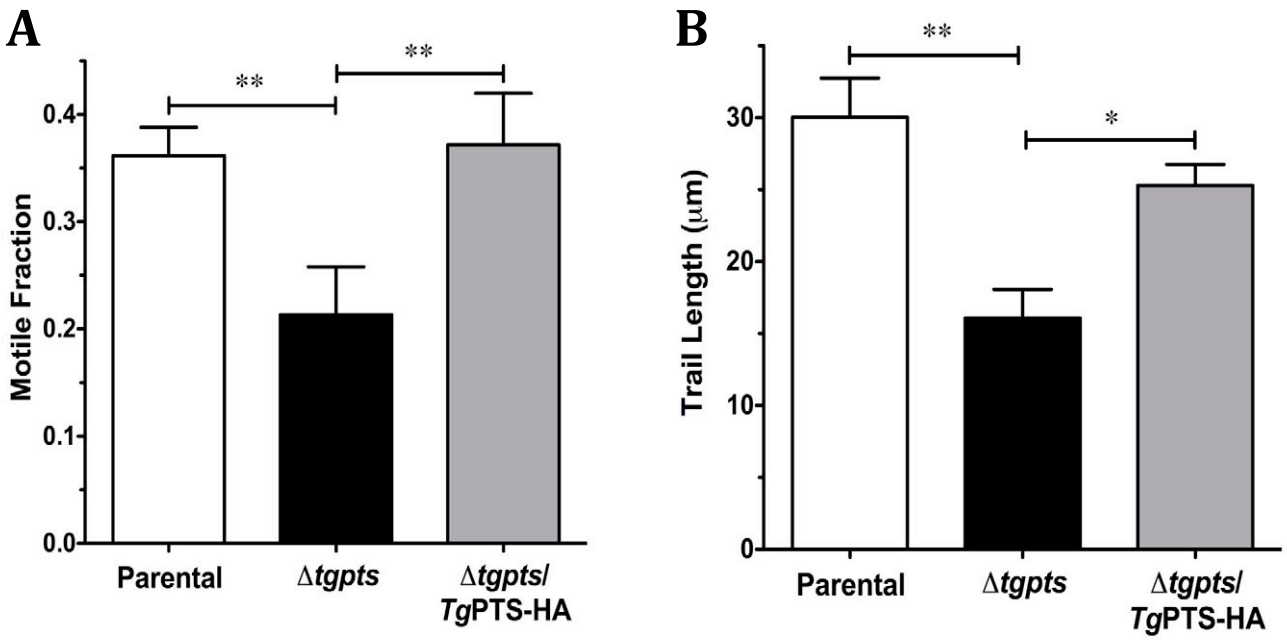

Fig. 24. *Δtgpts parasites display a reduced motility*. **(A)** Motile fractions of different strains. In total, 500-1000 parasites from 3 assays were scored for the presence or absence of a motility trail visualized by anti-*Tg*Sag1 antibody. **(B)** Motility of individual parasite strains from *panel A*, as deduced by the length of *Tg*Sag1-stained trails (± SEM from n=3 assays). *Panel A-B*, *p<0.05, **p< 0.01

3.1.11. Phosphatidylthreonine is required for the virulence of *T. gondii* in a mouse model and parasites lacking PtdThr exert protection against acute and chronic toxoplasmosis

To correlate the defective *in vitro* lytic cycle with the parasite virulence, we performed infection assays in C57/BL6 mice by intraperitoneal injection of freshly syringe-released tachyzoites of the parental and *Δtgpts* strains, and analyzed their survival. As observed (Fig 25), nearly all animals infected with the mutant *Δtgpts* parasites survived the acute infection, even at much higher doses than the parental strains (500, 5000 for *Δtgpts* vs. 50 tachyzoites for the parental), which was fully lethal between 8-10 days after infection. Interestingly, surviving *Δtgpts*-infected mice also turned completely resistant to a lethal challenge with the parental strain (Fig. 25), indicating a vaccination potential of metabolically attenuated parasites lacking PtdThr against acute toxoplasmosis.

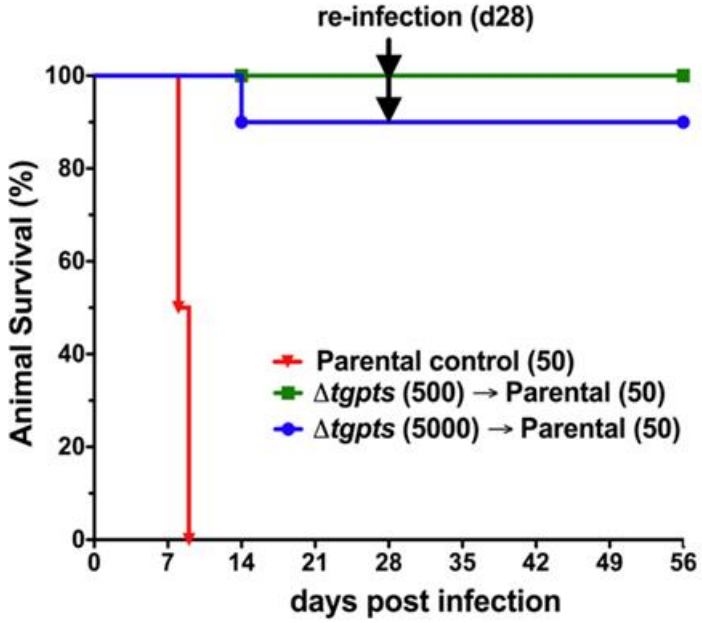

Fig. 25. *Lack of PtdThr impairs T. gondii virulence.* Infection of C57BL6/J mice with the *Δtgpts* and parental strains to test their virulence, and 'vaccination' potential of the mutant against acute toxoplasmosis. Naïve animals were infected with the *Δku80-hxgprt*⁻ (50 tachyzoites) or the mutant (500, 5000 tachyzoites) strains by intra-peritoneal route and monitored for 28 days (n=3 assays with 4 mice each). Animals surviving the *Δtgpts* infection were re-infected with a lethal dose of the parental strain and examined for additional 4 weeks. A control group of naïve mice (n=4) was also infected with the same parental inoculum.

Next, we evaluated the vaccination potential of the *Δtgpts* parasites against the chronic stage infection. As seen in Fig. 26, *Δtgpts*-immunized mice showed no detectable brain cysts after 28 days of infection with the cyst-forming type II strain (ME49), as screened by manual count, histology and qRT-PCR of *Tg*B2 as a marker of parasite load. On the other hand, a group of control naive mice presented high amounts of tissue cysts under the same conditions (~1200/brain). This result demonstrates the therapeutic potential of the *Δtgpts* strain also against chronic toxoplasmosis. These results also suggest that the impairment of the lytic cycle of *Δtgpts* parasites does not lead to cyst formation.

Mice infection and cyst screening assays were performed in collaboration with Dr. Ildiko R. Dunay and PhD student, Aindrila Biswas at the Institute of Medical Microbiology of Otto-von-Guericke University (Magdeburg, Germany).

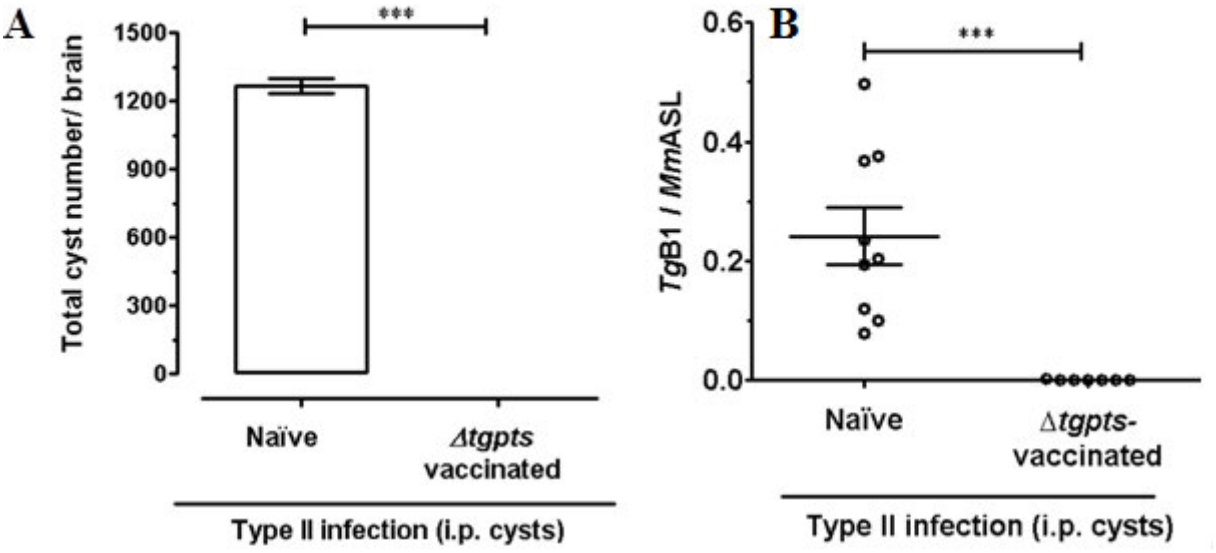

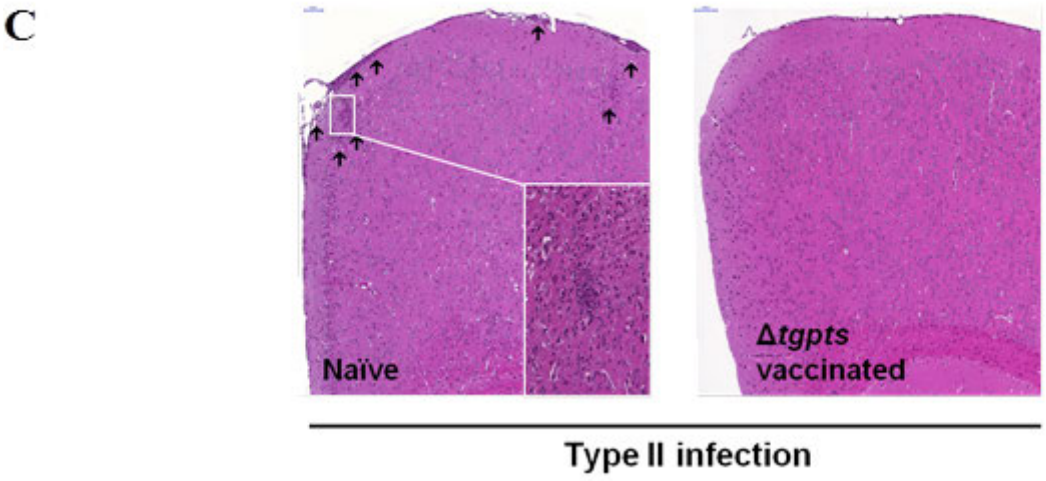

Fig. 26. *Δtgpts parasites protect against chronic toxoplasmosis*. C57/B6 mice were initially infected with the *Δtgpts* parasites (500 i.p.) and after 4 weeks, were challenged with three cyst (i. p.) of the ME49 type II strain. A control group of naïve mice was also included. After additional 4 weeks the outcome of the brain infection was evaluated. **(A)** Total number of cyst per brain of infected mice (n=5; ***p<0.001). **(B)** Relative expression of the *T. gondii* marker *Tg*B2 per infected brain, expression was normalized to the argininosuccinate lyase (*Mm*ASL) levels of the mouse (Bereswill et al., 2014). (n=7; ***p<0.001). **(C)** Brain histopathology of ME49-infected mice (naïve and *Δtgpts*-vaccinated*)*. Arrows indicate sites of pronounced inflammation caused by cyst development. Inset shows zoomed area of inflammation.

3.1.12. Cytoplasmic calcium pool is downregulated during egress upon phosphatidylthreonine depletion

Having defined the importance of PtdThr in the lytic cycle and virulence of *T. gondii*, we investigated the underlying mechanism. Egression and invasion events are regulated by the discharge of calcium to the parasite cytosol (Billker et al., 2009), which is primarily stored in acidocalcisomes and ER (Moreno et al., 2011); the latter of which hosts PtdThr synthesis (Fig 2). To correlate these events, we developed a method to monitor calcium in the parasite cytosol based on a genetically-encoded calcium indicator (GCamP6s) (Chen et al., 2013) in both, parental and *Δtgpts* strains. To this end, the GCamp6s ORF was cloned into the *pTgGRA2-UPKO* vector for targeted insertion at the non-essential *UPRT* locus after selection with fluoruracil deoxyribose (FUdR). Transgenic parasites expressing GCamP6s showed an intense Ca^{2+}-induced cytosolic fluorescence upon egression, whereas immature vacuoles harboring intracellular parasites were non-fluorescent (Fig 27A). An automated measurement of GFP fluorescence revealed a comparable level of cytosolic calcium during replication phase of the parental and mutant parasites, which was progressively elevated in both strains as they approached the end of their lytic cycles (42-50 hrs infection, Fig 27B). Quite noticeably, the *Δtgpts* mutant showed a significantly diminished fluorescence compared to the parental strain during the entire egression window (Fig 27B), indicating a defective release of calcium in the cytosol.

To determine a possible origin of this defect, we measured the levels of cytoplasmic calcium in the parental and mutant strains after treatment with 8% ethanol. Ethanol enhances phospholipase C (PLC) activity, which in turn activates the inositol 1,4,5-triphosphate (IP3)-sensitive calcium channels of the endoplasmic reticulum in mammalian cells (Hoek et al., 1987) and also in *T. gondii* (Arrizabalaga and Boothroyd, 2004; Lovett et al., 2002). As shown in Figure 27C, ethanol induced a calcium surge in both strains after only 1 min exposure which remained constant, suggesting a saturation effect after depleting intracellular Ca^{2+}-storages. However, the cytoplasmic Ca^{2+} levels induced in the mutant parasites were significantly less compared to those achieved in the parental throughout the whole experiment. This result suggests an involvement of Phospholipase C and IP3-sensitive channels in the ER in the regulation of calcium signaling by PtdThr.

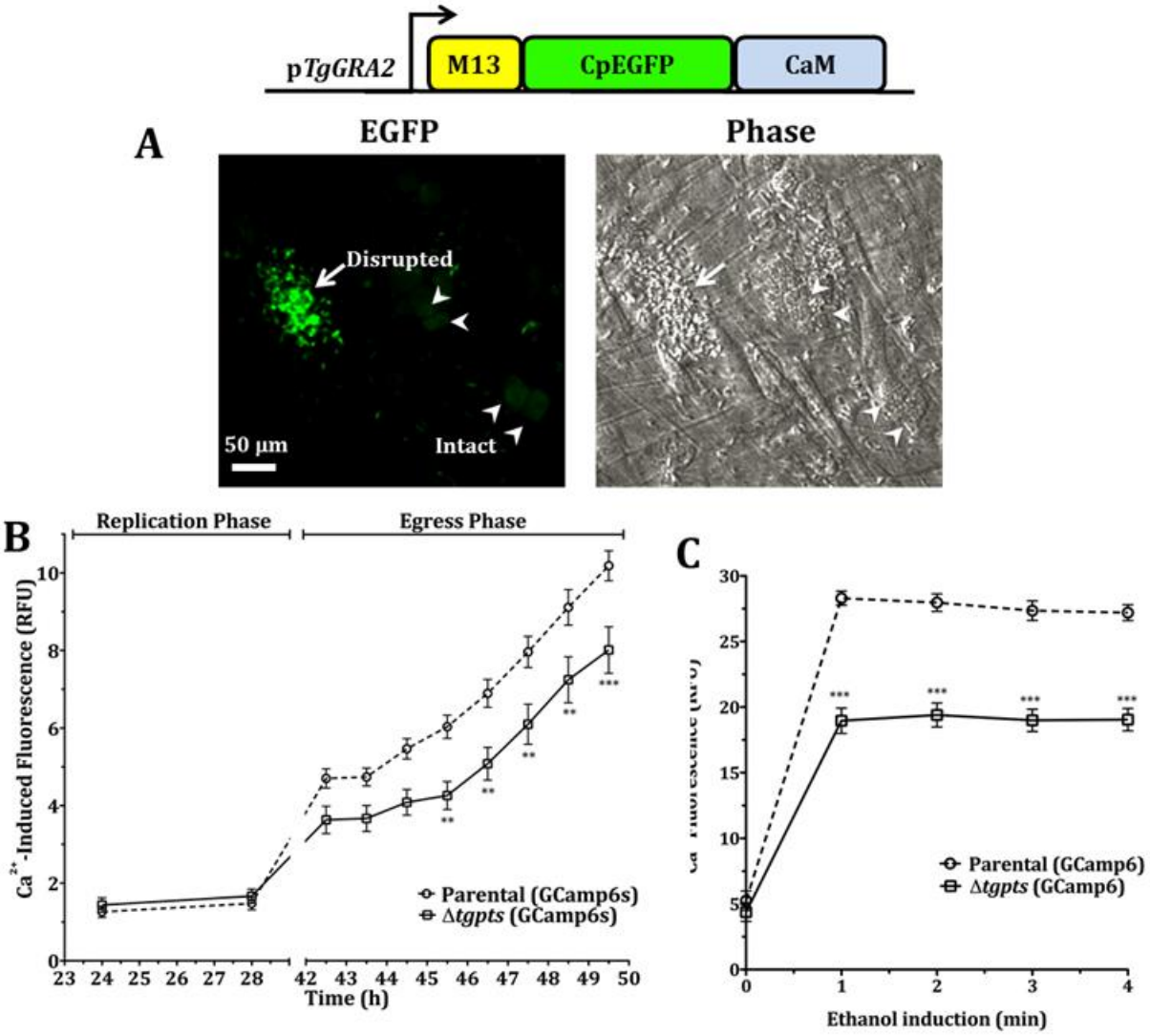

Fig. 27. *The Δtgpts mutant has an impaired mobilization of ER-derived Ca^{2+} into its cytosol during natural egress*. **(A)** Image showing an accentuated GFP fluorescence during parasite egress (arrow) and background intensity in the intact vacuoles (arrowheads). The parental or *Δtgpts* strains expressing GCamP6s (M13-CpEGFP-CaM fusion) under the control of the *TgGRA2* promoter were generated. The image shows the parental strain 44 hrs post-infection (MOI, 3). **(B)** Quantification of GFP fluorescence during the replication and egress phases of indicated strains. Human fibroblasts were infected with GCamP6s-transgenic parental or *Δtgpts* strains with an MOI of 3 and 3.75, respectively, to offset for the invasion defect (Fig 22C). Calcium-induced GFP fluorescence was measured in living parasite cultures using a microplate reader. Error bars indicate the mean ± SEM of 9 assays performed in triplicates. **(C)** Calcium-induced fluorescence after ethanol (8%) exposure of transgenic parasites expressing a genetically-encoded calcium indicator, GCamp6s. Ethanol treatment was performed 42 hrs post-infection followed by fluorescence quantification. *p<0.05, **p<0.01, ***p<0.001.

3.1.13. Ionophore-induced calcium entry bypasses egress defect upon phosphatidylthreonine depletion

The *Δtgpts* mutant also exhibited a reduced calcium level following treatment with an ionophore (A23187, Fig. 28A), again implying an impaired ion mobilization to the parasite cytosol. The calcium level in ionophore-induced samples was nevertheless notably higher than the natural amount in control samples. Only 1 min of drug exposure triggered a prominent calcium spike (Fig. 28A), which was greater than the apex calcium level achieved in both strains under non-induced control conditions (Fig. 28B). Consistently, such an elevated flux of calcium also restored the egress defect in the ionophore-treated mutant (Fig 28B), which indicated a need of minimum threshold for the natural egression. Collectively, these results also implied a regulatory role of lipids upstream of calcium signaling in *T. gondii.*

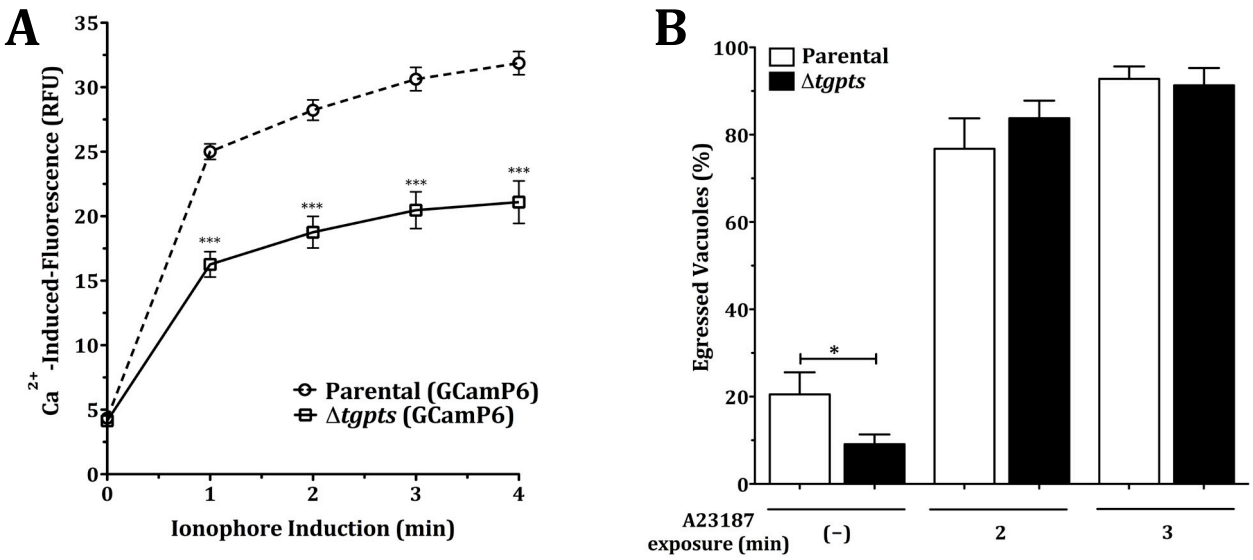

Fig. 28. *Ionophore-induced influx of calcium can repair egress defect*. **(A)** Calcium response following the ionophore (A23187) exposure of parasites expressing GCamp6s (42 hrs post-infection). **(B)** Ionophore-induced egress in the parental or *Δtgpts* parasites. Parasitized cultures (MOI, 1; 48 hrs infection) were stimulated with 5 μM A23187 up to 3 minutes before fixation. Percentage of egressed vacuoles was scored in at least 10 random fields at each time point (n=3). Note a natural egress defect in the mutant in the absence of A23187; which is amended within 2-3 min of drug exposure. *p<0.05, **p< 0.01, ***p<0.001. Error bars, S.E.

3.1.14. Phosphatidylthreonine depletion induces higher endogenous PSS activity in *T. gondii*

To determine if *de novo* synthesis of phosphatidylserine rather than scavenging from the host cell was the mechanism behind the observed increase in PtdSer content in the mutant parasites, metabolic labeling of fresh extracellular parasites with ^{14}C-serine was performed. Incorporation of ^{14}C-serine into total lipids was about 2.5-fold higher in the mutant compared to the parental strains (1652.39 vs. 662.07 pmol/10^8 parasites). This correlated with a 2.3-fold increase in PtdSer synthesis as determined by autorradiography (Fig. 29A) and counts of corresponding scraped silica bands of TLC-resolved lipids (Fig. 29B). PtdSer synthesis returned to normal levels upon ectopic expression of *Tg*PTS-HA in the *Δtgpts* parasites (Fig. 29B). Interestingly, PtdEtn labeling remained about the same in all three strains, indicating surprisingly similar PtdSer decarboxylation rates despite the increased synthesis of PtdSer in the mutant parasites (Fig. 29B).

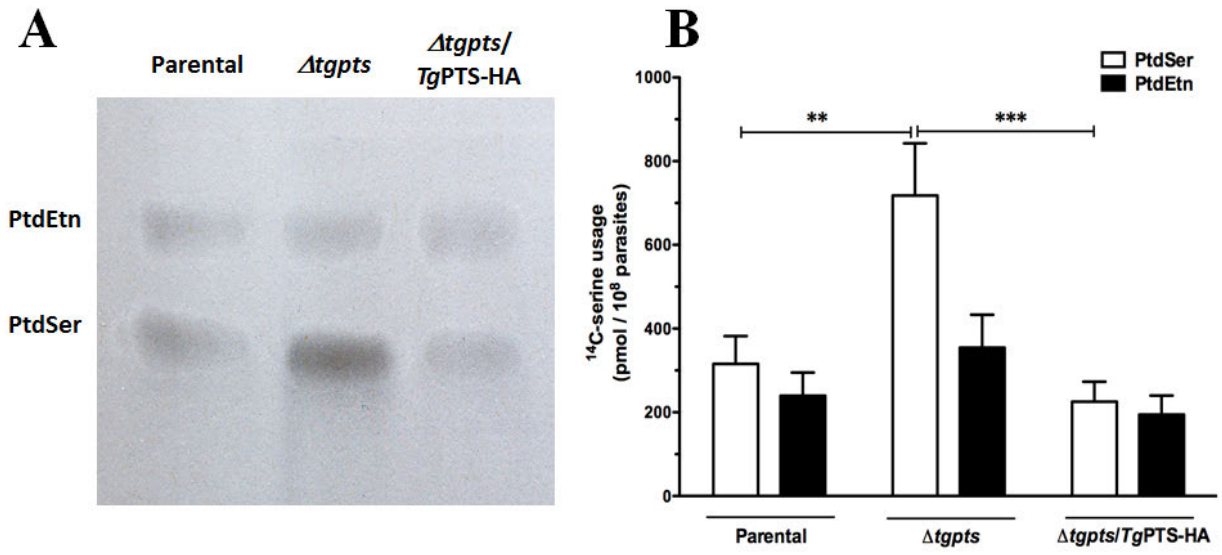

Fig. 29. *Loss of PtdThr upregulates PtdSer synthesis in T. gondii*. **A.** Autoradiography of TLC-resolved lipids of freshly syringe-released extracellular tachyzoites of the indicated strains labeled with ^{14}C-Ser (2μCi, 2hrs, 37°C, 5x10^7 parasites each). Solvent system used was chloroform/ethanol/water/triethylamine (30/35/7/35, v/v). **B.** Individual phospholipid bands from A were scraped for scintillation counting, and incorporation of ^{14}C-Ser was determined (n = 4 assays; **, $p < 0.01$; ***, $p < 0.001$). Error bars, S.E.

3.1.15. Gene expression analysis suggest product-inhibition/activation rather than a transcriptional control of *Tg*PTS and *Tg*PSS regulating the phosphatidylserine/ phosphatidylthreonine balance in *T. gondii*

To correlate the observed reversible increase in endogenous PtdSer synthesis in the *Δtgpts* parasites with the gene expression levels of *Tg*PSS and *Tg*PTS, quantitative real time PCR analysis was performed for the parental, mutant and complemented strains (Fig. 30).

As expected, the *Tg*PTS transcript levels in the *Δtgpts* strain were below the limit of detection, while the complemented strain with a *Tg*PTS-ORF under the foreign *Tg*GRA2 promoter showed a ~100 fold increase compared to the parental. Despite this, however, the PtdThr levels remained fairly normal in the complemented strain (Fig. 30), what would suggest an end-product inhibition feedback of *Tg*PTS. On the other hand, the *Tg*PSS transcript levels remained unexpectedly unaltered in the *Δtgpts*. This result suggests a post-transcriptional mechanism concerning the observed upregulation of the activity of the *Tg*PSS and the consequent PtdSer/PtdThr balance.

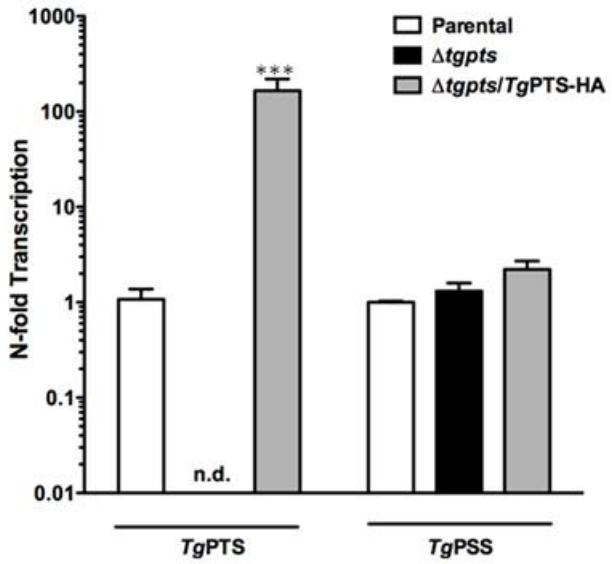

Fig. 30. *Relative abundance of the TgPSS and TgPTS transcripts of indicated strains as detected by qRT-PCR*. 100 ng of total RNA were transcribed into the first-strand cDNA using Oligo(dT) and random hexamer primers at Ta of 60°C. The transcript abundance was calculated as Δct by subtracting the Ct from the housekeeping transcripts (TGGT1_124740, *Tg*GT1; TGGT1_231770, *Tg*TUB8α) and then normalized to parental values. n. d.: not-detected below 30 cycles of amplification. (n = 3 assays; **, $p < 0.01$; ***, $p < 0.001$). Error bars, S.E.

3.2. Phosphatidylserine synthesis in *T. gondii*

3.2.1. *Tg*PSS and *Tg*PTS can produce PtdSer, but only *Tg*PTS utilizes threonine in *E. coli*

E. coli (M15) were transformed with the empty pQE60 plasmid, pQE-60-*Tg*PSS-6his, -*Tg*PTS-6his or -*At*PSS-6his as a positive control (Yamaoka et al., 2011). Next, we ran lipid extracts of the above mentioned *E. coli* strains on TLC, and identified amine-containing phospholipids by ninhydrin staining (Fig 15). While control *E. coli* harbouring the empty vector only showed PtdEtn band, *Tg*PSS, *At*PSS (positive control) and also *Tg*PTS-expressing *E. coli* produced PtdSer when cultured in the presence of 5 mM Ser after IPTG induction. However, when cultured in presence of excess threonine (5mM), only *Tg*PTS-expressing cultures produced significant amounts of PtdThr (Fig 31).

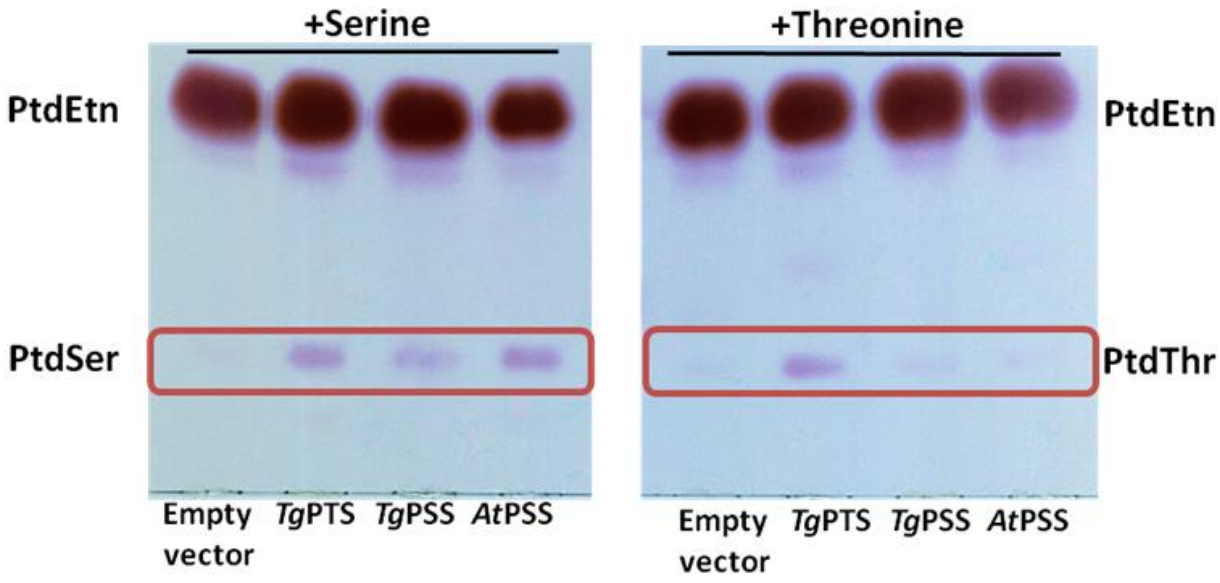

Fig 31. *TgPSS and TgPTS can produce PtdSer, but only TgPTS makesPtdThr in E. coli.* Lipid profiles of indicated *E. coli* strains (after induction in IPTG 1.5mM) cultured in presence of either 5mM serine or 5mM threonine by one dimensional-thin-layer chromatography. Solvent system used was $CHCl_3$/Methanol/Acetic acid (130/50/20). Aminophospholipids (PtdEtn, PtdSer and PtdThr) were visualized by ninhydrin staining.

3.2.2. *Tg*PTS but not *Tg*PSS has a growth-enhancement effect in PtdSer-defficient yeast

The *cho1*Δ yeast strain (JSY94A, a W303a derivative; (Choi et al., 2010)) lacks any PtdSer synthase activity and show no detectable amounts of PtdSer in its membranes (Hikiji et al., 1988). Yeast PtdSer synthase (*Sc*PSS), however is a CDP-DAG dependent enzyme and in absence of choline constitutes the primary source of PtdCho, by decarboxylation to PtdEtn followed by 2 consecutive methylations (Choi et al., 2004). The *cho1*Δ strain can grow when supplied with choline or ethanolamine, which feed the alternative Kennedy pathways to produce both major phospholipids, although full recovery is not achieved due to the absence of PtdSer. In an attempt to functionally characterize *Tg*PSS and *Tg*PTS, the *cho1*Δ strain was transformed with the pESC-URA-*Tg*PSS, -*Tg*PTS, -*Sc*PSS (positive control) and empty plasmids (negative control). Transgenic expression was induced in medium with galactose. As seen in Fig. 32, *Sc*PSS-expressing strain grew normally in both, media supplied with and without choline, in stark contrast to *Tg*PSS- or empty plasmid transfected strains, which only grew modestly in presence of choline. On the other hand, although not able to complement the growth defect in absence of choline, *Tg*PTS did enhance the growth of the *cho1*Δ mutant under permissive conditions (Fig. 32).

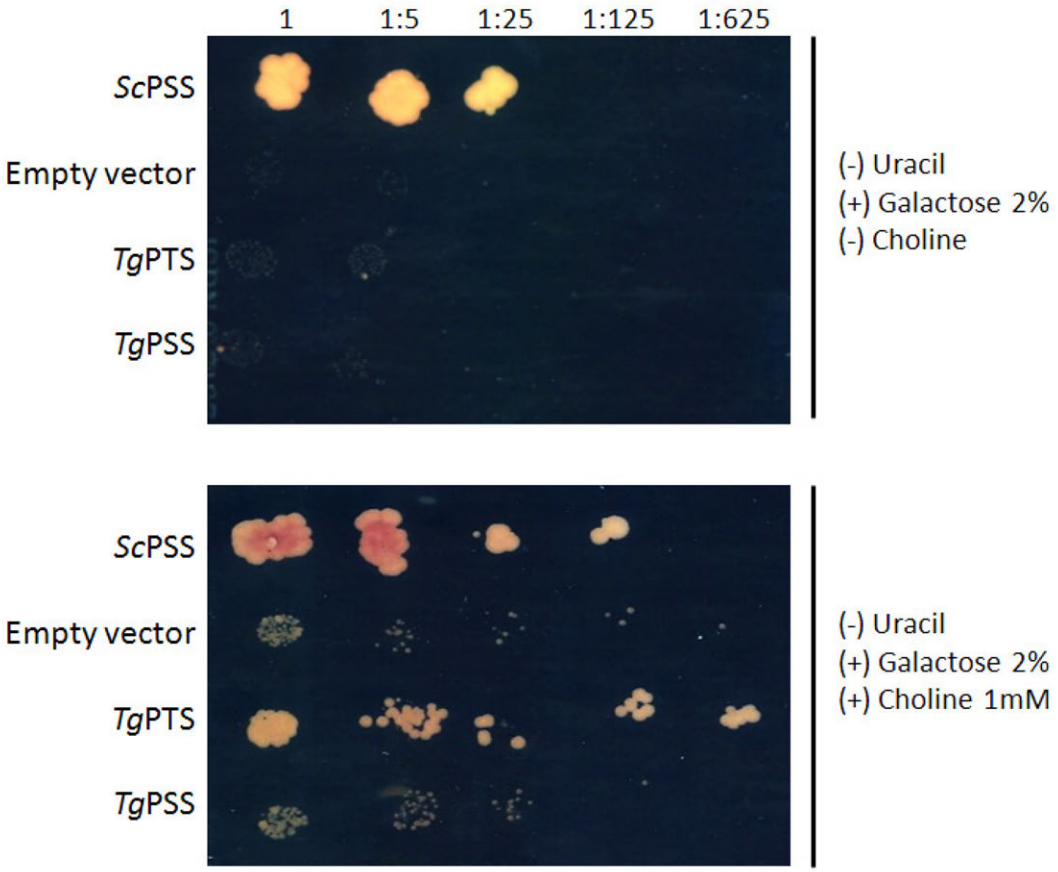

Fig. 32. *TgPTS enhances but does not complement the growth of a PtdSer-defficient yeast strain.* Dilution plate assay showing the growth of the indicated transformants of the *cho1Δ* (JSY94A) yeast strain.

The growth enhancement bestowed by *Tg*PTS expression was also observed when the transgenic yeast strains were cultured on lactacte as main carbon source (Fig. 33), which requires a functional mitochondrial respiratory chain to be utilized (Choi et al., 2004). This discards a differential mitochondrial unstability, which has been reported for the *cho1Δ* mutant (formation of "petite" colonies) as responsible for the observed growth.

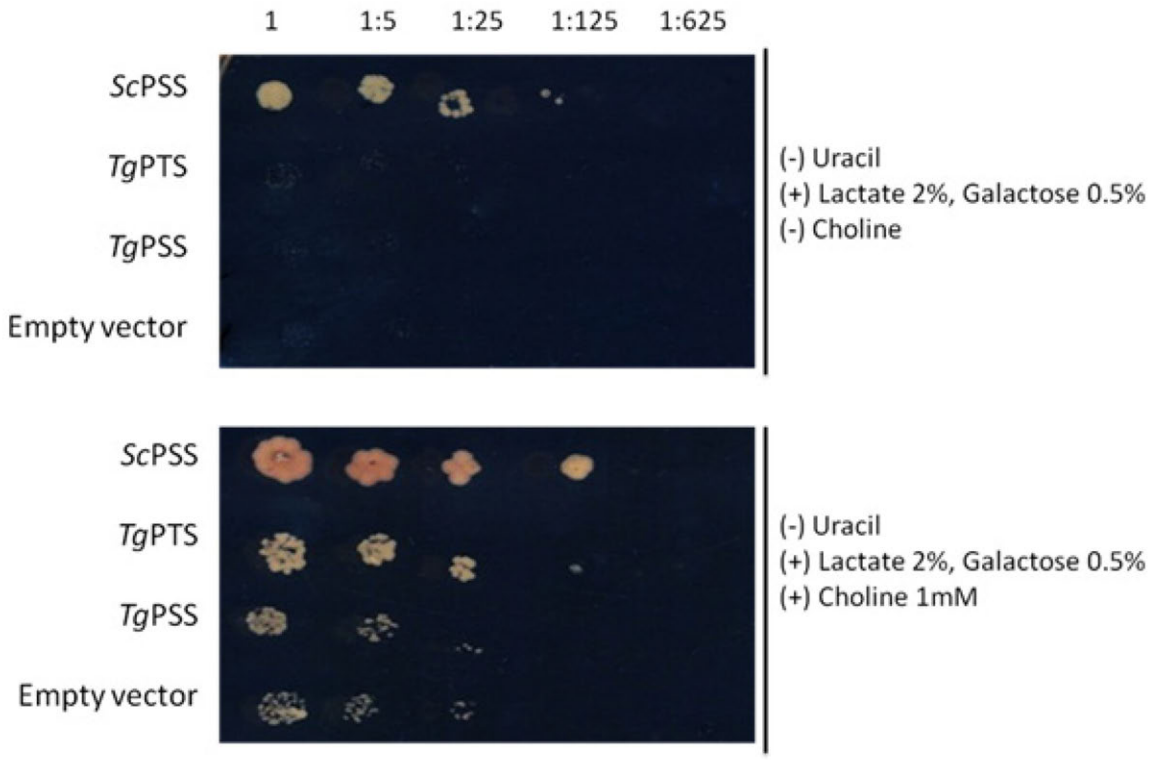

Fig. 33. *Growth enhancement of a PtdSer-defficient yeast strain granted by TgPTS is not due to higher mitochondrial stability.* Dilution plate assay showing the growth of the indicated transformants of the *cho1Δ* (JSY94A) yeast strain in medium containing lactate as main carbon source, which requires functional mitochondria for its utilization.

On the other hand, expression of *Tg*PSS, *a bona fide* PSS (as shown directly by our data in *T. gondii* and *E. coli*) had no effect on *cho1*Δ growth in minimal or permissive medium. The reason for this lack of complementation lies in the different nature of the reactions synthesizing PtdSer in yeast and *T. gondii*. While *Toxoplasma* and mammalian enzymes utilize a base-exchange mechanism, and rely in already present PtdEtn and PtdCho; yeast as well as bacterial PSS generate *de novo* PtdSer from CDP-DAG and serine. Therefore *Tg*PSS would utilize the same PtdEtn pool that would be required for the PtdCho production needed by the *cho1*Δ mutant to grow in absence of choline. It is also possible that *Tg*PSS is not active in yeast due to a different environment or misfolding, in fact there has not been any report of functional expression of base-exchange PSS in yeast.

The enhancement effect of *Tg*PTS on *cho1*Δ in presence of choline would correlate with the increase in PtdCho observed in *Δtgpts* parasites (Fig. 19B) and would support PtdCho as substrate of *Tg*PTS. Following this reasoning, when PtdCho from the Kennedy pathway is available, *Tg*PTS could utilize it to synthesize PtdThr, which, given its structural analogy to PtdSer, could also fulfill some of its functions and increase the deficient growth of the *cho1*Δ yeast mutant. Conversely, the secondary PSS activity of *Tg*PTS, shown by the absence of defined minor PtdSer species in the *Δtgpts* parasites (Fig.20A) and the production of PtdSer in *Tg*PTS-expressing *E. coli* in high serine-content medium (Fig. 31), may also contribute to this growth enhancement. Further biochemical characterization of the PSS and PTS activities and determination of the phospholipid composition of these transgenic yeast strains should address these issues.

3.2.3. Conditional knockdown of *Tg*PSS does not affect the parasite growth

To assess the function and essentiality of the putative *Tg*PSS, a direct knock-out approach was initially performed. However multiple attempts to generate stable clonal lines with a deleted or disrupted *Tg*PSS locus by double homologous recombination were unsuccessful under different selections markers (chloramphenicol, MPA/XA and pyrimethamine). While the pool of transfected parasites showed evidence for recombination events at the 5' and 3' ends, none of the selected clones had double homologous recombination and only underwent either single 3' or mostly 5'- crossover (Appendix 5).

Given these results, a conditional knockdown of *Tg*PSS was approached. A C-terminally HA-tagged copy of the *Tg*PSS ORF under the tetracycline-regulatable promoter *pTeto7sag1* (Meissner et al., 2002) and the *NTP3*-3'UTR was cloned into the plasmid *pTetUPKO*. The expression cassette was flanked by 800 bp of the 5'- and 3'-UTRs of the non-essential *Tg*UPRT (uracil phosphoribosyl transferase) gene for the insertion of *Tg*PSS-HA at the locus by double crossover to generate a merodiploid parasite line, expressing both, the inducible and the endogenous *Tg*PSS gene copies. Selection of recombinant parasites was achieved in presence of fluoro-deoxyuracil (FudR) 5 μM for 2-3 weeks (Donald and Roos, 1995).

Next, the merodiploid *Tg*PSS/*Tg*PSS-HA_i strain was transfected with a *Tg*PSS knockout plasmid. To this end, the 5' and 3' UTRs of *Tg*PSS (1 Kb each) were cloned into the *pTKO-DHFR-TS* vector, flanking the resistance cassette. Stable parasites were then selected by

resistance to 1 µM pyremithamine for one week (Donald and Roos, 1993). Clonal resistant parasites obtained by serial dilution were analyzed for double homologous crossover at the *Tg*PSS locus by PCR. 5' and 3'-specific PCRs amplified the expected bands in the *Δtgpss*/*Tg*PSS-HA$_i$ clones, but not in the parental *(Δku80*-TaTi) or the control knockout plasmid (Fig. 34). The identity of both crossover DNA fragments was confirmed by sequencing, validating the deletion of the endonenous *Tg*PSS gene.

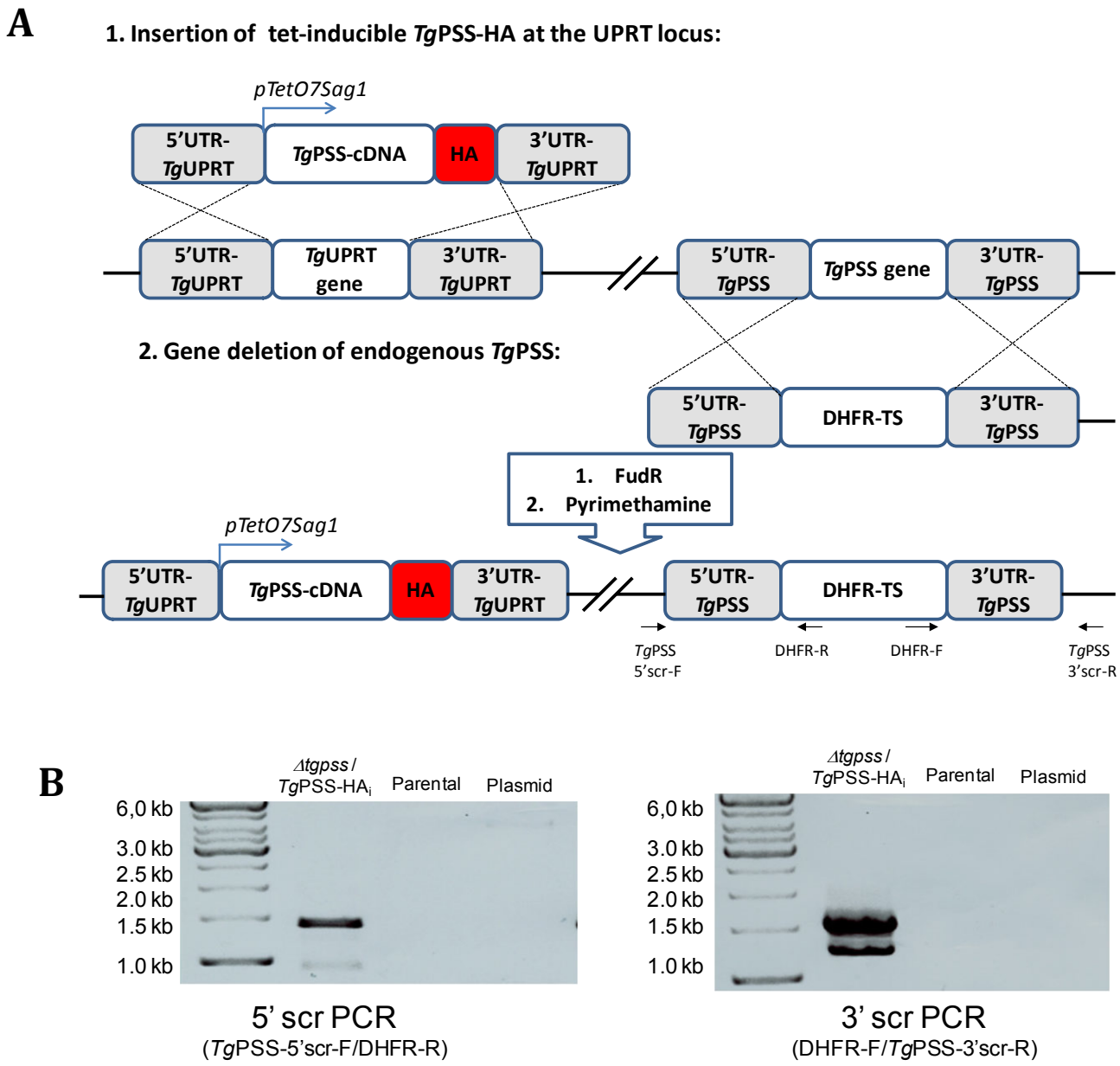

Fig. 34. *Conditional mutagenesis of TgPSS*. **(A)** Scheme depicting the generation of a regulatable *Tg*PSS-knockdown line in two steps. First, *Tg*PSS-HA under the control of the *pTetO7Sag1* promoter

(*Tg*PSS-HA$_i$) was cloned into *pTetUPKO* plasmid, which allows the selection of transgenic parasites with FUDR (5 μM) for stable integration at the *Tg*UPRT locus. In the next step, the 1kb of 5'- and 3'-UTRs of *Tg*PSS were introduced into *pTKO-DHFR-TS* flanking the resistance cassette, and the *NotI*-linearized construct was transfected into the *Δku80*-TaTi strain of *T. gondii* expressing the *Tg*PSS-HA$_i$ (merodiploid). Stable parasites were selected with 1 μM pyrimethamine and cloned by limiting dilution. **(B)** Recombination-specific PCR using *Tg*PSS-5'Scr-F/DHFR-R and DHFR-F/*Tg*PSS-3'Scr-R revealed 5'- and 3'-crossovers in the *Δtgpss/Tg*PSS-HAi mutant, but none in the in the plasmid or in the parental gDNA.

The regulation of the *Tg*PSS expression by aTC was analized at the mRNA level by quantitative RT-PCR (Fig. 35A). Interestingly, the *Δtgpss*/*Tg*PSS-HA$_i$ showed ~8-fold overexpression of *Tg*PSS mRNA in the absence of aTC, which was downregulated after 6 days in the presence of 1 μM aTC to about 3-fold less the parental levels. *Tg*PTS transcript levels were not significantly influenced neither by the aTC treatment nor the *Tg*PSS gene deletion, although there was a slight increase (~1.8-fold) at the *off* state of the *Δtgpss*/*Tg*PSS-HA$_i$ mutant.

In the same way, the regulation of the *Tg*PSS-HA$_i$ protein was confirmed by western blot (Fig. 35B), where *Tg*Hsp90 served as a loading control. Two protein bands were observed, one of about 62 KDa, corresponding to the expected full-length size of *Tg*PSS-HA and a shorter one of about 45 KDa, both of which were regulatable by aTC. The full-length *Tg*PSS (blue rectangle, Fig. 35B) was downregulated after 2days in aTC and was almost undetectable after 4 days in presence of the drug. Upon removal of aTC, *Tg*PSS-HA was rapidly recovered, indicating the specificity of the drug treatment for the control of *Tg*PSS-HA expression in the *Δtgpss*/*Tg*PSS-HA$_i$ strain. Interestingly, however, there was an additional 40 KDa protein band which remained resistant to aTC regulation. Immunofluorescence assays revealed the expected perinuclear localization (endoplasmic reticulum) of the inducible HA-tagged copy of *Tg*PSS, and also confirmed its regulation in the presence of anhydrotetracycline (aTC) (Fig. 35C).

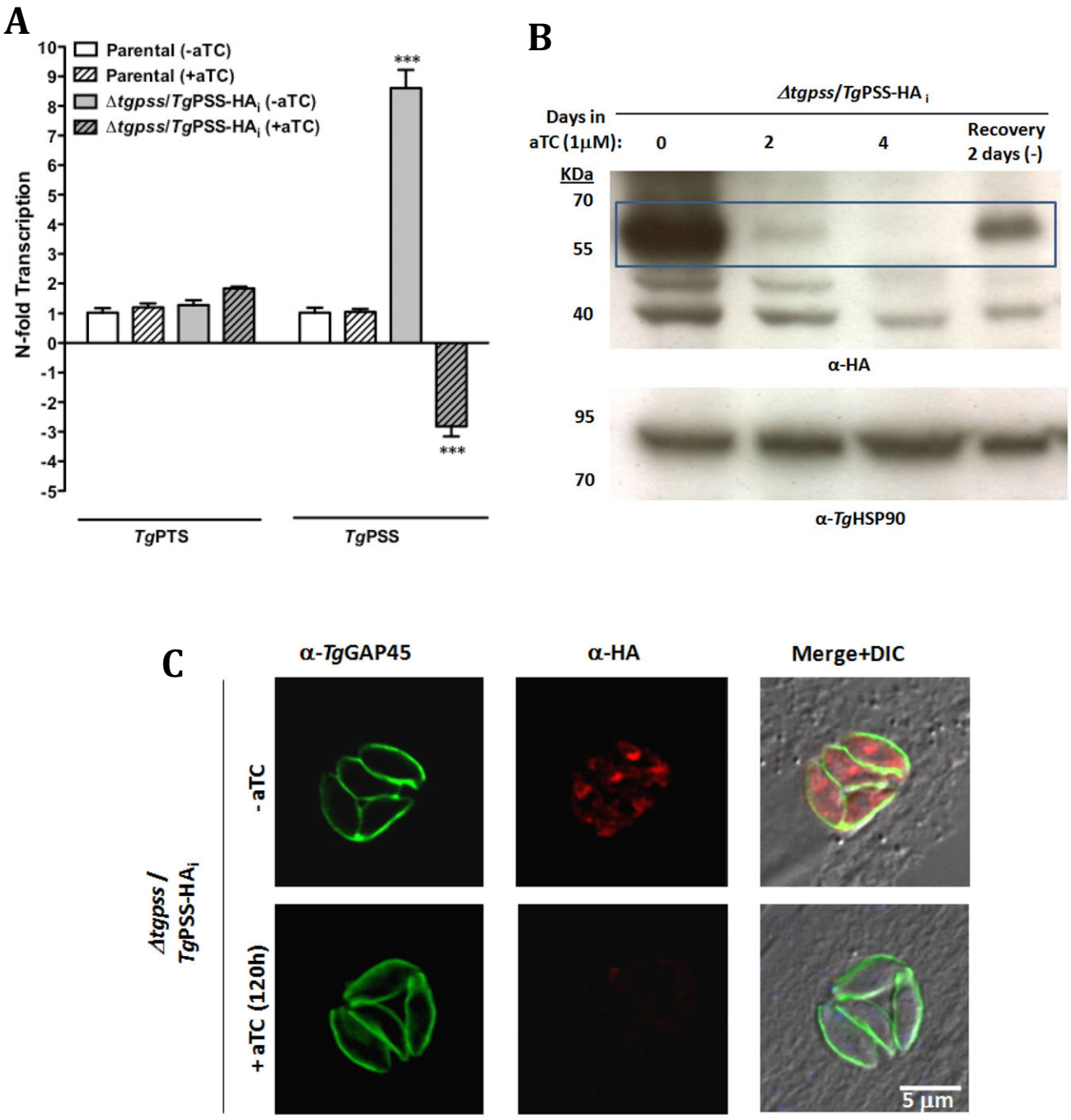

Fig. 35. *Regulation of a tetracycline-inducible TgPSS knockdown in T. gondii.* **(A)** Transcription-fold changes of *Tg*PTS and *Tg*PSS in the parental *(Δku80*-TaTi) or mutant *(Δtgpss*/*Tg*PSS-HA$_i$) grown in absence or presence of 1 μM anhydrotetracycline (aTC) for 6 days. (n = 3; ***, $p < 0.001$). Error bars, S.E. **(B)** Western-blot analysis of aTC dependence of *Tg*PSS-HAi protein levels. Blue rectangle encases expected band of ~62 KDa (upper panel). *Tg*HSP90 was used as a loading control (lower panel). **(C)** Representative immunofluorescence images showing regulation of *Tg*PSS-HA$_i$ staining by aTC (1μM).

The growth of the *Δtgpss*/*Tg*PSS-HA$_i$ strain was then evaluated by plaque assays. There was no difference in none of the conditions regarding the number of plaques (Fig. 36B), which would suggest a similar ability to invade/egress from the host cell. The size of the plaques, however, was only about 76% the size of the parental for the *Δtgpss*/*Tg*PSS-HA$_i$ in the *on* state (without aTC, Fig. 36C). Unexpectedly, the addition of aTC and the consequent downregulation of *Tg*PSS caused a recovery, rather than a decrease in the plaque size (~94%), which was further increased upon pre-incubation for 5 days before setting up the plaque assay (~110%). Our further work showed that the growth defect of *Δtgpss*/*Tg*PSS-HA$_i$ parasites at the *on* state of *Tg*PSS expression was due to a slower intracellular replication as deduced by a lower proportion of bigger vacuoles (with 16 parasites) and a correspondent increase in smaller vacuoles (with 4 parasites) when aTC was present in culture (Fig. 36D).

Summing up, these results show that the overexpression of *Tg*PSS under the foreign *pTetO7sag1* promoter, but not the knockdown of full-length *Tg*PSS affects negatively the parasite growth, in particular by slowing down the intracellular replication of *T. gondii*.

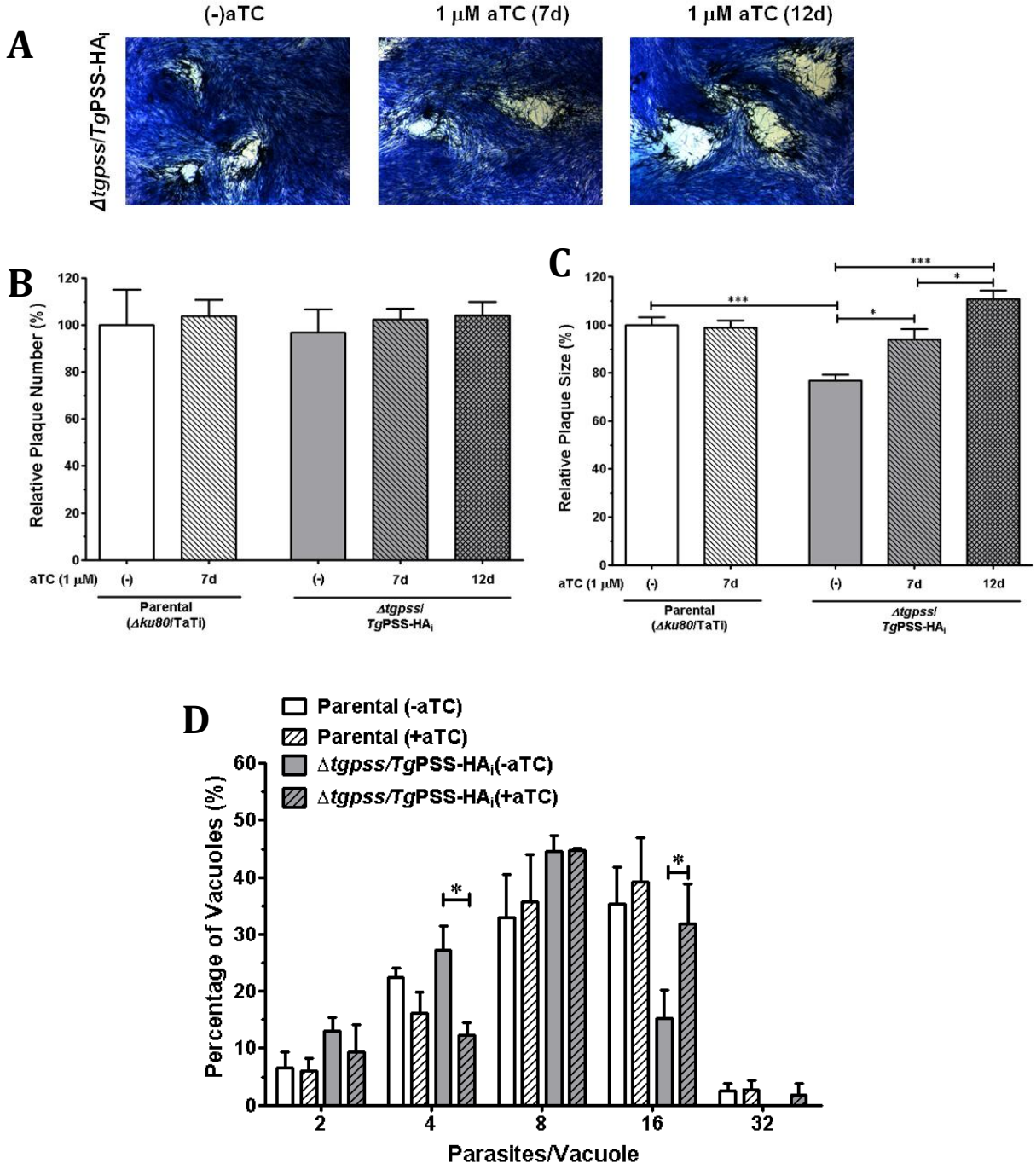

Fig. 36. *In vitro growth phenotype of conditional knockdown of TgPSS.* **(A)** Representative plaques formed by the *Δtgpss*/*Tg*PSS-HA$_i$ mutant in absence or presence for 7 or 12 days of aTC. Number **(B)** and size **(C)** of plaques formed by indicated strains in presence or absence of aTC (1μM). Notice enhanced growth of the mutant upon prolonged incubation in aTC. **(D)** Replication assays showing the number of parasites per vacuole 30 h post-infection. (n = 3 assays; *, p<0.05; **, p < 0.01; ***, p < 0.001). Error bars, S.E.

3.2.4. The endogenous synthesis and the content of phosphatidylserine are decreased, but not abolished upon conditional knockdown of *Tg*PSS

To analyze the effect of *Tg*PSS knockdown on the autonomous PtdSer synthesis of *T. gondii*, the incorporation of ^{14}C-Ser into lipids of extracelluar parasites was studied. Next, parasite lipids were resolved by one-dimensional TLC (chloroform/ethanol/water/triethylamine (30/35/7/35, v/v). Major lipid bands were identified by co-migration with authentic standards and silica was scrapped to measure radioactivity by liquid scintillation counting. Incorporation of [14C]-serine into total parasite lipids at the *off* state of the *Δtgpss*/*Tg*PSS-HA$_i$ strain was decreased ~20% compared to the parental strain and about the half when compared to the *on* state in the absence of aTC, which showed in turn an increase of about 50% incorporation compared to the parental control (Fig. 37B). These results correlated with a ~30% decrease in the PtdSer synthesis of *Δtgpss*/*Tg*PSS-HA$_i$ strain at the *off* state compared to the parental. On the other hand, the *Δtgpss*/*Tg*PSS-HA$_i$ mutant also showed an increase in the incorporation of 14C-Ser into PtdSer at the *on* state, matching the observed increase in total lipids. Interestingly, incorporation of 14C-Ser into PtdEtn by PtdSer decarboxylation (Hartmann et al., 2014) remained unaltered upon *Tg*PSS knockdown, despite a decrease in the active synthesis of PtdSer. However, at the *off* state, when *Tg*PSS is overexpressed, PtdEtn decarboxylation was increased to almost the double the parental level (Fig. 37C-D).

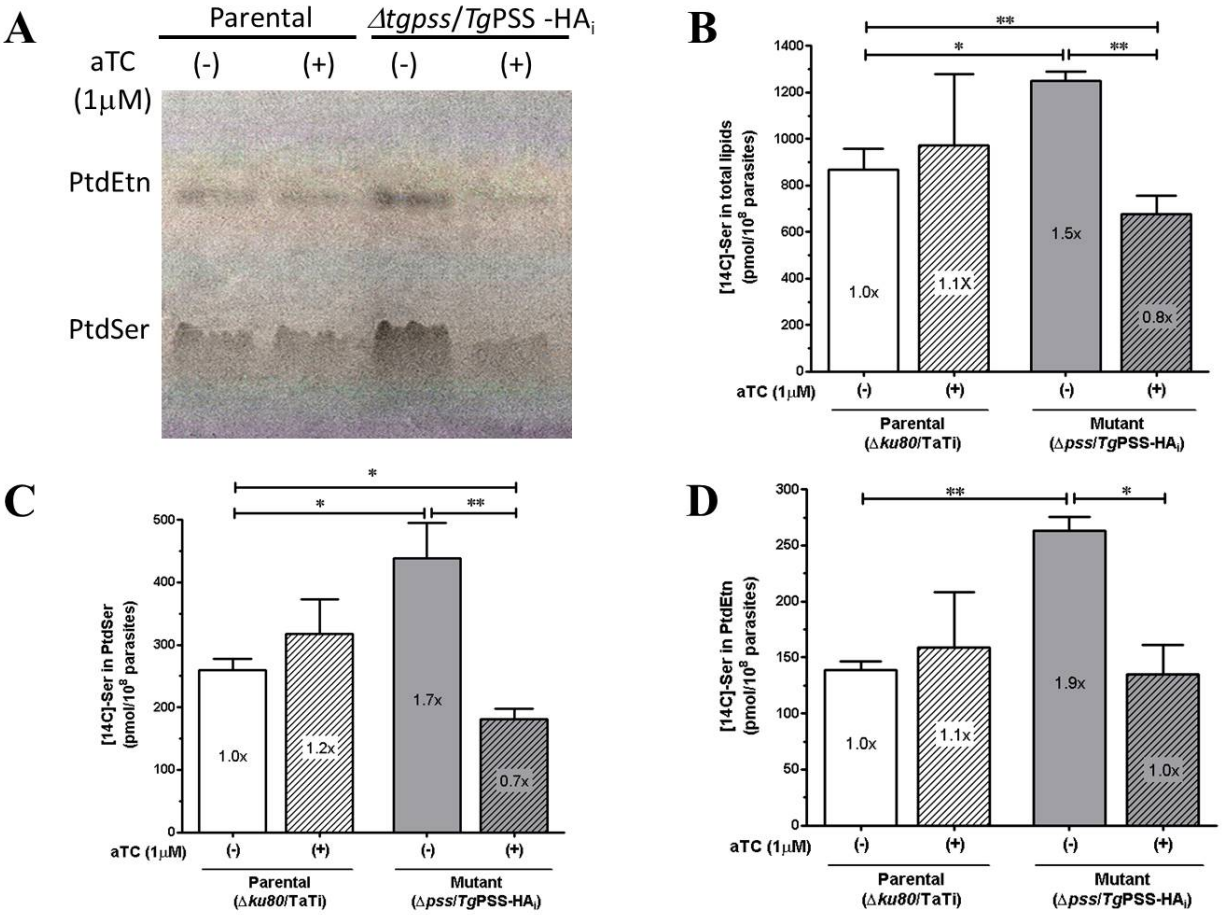

Fig. 37. *Conditional knockdown of TgPSS downregulates PtdSer synthesis in T. gondii*. **(A)** Autoradiography of TLC-resolved lipids of freshly syringe-released extracellular tachyzoites of the indicated strains labeled with ^{14}C-Serine (2 μCi, 2hrs, 37°C, 5x10^7 parasites each). Solvent system used was chloroform/ethanol/water/triethylamine (30/35/7/35, v/v). (**B)** Incorporation of ^{14}C-Serine into total lipid fraction of parental and mutant strains pre-cultured in absence or presence of aTC. **(C, D)** Individual phospholipid bands from A were scraped for scintillation counting, and incorporation of ^{14}C-Ser was determined (n = 4 assays; *, p<0.05; **, p < 0.01; ***, p < 0.001). Error bars, S.E.

Next, the lipid composition of the *Δtgpss*/*Tg*PSS-HA$_i$ mutant was analyzed and compared to the parental in absence or presence of aTC (for at least 6 days) by chemical phosphorus assay of 2D-TLC-resolved lipids (Rouser et al., 1970). Figure 38 illustrates that most major phospholipids, including PtdThr, remained unaltered. PtdSer, however, was reduced to 70% of the parental level upon conditional knockdown of *Tg*PSS. In contrast, at the *on* state, PtdSer was incremented to 134% of the parental level.

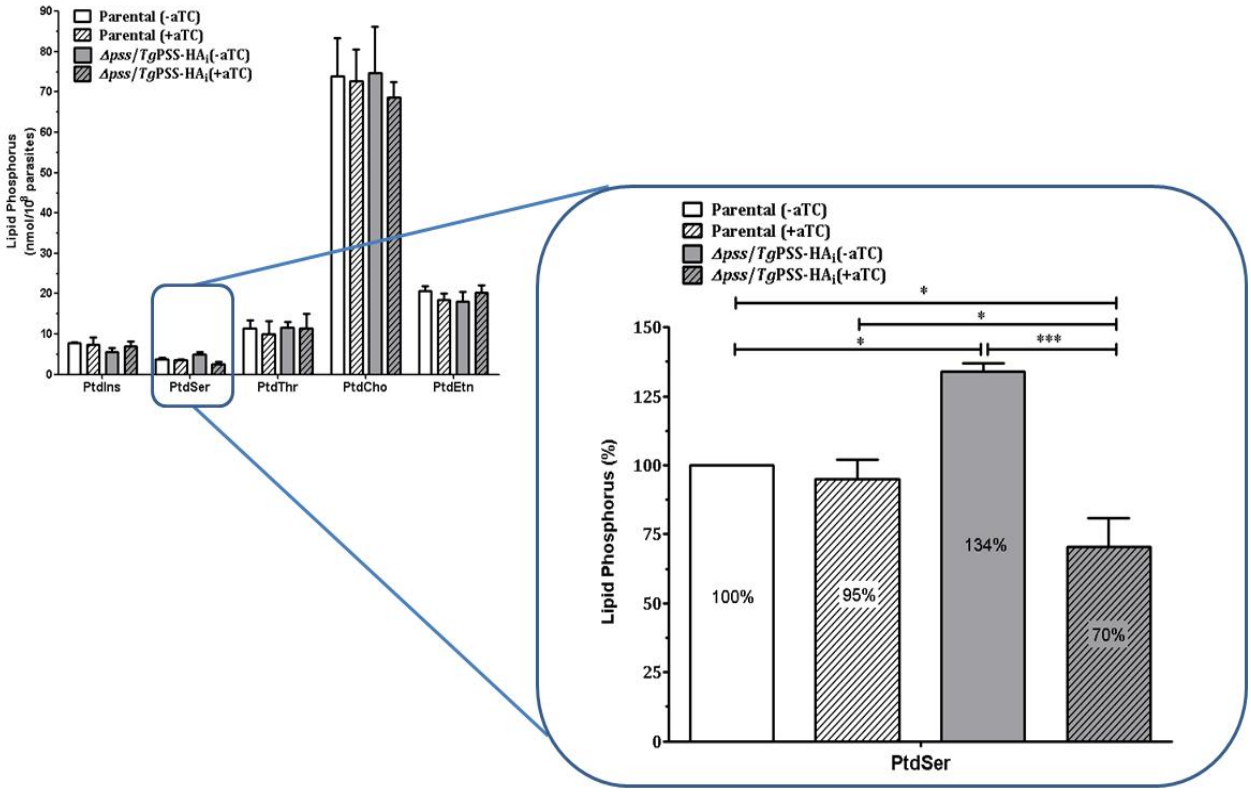

Fig. 38. *Conditional knockdown of TgPSS does not abolish PtdSer content of T. gondii*. Lipid phosphorus assays of the annotated strains. Zoom window of the relative phosphatidylserine content shows a 30% reduction in the *Δtgpss*/*Tg*PSS-HA$_i$ strain in presence of aTC and a 34% increase at the *on* state in absence of the drug. No significant changes were observed in the parental strain or in other major phospholipid classes. (n = 3 assays; *, p<0.05; **, p < 0.01; ***, p < 0.001). Error bars, S.E.

These results correlate tightly with the above-described alterations in the endogenous PtdSer synthesis, confirming the PtdSer synthase activity of *Tg*PSS. They also suggest that the major contribution of the PtdSer pool of *T. gondii* is produced by the parasite itself, rather than scavenged from the host cell, nevertheless this last possibility cannot be discarded. They also indicate that PtdSer can be safely decreased up to 30% without impairing the parasite growth (Fig. 36B). On the other hand, despite a major knockdown of *Tg*PSS, the parasite is still able

to produce most of the PtdSer it needs. The short 40 KDa protein which was not repressed by aTC (Fig 35B) may contribute to most of the PtdSer synthase activity when the full-length protein is absent.

3.2.5. Conditional degradation of *Tg*PSS demonstrates its PtdSer synthase activity and control over PtdSer content in *T. gondii*

Due to the observed deleterious effect of *Tg*PSS overexpression under the conditional promoter used in our tetracycline-induced knockdown and the modest reduction in PtdSer synthesis and content, we resorted to a conditional protein destabilization approach, which does not depend on foreign promoter elements as the tetracycline system (Striepen, 2007). To this end, the C-teminal end of the endogenous *Tg*PSS locus was tagged with an FKBP-destabilization domain (DD) in addition to a double hemagluttinin (2HA) epitope, by single homologous recombination (Fig. 39A). The destabilization domain targets either N- or C-terminal tagged proteins to the proteasome where they are rapidly degraded unless a small ligand (Shield1) binds to this domain and avoids their recruitment to the proteasome (Banaszynski et al., 2006; Hartmann et al., 2013; Herm-Götz et al., 2007). Stable transgenic parasites were selected with 1 μM pyrimethamine for 1 week. Positive recombinant clones expressing the 2HA-DD tagged *Tg*PSS were obtained by serial dilution and identified by immunofluorescence assay (Fig. 39B). Parasites were constantly maintained in medium with 0.5 μM of the small ligand Shield1 (Shld-1), unless stated otherwise. Effective and rapid targeting of *Tg*PSS-2HA-DD to proteasomal degradation in absence of Shld-1 was confirmed by IFA and western blotting (Fig. 39B-C).

Next, we proceeded to characterize the growth phenotype of endogenous *Tg*PSS destabilization by means of plaque assays (Fig. 39D). Neither the plaque size nor the plaque number were significantly different in absence or presence of Shld-1, indicating no major effect of *Tg*PSS destabilization on the *in vitro* growth of *T. gondii*. These results agreed to those found in our tetracycline-induced knockdown system. They also confirmed no toxic effect of Shield1 upon prolonged incubation at the dose used in this study. However, when the intracellular replication of the *Tg*PSS-HA-DD strain was evaluated by immunofluorescence assay, there was a slight shift towards smaller vacuoles in absence of Shld-1, suggesting a minor replication defect when *Tg*PSS is destabilized.

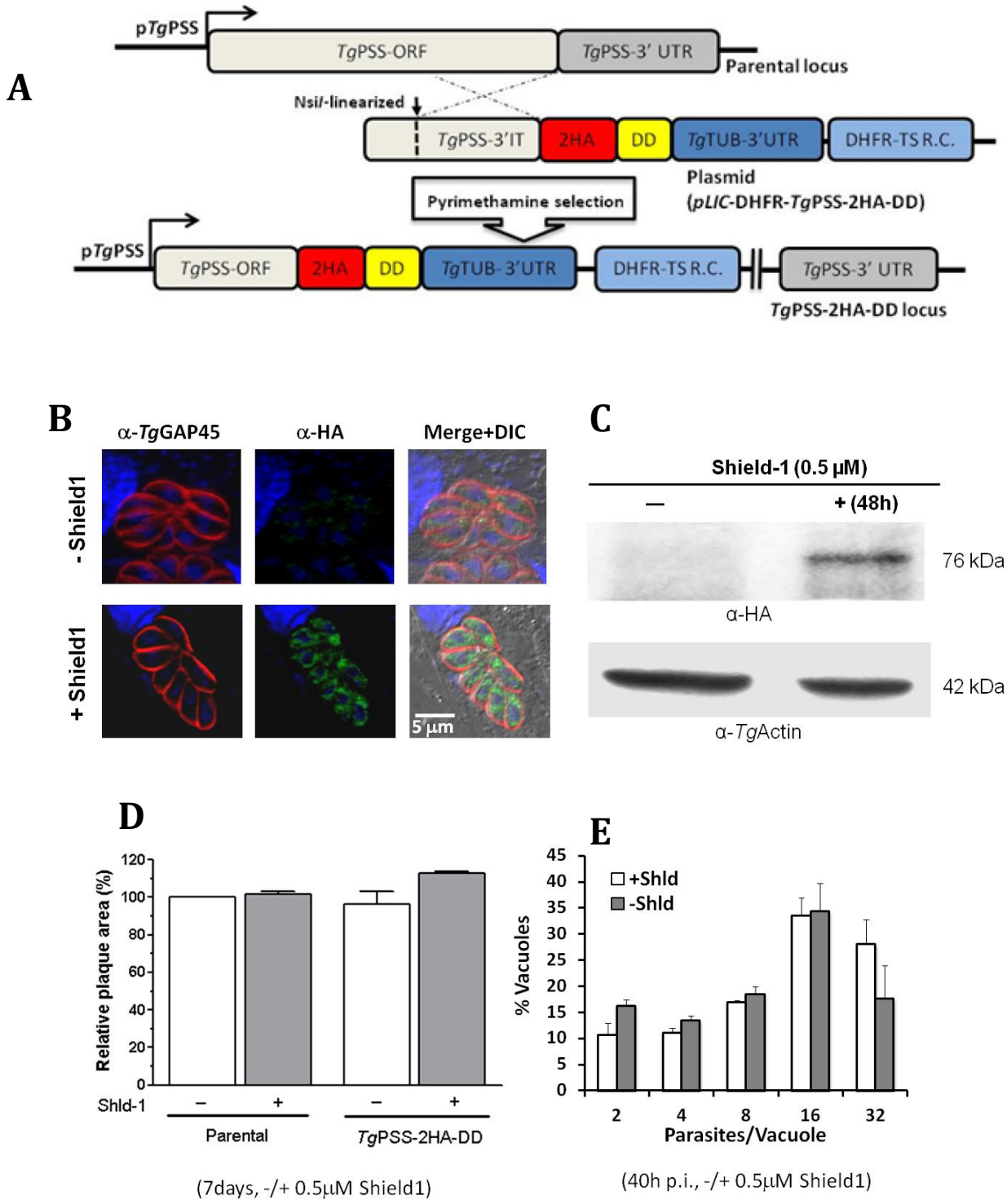

Fig. 39. *Conditional destabilization of endogenous TgPSS does not alter significantly the parasite growth.* **(A)** Scheme showing the strategy for tagging the *Tg*PSS locus with a C-terminal hemaglutinin-destabilization domain fusion (2HA-DD) epitope by single homologous recombination. Regulation of *Tg*PSS protein levels by Shield 1 as detected by immunofluorescence **(B)** and Western Blot **(C)**. Parasite growth of the parental *(Δku80-TaTi*) and transgenic (*Tg*PSS-2HA-DD) strains as assessed by plaque **(D)** and replication **(E)** assays. (n=3 assays).

Subsequently, the synthesis of PtdSer by extracellular parasites was evaluated. As seen in Figure 40, destabilization of *Tg*PSS in absence of Shield-1 caused a ~55% decrease in incorporation of ^{14}C-Serine into total parasites lipids, and particularly into PtdSer (~70%) and PtdEtn (~64%) via PtdSer decarboxylation compared to the parental strain. These alterations were fully reversible when *Tg*PSS-HA-DD parasites were treated with Shield-1 for 42hrs before and during metabolic labeling (2 hrs). On the other hand, Shield-1 did not have any effect on the incorporation of ^{14}C-Serine by parental (*Δku80/TaTi*) parasites.

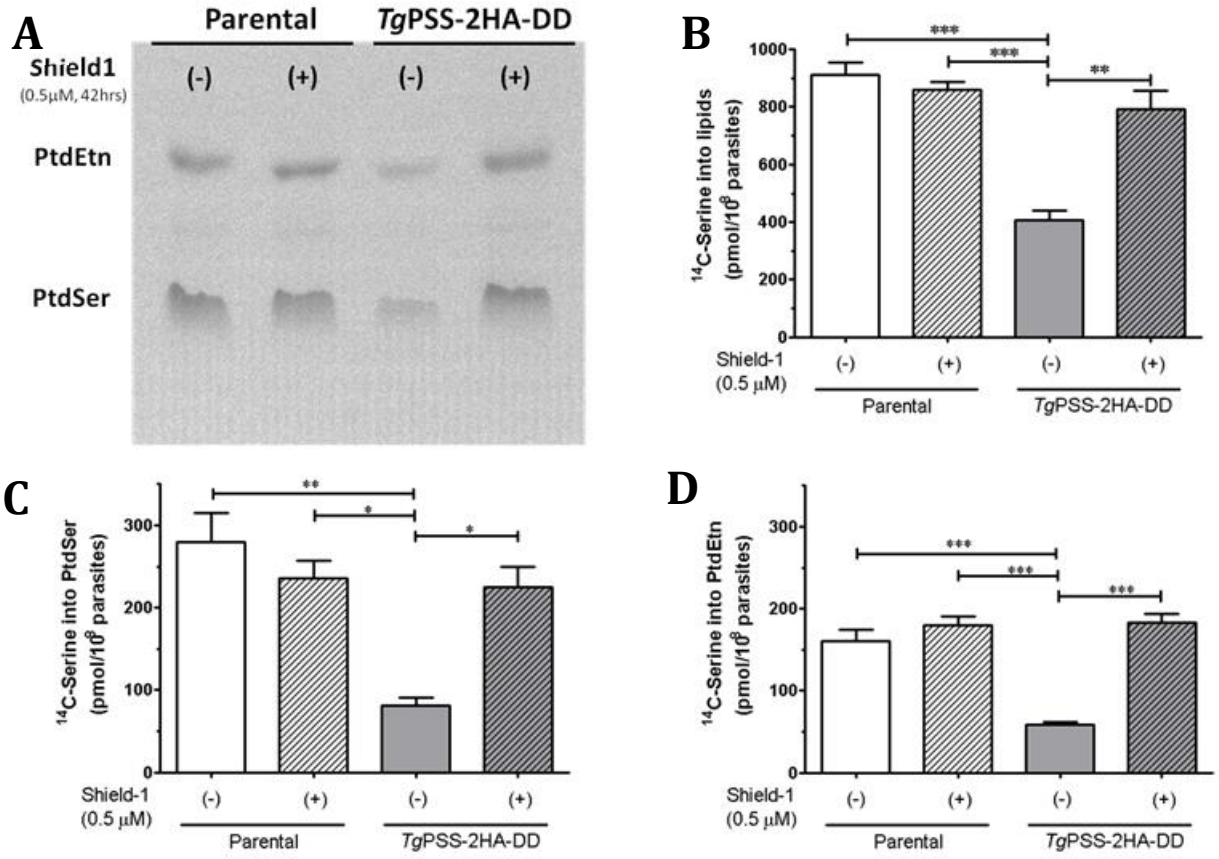

Fig. 40. *Conditional destabilization of TgPSS downregulates PtdSer synthesis in T. gondii*. **(A)** Autoradiography of TLC-resolved lipids of freshly syringe-released extracellular tachyzoites of the indicated strains labeled with ^{14}C-Serine (2 μCi, 2hrs, 37°C, 5x10^7 parasites each). Solvent system used was chloroform/ethanol/water/triethylamine (30/35/7/35, v/v). Individual phospholipid bands were identified by co-migration of authentic standards. **(B)** Incorporation of ^{14}C-Serine into total lipid fraction of parental and transgenic strains pre-cultured in absence or presence of Shield-1. **(C, D)** Individual phospholipid bands from (A) were scraped for scintillation counting, and incorporation of ^{14}C-Ser was determined (n = 3 assays; *, p<0.05; **, p < 0.01; ***, p < 0.001). Error bars, S.E.

This decrease in PtdSer synthesis in the *Tg*PSS-2HA-DD strain in absence of Shield1 was mirrored by a similar drop of PtdSer content compared to the parental strain, (2.2% vs. 5% of total phospholipids, Fig. 41).

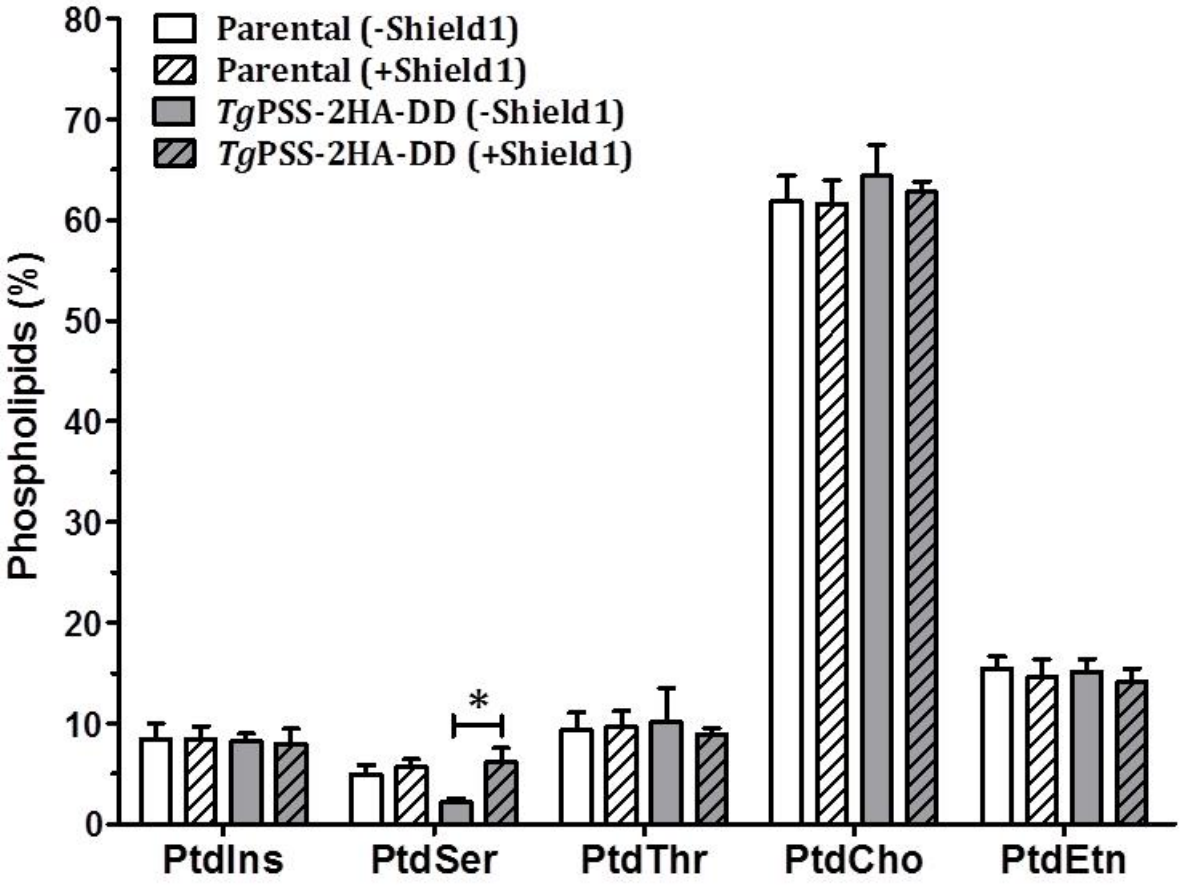

Fig. 41. *Conditional degradation of TgPSS specifically downregulates PtdSer content in T. gondii.* Phosphorous assays showing the content of major phospholipid classes of the indicated strains in absence or presence of Shield1. Notice lack of effect of the drug in the parental strain, but reduced PtdSer content in its absence for the *Tg*PSS-2HA-DD strain.

3.3. Amplified PtdSer content is not involved in the phenotype of *Δtgpts* parasites

To further address the increase in PtdSer synthesis and content observed when PtdThr is depleted in *T. gondii* as a possible compensatory mechanism and to discard its effect on the *Δtgpts* phenotype, we targeted the 2HA-DD tag to the *Tg*PSS locus of the *Δtgpts* strain as described above (Fig. 42A). Shield1-regulation of *Tg*PSS protein was also achieved in the *Δtgpts* background as shown by immunofluorescence and western blot analysis (Fig. 42B-C).

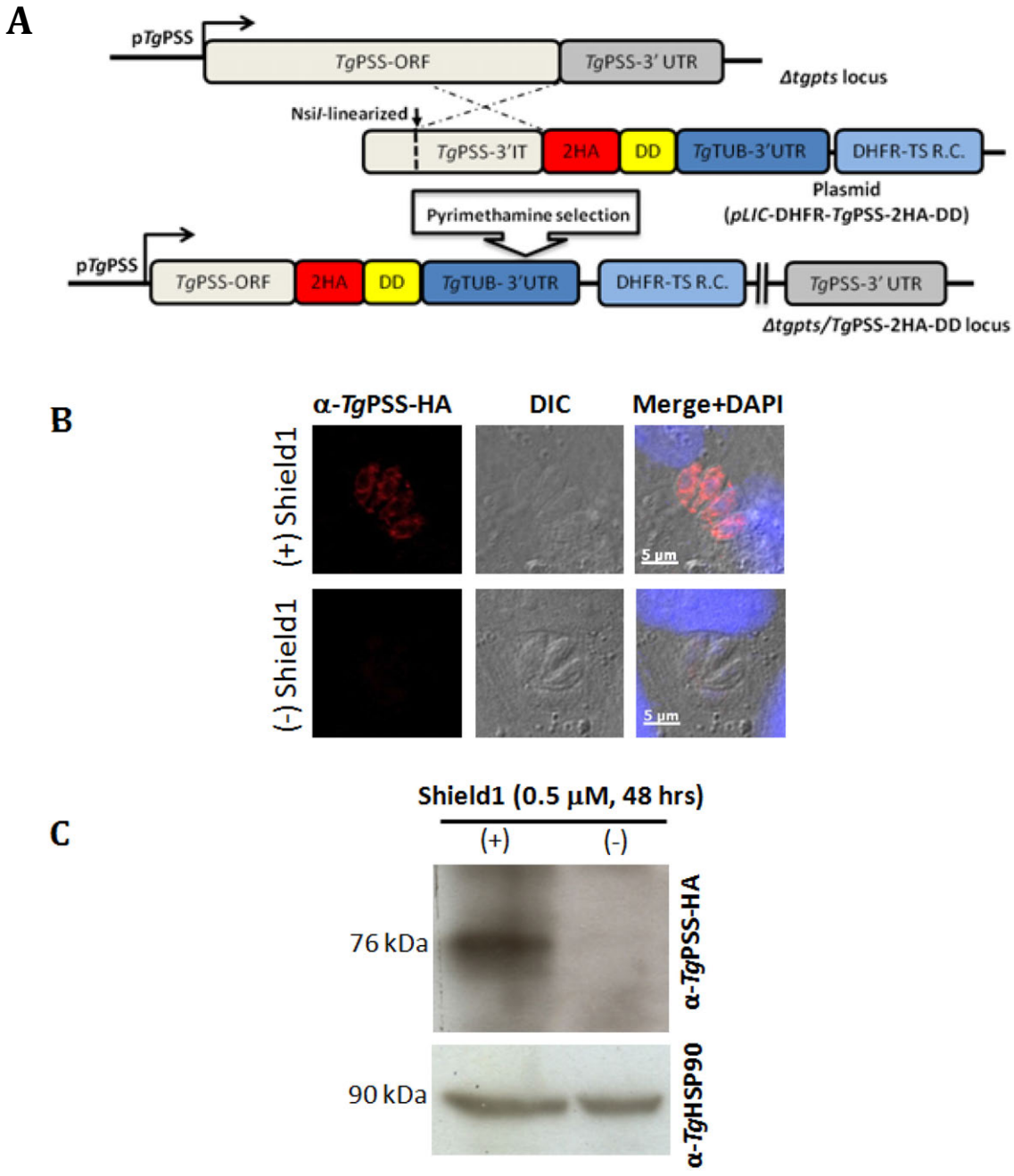

Fig. 42. *Protein regulation of TgPSS by a conditional destabilization approach in Δtgpts background*. **A.** The endogenous *Tg*PSS locus of the *Δtgpts* strain was C-terminally tagged with a DD-2HA epitope by single homologous recombination. Selection of recombinant parasites was done by pyrimethamine resistance. Shield1-control of *Tg*PSS was assessed by immunofluorescence **(B)** and western blot **(C)** analysis.

The biochemical characterization of the *Δtgpts*/*Tg*PSS-2HA-DD strain also showed a proportionate decrease in the incorporation of ^{14}C-serine into total lipids (Fig. 43B). In particular PtdSer synthesis returned to about the same levels of the parental strain (Fig. 43A, C). Concurrently, there was also a proportionate decrease in the PtdSer decarboxylation as measured by the incorporation of ^{14}C-serine into PtdEtn (Fig. 43A, D). These changes were mirrored in the phospholipid composition of the double mutant (*Δtgpts/Tg*PSS-2HA-DD) in absence of Shield with a significant drop in the PtdSer content down to the parental levels (Fig 43E). Interestingly, there was a concurrent increase in the PtdIns levels, another major anionic phospholipid, but no alteration in PtdEtn amount, despite the observed decrease in decarboxylation (Fig. 43E).

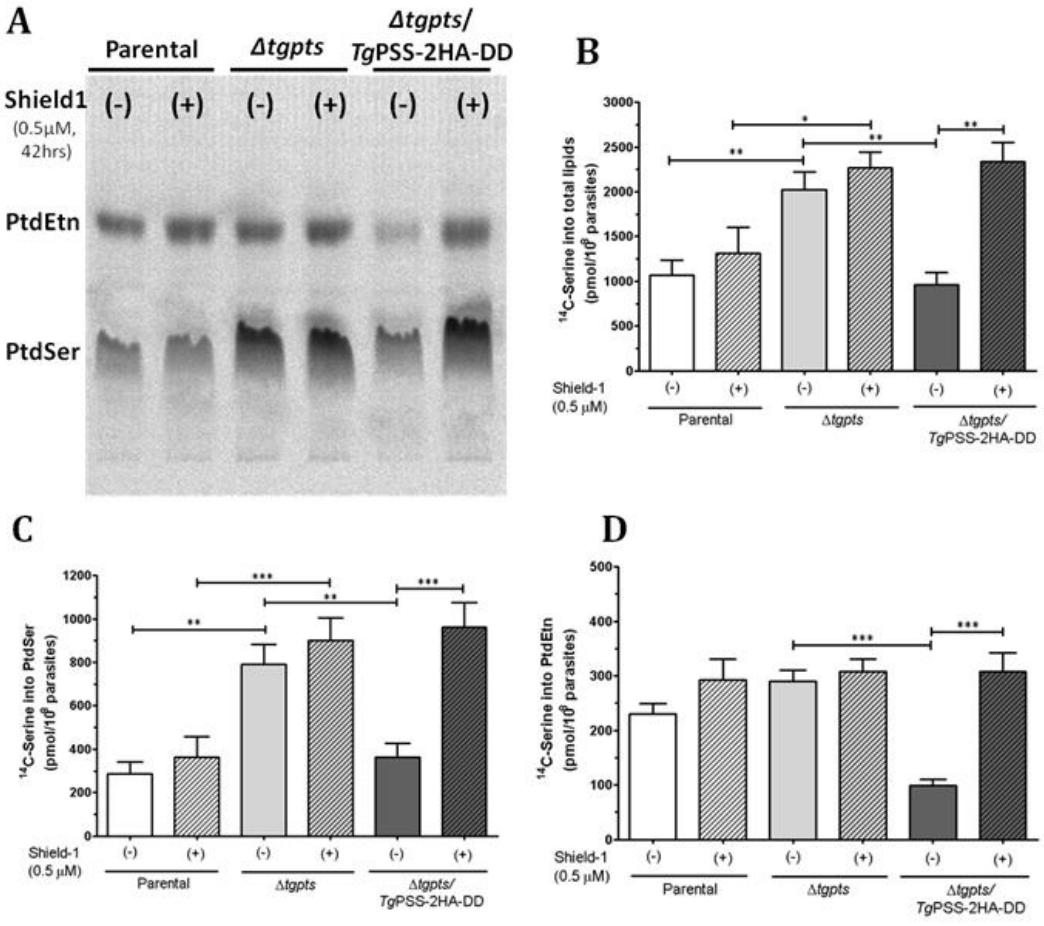

E

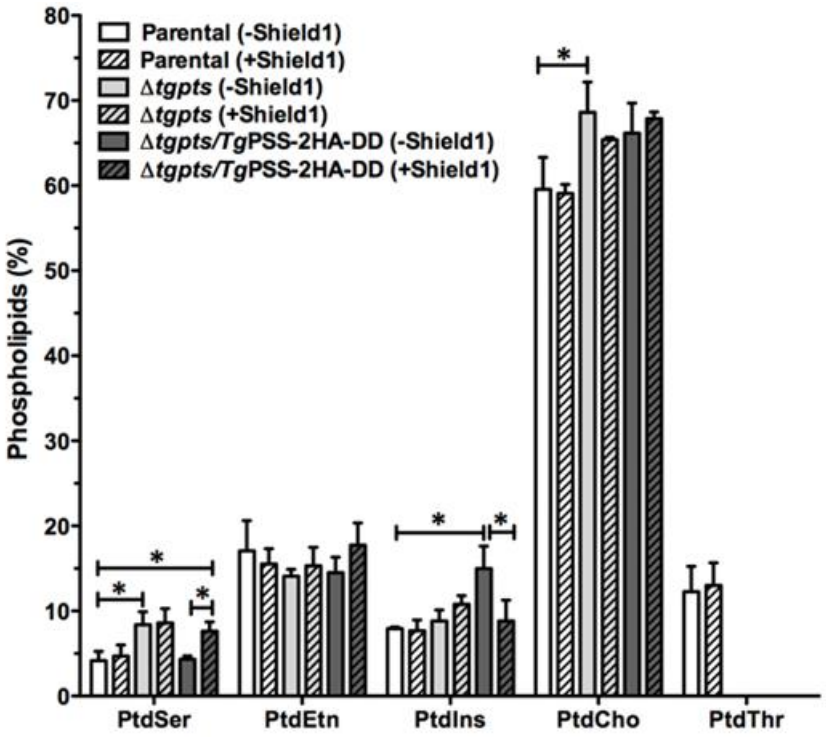

Fig. 43. *Conditional destabilization of TgPSS returns PtdSer synthesis and content to parental levels in PtdThr-deficient parasites*. **(A)** Autoradiography of TLC-resolved lipids of freshly syringe-released extracellular tachyzoites of the indicated strains labeled with ^{14}C-Serine (2 µCi, 2hrs, 37°C, 5x10^7 parasites each). Solvent system used was chloroform/ethanol/water/triethylamine (30/35/7/35, v/v). Individual phospholipid bands were identified by co-migration of authentic standards. **(B)** Incorporation of ^{14}C-Serine into total lipid fraction of parental and transgenic strains pre-cultured in absence or presence of Shield-1. Individual phospholipid bands from (A) were scraped for scintillation counting, and incorporation of ^{14}C-serine was determined for PtdSer **(C)** and PtdEtn **(D)**. **(E)** Total lipids of the indicated strains and conditions (0.8-1x10^8 parasites harvested after 40-48h in presence or absence of Shield1) were resolved by two-dimensional thin layer chromatography in chloroform/methanol/ammonium hydroxide (65/35/5, v/v) and chloroform/acetic acid/methanol/water (75/25/5/2.2, v/v), visualized by iodine vapor staining, and then subjected to phosphorus measurements of lipid bands (n = 3 assays; *, $p<0.05$; **, $p < 0.01$; ***, $p < 0.001$). Error bars, S.E..

Assessment of the growth phenotype by plaque assay did not show any further alteration in absence of Shield1 (Fig. 44), when *Tg*PSS and PtdSer levels are largely decreased. These results indicate that the upregulation of PtdSer synthesis and content observed in the *Δtgpts* mutant is not responsible for its defective lytic cycle.

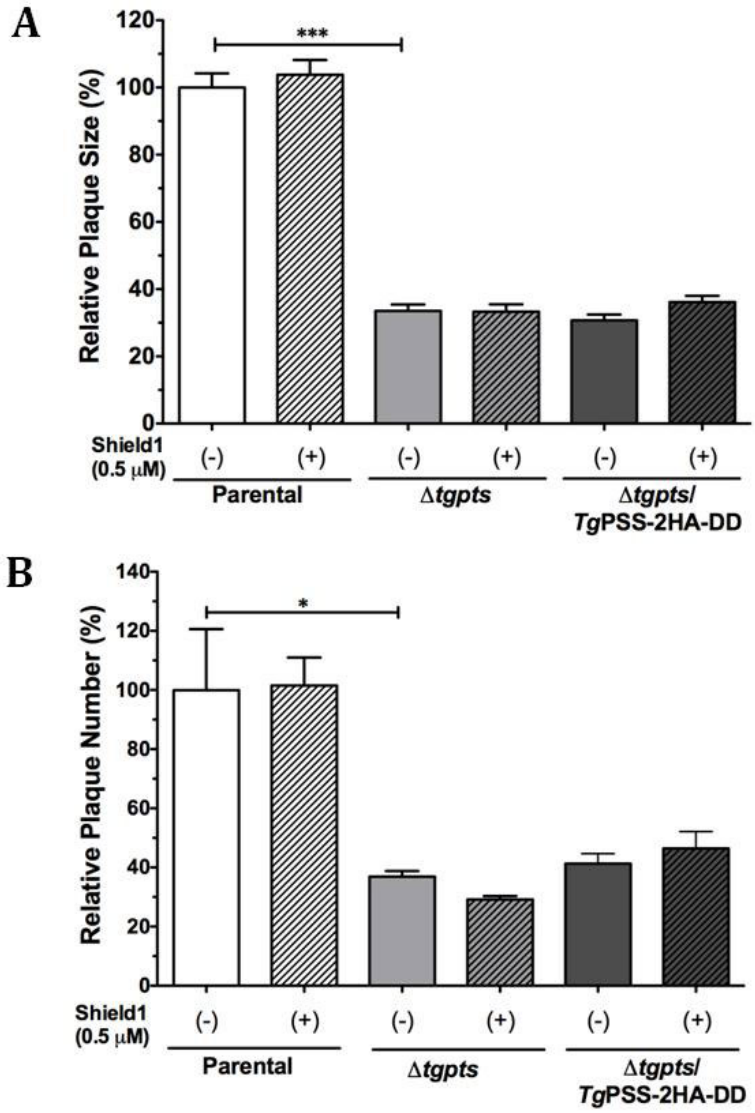

Fig. 44. *Elevated PtdSer synthesis and content are not responsible for defective growth of Δtgpts strain*. Quantification of the *in vitro* growth of the indicated strains in presence or absence of Shield1, as determined by the relative size **(A)** and number **(B)** of plaques formed. Error bars indicate the mean ± SEM (n=3; *p<0.05, **p<0.01, ***p<0.001).

3.4. Distribution of PtdSer in *T. gondii*

Lact-C2-GFP ORF was amplified from the pEGFP-Lact-C2 plasmid (Addgene) and cloned into *pGRA2-UPKO*. Tachyzoites were transiently transfected with the *pGRA2-UPKO-Lact-C2-GFP* plasmid to study the distribution of phosphatidylserine in the parental and *Δtgpts* strains. In Figure 45 we can see different localization patterns of the PtdSer probe for both strains, while about 80% of the *Δtgpts* parasites showed an almost exclusive plasma

membrane localization of PtdSer, for the parental strain this fraction corresponded to only 60% and showed a higher proportion of parasites with the more complex internal pattern, including vesicle-, ER- and Golgi-like structures, likely involved in the endocytic/secretory pathway of *T. gondii*. A similar pattern for PtdSer distribution, using a Lact-C2-GFP probe, has been described for other eukaryotic cells, like yeast and macrophages, where it is thought to regulate the sorting of cationic proteins (Yeung et al., 2008). The observed increase of the surface-only pattern in the mutant parasites may be a consquence of the augmented amount of PtdSer of this strain, which would be mostly targeted to the plasma membrane to maintain a normal membrane potential, given the loss of PtdThr, one of the main anionic phospholipids in *T. gondii*. Alternatively, it may be possible that Lact-C2-GFP has a minor affinity for PtdThr and that the loss of internal-type fluorescence in the mutant is due to the loss of this lipid, which would be predominantly localized in the ER. Future studies with pure PtdThr liposomal preparations should help know if Lact-C2-GFP shows indeed this affinity and if it can be improved by site-directed mutagenesis to be used as an exclusive PtdThr probe for dynamics studies on the behavior of this lipid during signaling or vesicle transport events.

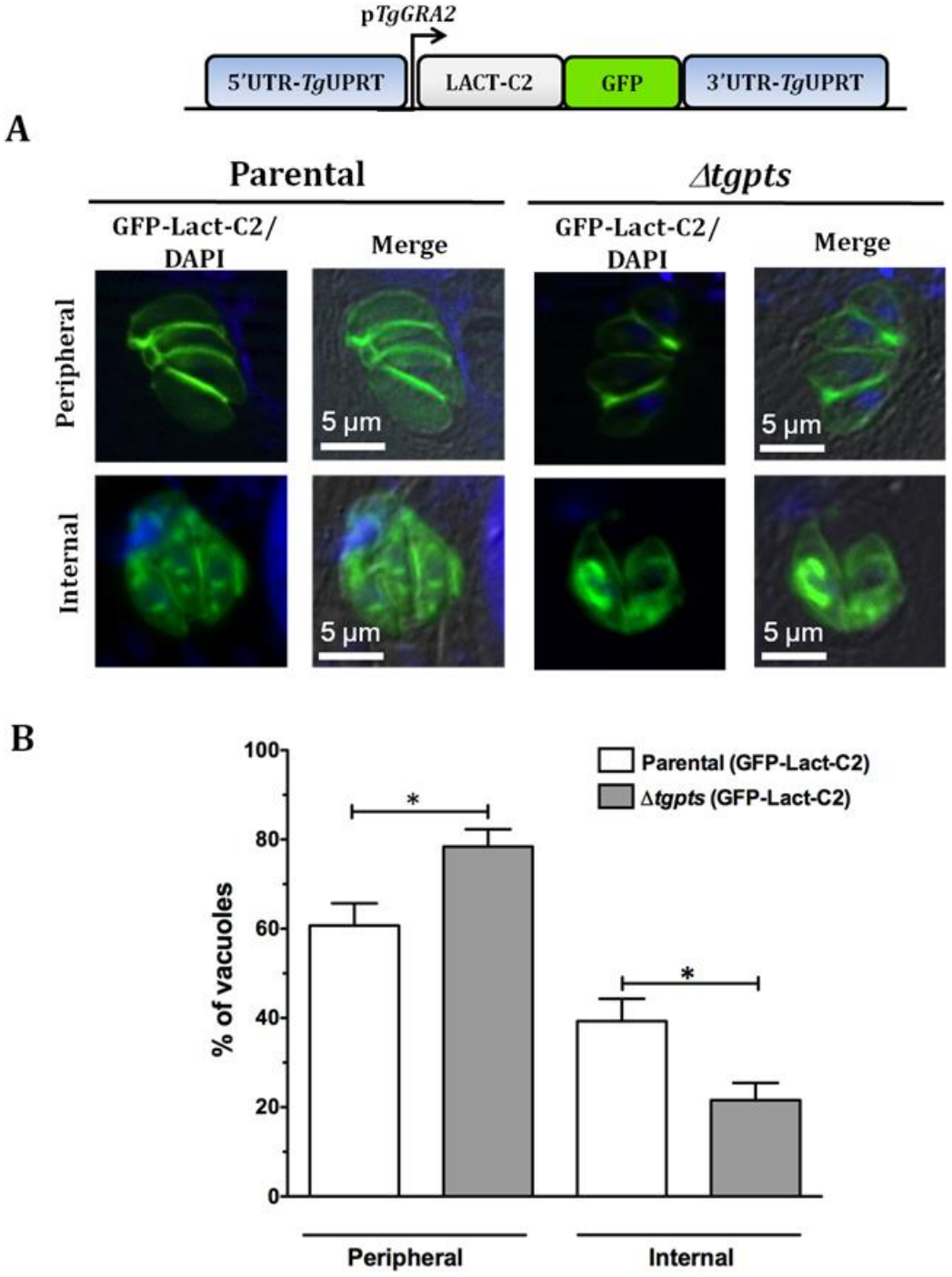

Fig. 45. *Distribution of PtdSer pool is altered in Δtgpts parasites.* **A**. Representative epifluorescence images showing localization of the PtdSer probe GFP-Lact-C2 (Yeung et al. 2008) in parental and *Δtgpts* intracellular parasites. Notice exclusive plasma membrane localization pattern of GFP fluorescence compared to more complex internal perinuclear and vesicle-like pattern in both strains. **B.** Quantification of observed fluorescence patterns in GFP-Lact-C2-expressing parasite vacuoles of parental and *Δtgpts* strains. (n=3 independent transient transfections; *$p<0.05$). Error bars indicate the mean ± SEM.

4. Discussion

4.1. PtdSer and PtdThr pathways of *Toxoplasma gondii*

PtdSer is the third most abundant phospholipid in eukaryotic cells (~10%) after PtdCho and PtdEtn. It is a very important lipid, whose functions extend to apoptosis (Fadok et al., 1992; Li et al., 2003), membrane potential (Leventis and Grinstein, 2010), protein sorting and secretion (Uchida et al., 2011) and as a precursor of other phospholipids (Gupta et al., 2005; Vance, 2008; Voelker, 1984). Many of the PtdSer functions depend on the acidic nature and negative charge of this phospholipid, which allows it to associate with calcium ions and cationic proteins, and to help in the maintenance of the membrane potential at the inner leaflet of the plasma membrane (Leventis and Grinstein, 2010). A vital role for PtdSer has been shown in many species like mammals (Kuge et al., 1997) and plants (Yamaoka et al., 2011), which cannot survive in the absence of PtdSer synthesis. PtdSer levels in *T. gondii* were however very low (<5%), and instead an otherwise rare analogue, PtdThr, was present and was the most abundant anionic phospholipid in *T. gondii* (Figs. 19, 38, 41, 43). Our work managed to identify *Tg*PTS as the sole parasite enzyme responsible for the synthesis of PtdThr in *T. gondii*. The relationship between the functions of both analog phospholipids for the parasite morphology and membrane biogenesis is shown by the fact that the parasites lacking *Tg*PTS and therefore PtdThr, replicate at a normal rate and maintain a normal organelle morphology, including endoplasmic reticulum, micronemes, rhoptries and mitochondria (Appendix 6), and increase proportionally its PtdSer levels (Fig. 19B). Additionally the reversible increase in PtdCho content upon PtdThr depletion in *T. gondii* (Fig. 19B) suggests PtdCho as the substrate of the base-exchange reaction catalyzed by *Tg*PTS. A proposed scheme showing the main PtdSer and PtdThr synthetic pathways in *T. gondii* is shown in Figure 46.

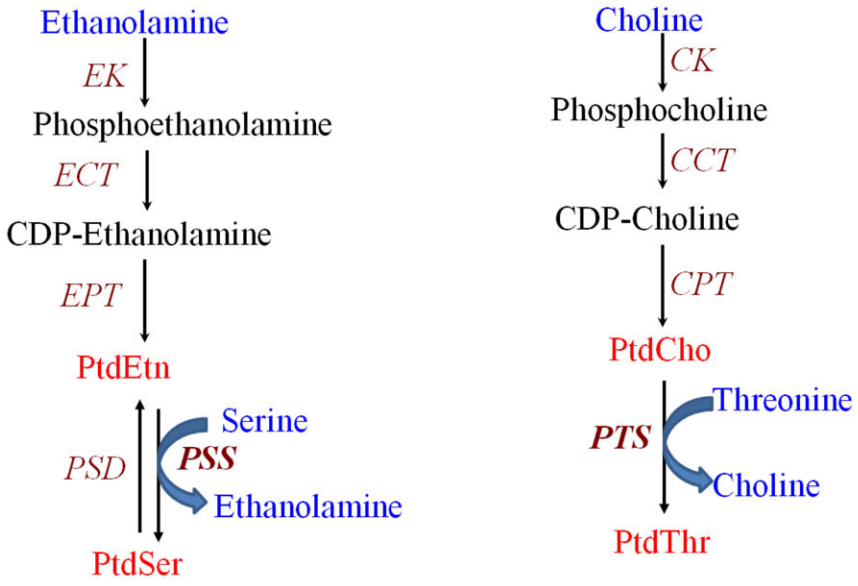

Fig. 46. *Proposed model of metabolic pathways involved in the biogenesis of PtdSer and PtdThr in T. gondii. C/EK*: choline/ethanolamine kinase; *CCT*: CTP:phosphocholine cytidylyltransferase; CPT: 1,2-diacylglycerol cholinephosphotransferase; *ECT*: CTP:phosphoethanolamine cytidylyltransferase; *EPT*: 1,2-diacylglycerol ethanolaminephosphotransferase; *PSS*: base-exchange phosphatidylserine synthase; *PTS*: base-exchange phosphatidylthreonine synthase.

Our tetracycline-inducible knockdown system was only modestly effective and showed that *T. gondii* can safely tolerate a 30% reduction in PtdSer synthesis, which translated into a similar decrease of PtdSer levels. Our *Δtgpss/Tg*PSS-HAi mutant showed shorter protein bands by western blot analysis, that were not regulated by aTC and which may be responsible for the high remaining PtdSer synthase activity in presence of the drug. In this regard, a similar tetracycline-inducible knockdown approach for the choline kinase gene of *T. gondii* (*Tg*CK) also showed only a modest reduction in PtdCho biogenesis despite an effective suppression of full-length transcript and protein (Sampels et al., 2012). To recompense for the loss of full-length *Tg*CK, the mutant of this study makes use of an alternative promoter and/or start codon, resulting in the expression of a shorter but active *Tg*CK isoform, which correlated with the persistent choline kinase activity.

On the other hand, a targeted DD-tagging system effectively destabilized *Tg*PSS protein and further decreased by 55-70% the PtdSer content and synthesis (Figs. 40, 41) with only a slight decrease of *T. gondii* replication (Fig. 39E.). This indicates that *T. gondii* can dispense a major

fraction of PtdSer, whose functions can be probably overtaken by its anlog PtdThr or other anionic phospholipids. The present report is also one of the first showing efficient regulation of an endoplasmic-reticulum protein by a Shield1-dependent destabilizing domain (Sellmyer et al., 2012). Interestingly, however, the relative overexpression of *Tg*PSS under the *pTetO7Sag1* (Fig. 35A) caused an enhanced synthesis and content of PtdSer (Figs. 37, 38), which in turn slowed down the intracellular parasite replication (Fig. 36D), as well as induced vacuolization of the endoplasmic reticulum in some instances (Appendix 7). In a similar way, it has been shown that overexpression of PtdSer synthase, Pps1, in *Sacharomyces pombe* produces severe defects in cell morphology and cytokinesis leading to a poor growth (Matsuo et al., 2007). These independent observations suggest a dosage-dependent role for PtdSer regulating these processes also in *T. gondii*.

The fact however, that *Tg*PSS remained resilient to several attempts of direct gene deletion or disruption (Appendix 5) strongly suggests that endogenous PSS activity and PtdSer are essential for *T. gondii*, although the parasite can tolerate safely a certain decrease in both, emphasizing *T. gondii* plasticity regarding its phospholipid metabolism. Further studies using most recent reverse genetic approaches like the conditional Cre-knockout system (Andenmatten et al., 2013) should determine the essentiality of *Tg*PSS. In any case, given the similarity of the reactions catalized and its homology to the orthologs of its mammalian peers, the potential of *Tg*PSS as a therapeutic target against toxoplasmosis seems very limited.

4.2. Interregulation of the analog phospholipids, phosphatidylthreonine and phosphatidylserine in *T. gondii*

The proportional increase in PtdSer content upon *Tg*PTS gene disruption and the consequent PtdThr depletion seemed to suffice for a normal replication of the *Δtgpts* parasites, however, these remained defective in their motility, invasion and egress. This result suggests that *T. gondii* can replace PtdThr for PtdSer regarding the membrane biogenesis necessary for a normal intracellular replication while other steps of the lytic cycle require PtdThr to be optimal.

Another possibility is that the observed upregulation of the PtdSer production in the *Δtgpts* parasites may be responsible for their defective growth phenotype. The role of PtdSer in Ca^{2+} -induced exocytosis, which is central for the lytic cycle of *T. gondii*, is known since more than

three decades (Martin and Lagunoff, 1979). Indeed, gain-of-function mutations of the *Hs*PSS1 gene have been identified as the cause of the rare Lenz-Majewski dwarfism syndrome in humans, which is characterized by altered Ca^{2+} homeostasis leading to excessive bone density and malformations (Sousa et al., 2014). These mutations induce abnormally high PtdSer synthesis, due to loss of the end-product inhibition of PSS1 activity by PtdSer (Ohsawa et al., 2004; Sousa et al., 2014). On the other hand, however, downregulation of *Tg*PSS activity and PtdSer content to parental levels upon degradation of *Tg*PSS in a *Δtgpts* background did not lead to neither improvement nor further impairment of the lytic cycle (Fig. 44), confirming that the increase in PtdSer synthesis observed upon PtdThr depletion is not responsible for the impaired lytic cycle. Interestingly, the levels of another major anionic phospholipid in the parasite, PtdIns, were increased when PtdSer was brought to normal amounts in absence of Shield1 in the *Δtgpts*/*Tg*PSS-DD-HA strain (Fig. 43E). This result emphasizes the importance of maintaining the net membrane charge by altering the phospholipid composition of the parasite. In fact, the relative proportion of all anionic phospholipids (PtdThr, PtdSer and PtdIns) was maintained relatively constant, despite the profound alterations observed in each individual phospholipid (Fig. 47). Similar compensatory mechanisms have been documented in other species like *Neurospora crassa* (Hubbard and Brody, 1975), and *Sacharomyces cerevisiae* (Hikiji et al., 1988) and would be sufficient to maintain a normal intracellular replication, but cannot address PtdThr-specific functions for the parasite egress, invasion and motility.

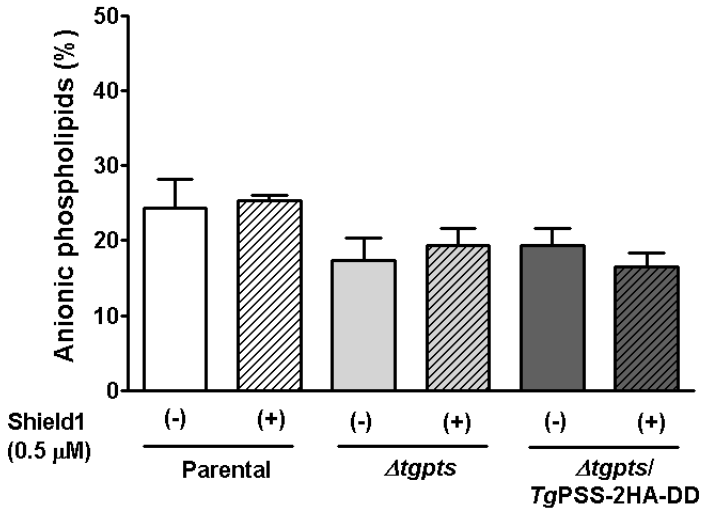

Fig. 47. *Anionic phospholipid content is maintained despite PtdThr loss and PtdSer reduction in T. gondii*. Total anionic phospholipid content (PtdSer+PtdThr+PtdIns) for the indicated strains and conditions was calculated from phosphorus assays shown in Fig. 43E. Error bars indicate the mean ± SEM (n=3).

It is also possible that the increase in PtdSer is mainly due to the missing amount of PtdThr, which would be acting as a repressor of *Tg*PSS activity in wild-type parasites. It is known that base-exchange PtdSer synthases are repressed by its product, phoshatidylserine, by interaction with specific residues, e.g. the Arg95 in *Cg*PSS1 (Hasegawa et al., 1989; Kuge et al., 1998; Ohsawa et al., 2004). In Fig. 48 we can observe that some basic or sulfured amino acid residues crucial for PtdSer-induced inhibition of base-exchange activity (His97, Cys189 and Arg262 in *Cg*PSS1) are substituted by short-chained residues at the equivalent positions in *Tg*PSS (Thr132, Leu219 and Gly351). These substitutions may be responsible for a higher affinity for PtdThr instead of PtdSer controlling the end-product feedback inhibition of *Tg*PSS. To support this hypotheis, lipid precursor labeling of parental and *Δtgpts* parasites with ^{14}C-serine was performed in absence or presence of 40 μM PtdSer (Avantis). There was no significant change of incorporation of ^{14}C-Ser into lipids between parasites labeled in absence or presence of PtdSer either for parental or *Δtgpts* strains. In contrast, labeling in presence of PtdThr extracted from *T. gondii* (from $2x10^8$ parasites, ~40 μM) was reduced, albeit poorly, for both mutant and parental parasites (Appendix 8). Although these results do not directly support the existence of PtdThr-driven feedback inhibition of *Tg*PSS, it is still possible that the provided lipids are not able to enter the parasite efficiently, despite previous reports based on fluorescent analogues showing their entrance, particularly for PtdSer (Charron and Sibley, 2002; Sampels and Marquadt, unpublished data). Fluorescent-phospholipid analogs like NBD-PtdSer have distorted fatty acyl chains and are also liable to metabolic conversion before incorporation, thus making inconclusive many traffic studies (Kay and Grinstein, 2011; Leventis and Grinstein, 2010).

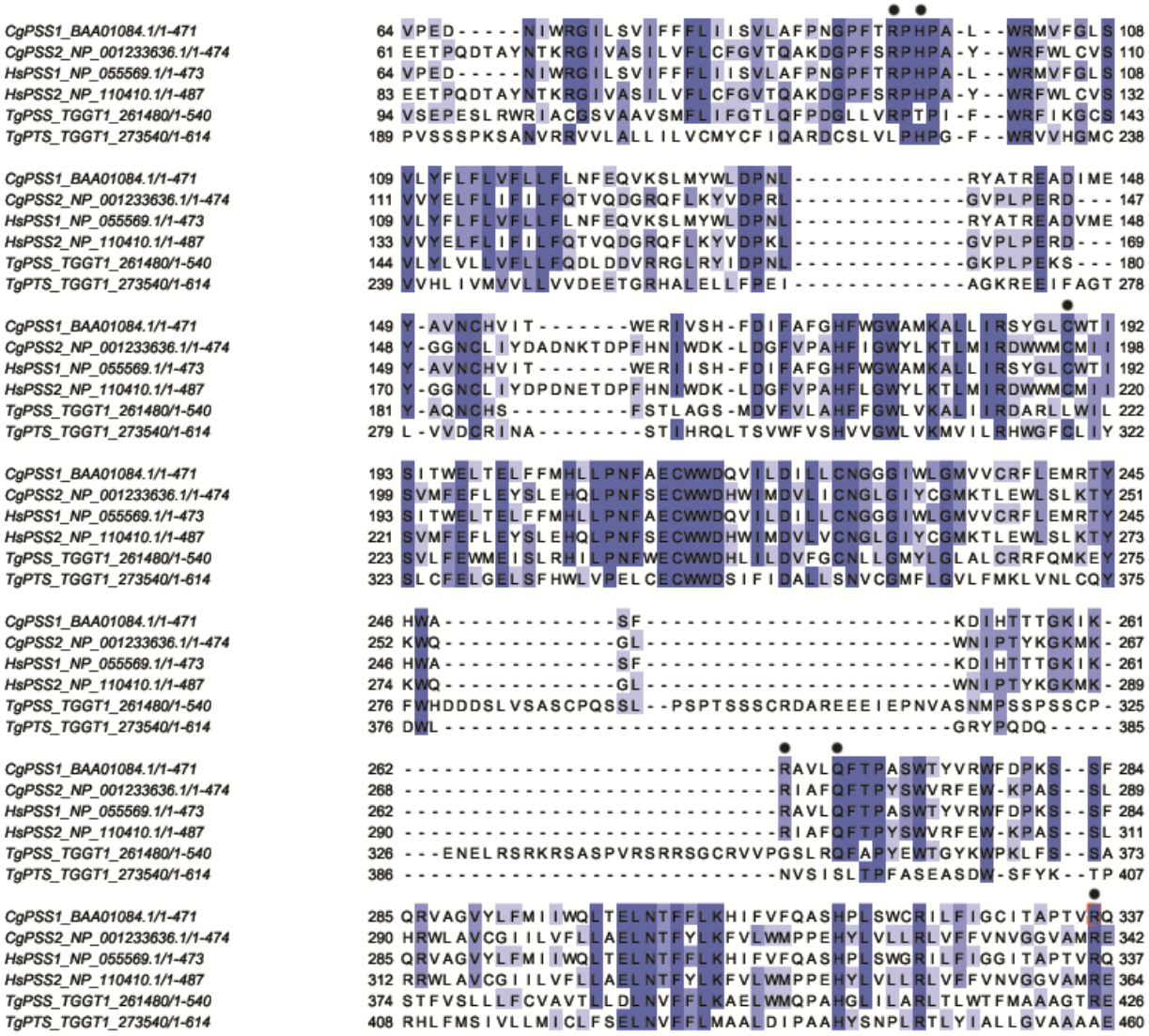

Fig. 48. *Crucial amino acid residues for PtdSer-driven regulation of base-exchange activity are missing in TgPSS and TgPTS.* Alignment of protein sequences of PSS and PTS from *Cricetulus griseus* (*Cg*), *Homo sapiens* (*Hs*) and *Toxoplasma gondii* (*Tg*). Amino acid residues indicated (filled circles) are crucial for product (PtdSer)-inhibition of *Cg*PSS1 (Ohsawa et al., 2004). Notice lack of conservation for His97, Cys189 and Arg262 at the equivalent positions of *Tg*PSS; and Arg95, Glu265 and Arg336 in the case of *Tg*PTS.

The fact that PtdSer synthesis was downregulated about 60-70% in either parental or *Δtgpts* background in absence of Shield1 when *Tg*PSS was DD-tagged (Figs. 40, 42), also shows that *Tg*PSS is the main PtdSer-producing enzyme in *T. gondii* and that the contribution of *Tg*PTS for the parasite PtdSer pool may be neglected. However, it remains in question whether the specific PtdSer species which are lost by *Tg*PTS deletion (Fig. 20A) are involved in the growth defect of the *Δtgpts* strain.

Although unlikely given the paralell perturbations observed in endogenous PtdSer synthesis by *Tg*PSS and parasite PtdSer content, we cannot discard the contribution of host PtdSer to the parasite membranes, in particular since it has been shown that the parasite is able to incorporate fluorescent PtdSer analogs from its host cell (Charron and Sibley, 2002), and that host PSS1 transcript levels are significantly upregulated in *T. gondii*-infected HFF cells (Kim et al., 2007).

Regarding the fatty acyl distribution of other major phospholipids, besides PtdSer and PtdThr, a significant increase of PtdCho (40:5) and a reduction in short-chained PtdIns species were observed between the parental and *Δtgpts* strains (Appendix 3). These changes may be directed to maintain a fluid membrane composition upon the loss of PtdThr, which is composed mostly of long polyunsaturated fatty acyl chains. Particularly the increase in PtdCho(40:5) would also reinforce the hypothesis of PtdCho as the substrate of *Tg*PTS, as PtdThr in *T. gondii* is dominated by such a species.

4.3. Role of phosphatidylthreonine for the lytic cycle of *T. gondii*

Our results show a non-customary role for a novel lipid in *T. gondii*, PtdThr, in the regulation of the lytic cycle of this intracellular pathogen. While been described already as a minor component of some mammalian cells mainly under serine starvation (Heikinheimo and Somerharju, 2002; Ivanova et al., 2010; Mark-Malchoff et al., 1978), the present report is the first one to identify a dedicated enzyme for its synthesis under normal cell culture conditions. Interestingly, the normal intracellular replication of the *Δtgpts* parasites lacking any PtdThr indicates no major role for this lipid regarding the bulk membrane biogenesis of the parasite. Instead, our work demonstrates that PtdThr is necessary for an optimal motility, which translates into a normal egress and invasion phenotypes.

Our assays clearly demonstrate the specificity of the observed phenotypes, by showing a large recovery of all these defects by genetic complementation of the mutant *Δtgpts* strain with an ectopic *Tg*PTS gene. However, the magnitude of the recovery in the complemented strain was not always full compared to the parental strains as observed in the plaque assays (Fig. 21). In this regard, the evaluation of the intracellular replication of the complemented *Δtgpts/Tg*PTS-HA strain showed a slight replication defect compared to the parental or the *Δtgpts* strains at later time points of infection despite a normal ER-localization (Appendix 9). This unexpected

defect may be due to the highly elevated expression level driven by the *Tg*GRA2 promoter (Fig. 30), which could divert the cellular machinery needed for a fast replication. Future work with a complemented strain with an ectopic *Tg*PTS copy under native promoter elements, should clarify this point.

In an effort to give more specificity to our results, and to find out if exogenously provided lipids were able to complement the growth defect produced by the loss of PtdThr; plaque assays were performed in medium containing exogenous PtdThr isolated from wild-type parasites (Appendix 10). Neither the plaque size nor the plaque numbers were significantly altered, suggesting no major contribution of exogenous PtdThr for the *Δtgpts* phenotype. However, it is possible that the added phospholipid cannot be readily incorporated by the host cells and therefore by the parasite; despite the observed evidence with fluorescent lipid analogs (Charron and Sibley, 2002), whose chemical structure and hydrophobicity are considerably altered by their fluorophore moiety (Leventis and Grinstein, 2010; Sarantis and Grinstein, 2012).

Our results also suggest an altered Ca^{2+} homeostasis as the cause of the impaired lytic cycle of the *Δtgpts* parasites (Fig. 27). Particularly, the calcium release responsible for triggering motility during egress (Arrizabalaga and Boothroyd, 2004; McCoy et al., 2012; Meissner et al., 2002) is reduced in absence of PtdThr, and this impaired release can be overcome by calcium ionophores or ethanol, a known phospholipase C inducer, which in turn controls the Ca^{2+} release from the ER via IP_3-sensitive channels (Fang et al., 2006; Hoek et al., 1987; Lovett et al., 2002). Indeed, the ionophore-induced calcium surge was sufficient to recover the egress defect of the *Δtgpts* strain (Fig. 28). It is then plausible that PtdThr serves as a more effective PtdSer analog for regulating the calcium pool, which is supported by the decreased Ca^{2+} response to ethanol (Fig. 27B), indicating a dysregulation of the PLC and/or IP_3-dependent calcium discharge from the parasite ER, which is the site of PtdThr synthesis. In this context, it is worth noting that late during the egress phase, the parasites sense a potassium gradient caused by host-cell damage after prolonged intracellular replication, which stimulates the parasite PLC activity and subsequently initiates their exit (Fruth and Arrizabalaga, 2007; Moudy et al., 2001). Additionally the observed loss of short-chained PtdIns species (Appendix 3) could be an effort of the mutant parasites to enhance their PLC activity, as it has been shown that *Tg*PLC has an important affinity for PtdIns (Fang et al., 2006) and that at higher doses short-chained PtdIns species act as inhibitors of PtdIns-

dependent PLC activity (Zhou and Roberts, 1998). Furthermore, it has been shown that chemically-synthesized PtdThr derivatives are much more potent inducers of secretion by mast cells than PtdSer, and the presence of defined fatty acyl chains exerts a maximal exocytosis (Iwashita et al., 2009), both of which are consistent with the natural and dominant existence of only selected PtdThr species in *T. gondii*. Similarly, anionic phospholipids differentially inhibit the calcium slippage into the cytosol by the sarcolemmal Ca^{2+}-ATPase, thus increasing the Ca^{2+} capture into the ER (Dalton et al., 1999). PtdThr as one of the most abundant anionic lipids in *T. gondii* may also regulate Ca^{2+}-ATPase and control the levels of Ca^{2+} in the parasite ER.

The other major pathway controlling Ca^{2+} release from the ER are the ryanodine-sensitive channels. The activity of these channels is usually controlled by the second messenger cADPR in *T. gondii*, (Chini et al., 2005). It is well known that caffeine can activate ryanodine-type channels and trigger a calcium realease from the ER in *T. gondii*, which then stimulates the microneme secretion (Lovett et al., 2002). Interestingly, when treated with caffeine we found a recovery in the fraction of motile parasites in the *Δtgpts* strain (Appendix 11), reinforcing the importance of the ER as the main Ca^{2+} pool involved in the impairment of calcium fluxes caused by the loss of PtdThr. It remains, however to be clarified whether this novel phospholipid controls rather the lelvel of the Ca^{2+} pool in the ER, or its mobilization into the parasite cytosol, particularly during egress. Last but not least, recently it has been shown that the Ca^{2+} entry from the extracellular medium also contributes significantly to the invasion and microneme secretion (Pace et al., 2014). In this regard, it has also been shown that anionic phospholipids interact with a variety of ionic channels, and control their activity (Crowley et al., 2005; Kasimova et al., 2014; Makielski, 1997). PtdThr as the most abundant anionic phospholipid in *T. gondii* may also be involved in the regulation of these channels.

It is well known that the secretion of specific micronemal proteins plays a pivotal step in different steps of the lytic cycle, e.g. MIC2 for invasion and motility (Huynh and Carruthers, 2006; Wetzel et al., 2004), and perforin-like protein1, PLP1, which is required to initiate a rapid host-cell egress (Kafsack et al., 2009; Roiko and Carruthers, 2013). In contrast, extracellular *Δtgpts* parasites showed a normal microneme secretion (Appendix 12), despite their reduced calcium mobilization in intracellular parasites. This result indicates that the threshold of Ca^{2+} needed for an efficient microneme secretion in extracellular parasites is lower than that needed for egress, and therefore it remains unaffected despite the reduced

calcium mobilization and/or pool in the ER of *Δtgpts* strain. In Figure 49, a scheme is showed summarizing the lytic cycle of *T. gondii* and possible checkpoints modulated by PtdThr.

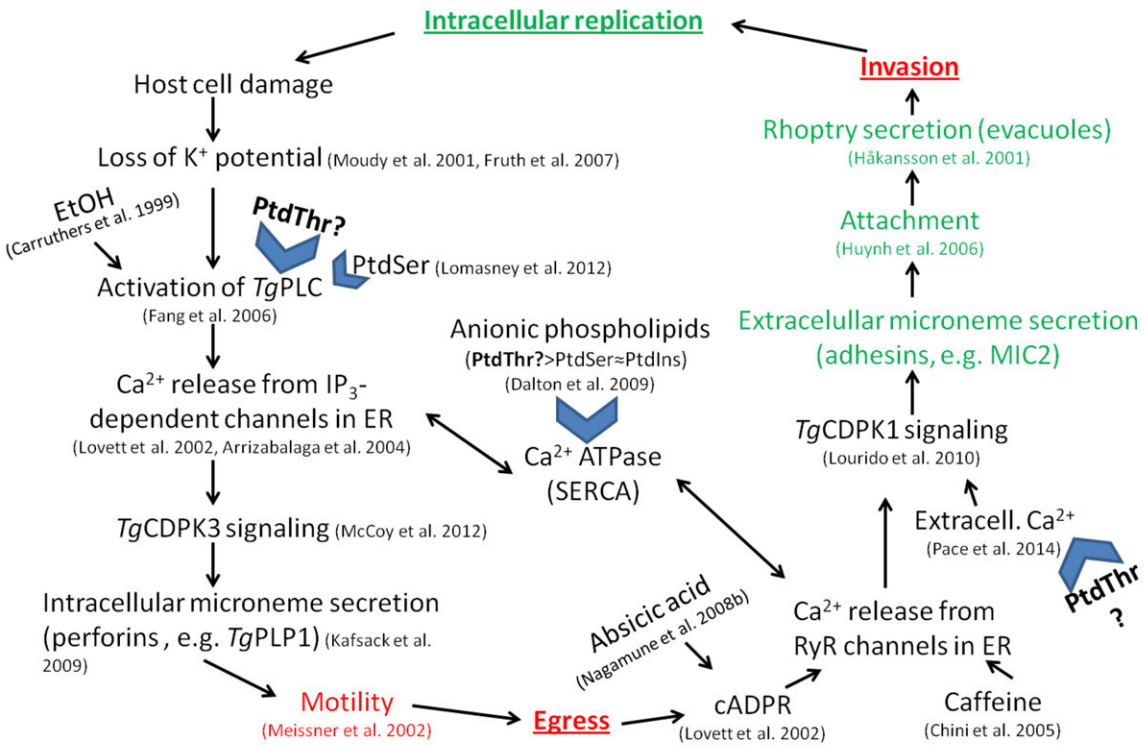

Fig . 49. *Scheme illustrating the regulation of the lytic cycle of T. gondii by Ca^{2+} pathways and steps in which PtdThr may be involved*. The blue arrowheads show possible checkpoints modulated by PtdThr. Red text indicates those steps of the lytic cycle which are compromised by PtdThr depletion, while those in green are not affected.

Finally, we were unable to detect PtdThr synthesis in extracellular parasites using radioactive threonine precursor, very likely due to a very low threonine transport system, as may be deduced from the low rates of ^{13}C-Thr incorporation into PtdThr in intracellular parasites (Fig. 13). Indeed, the parasite also harbors a pathway to produce threonine (www.ToxoDB.org, Appendix 13), an essential amino acid for its mammalian host cells, and therefore would not need an efficient threonine import system.

4.4. Phosphatidylthreonine as a parasite-adaptive trait in coccidians

Given the role of PtdThr for the lytic cycle and virulence of *Toxoplasma gondii*, we wanted to know if in other related parasites harboring orthologs of *Tg*PTS, such a lipid was also present

and may have a similar function. In this regard, we were able to identify PtdThr also in sporozoites of the related coccidian parasite *Eimeria tenella*. However, the fatty acyl chain composition of the main PtdThr species in *E. tenella* was radically different, instead of being dominated by the *Sn*1-20:1, *Sn*2-20:4 present in *T. gondii*, the most prevalent species was the *Sn*1-18:0, *Sn*2-18:1 (Appendix 14). Interestingly the identified ortholog *Et*PTS (ETH_00020770, Fig. 15) shows a maximal expression during the merogony phase of the life cycle (Appendix 14), where a synchronous egress from the schizont-infected host cells is necessary to define up to 3-4 generations of merozoites before gametogenesis can be initiated. This would suggest that also in *E. tenella* PtdThr may play a pivotal role in the regulation of the egress from host cells as it does in *T. gondii*. Future complementation studies of the *Δtgpts* strain generated in this study with *Et*PTS should help prove or discard this hypothesis.

Summing up, we have shown the PtdThr synthesis in determined apicomplexan parasites (*Toxoplasma*, *Eimeria*) as a parasite-specific trait, however, within the chromalveolate lineage orthologs of the PTS enzymes have been lost (e.g. *Plasmodium*, *Crytosporidium*) or retained (e.g. *Phytophtora*, *Perkinsus*) (Fig. 15). Gene loss or gain events are known to govern the evolution of chromalveolates and different parasitic strategies lead to the expansion or loss of specific metabolic pathways (Kemen et al., 2011) , and as such the PTS enzymes would be an ancestral feature of Chromalveolates that is maintained and exploited by *T. gondii* and possibly by other coccidians like *E. tenella* to optimize their lytic cycle.

4.5. Therapeutic potential of the *Δtgpts* strain

Our results highlight the importance and the profilactic potential of phospholipids and particularly of PtdThr to control the course of toxoplasmosis. It is worth noting that a similar role at controlling virulence has been shown for PtdSer in other pathogens like *Candida albicans* (Chen et al., 2010).

There is currently only one approved live-attenuated toxoplasmosis vaccine licensed for use in sheeps against spontaneous abortion (Buxton, 1993). This strain, S48, is unable to form tissue cysts after prolonged serial intraperitoneal passaging in mice, making its use acceptable in a food-producing animal. In this regard, our results show that the *Δtgpts* strain generated in this study in a type I background is also unable to form brain cysts, as it is derived from the highly virulent RH strain, which is widely considered to have lost this ability upon years of

cell culture passaging (Sullivan and Jeffers, 2012), and that they also protect against brain-cyst formation by a type II strain (Fig. 26). However, further studies with a *Δtgpts* strain in a type II background are required to answer the question of whether the impairment of the lytic cycle conferred by the lost of PtdThr also affects the tachyzoite to bradyzoite conversion, particularly since it has been described that insults that interfere with the calcium-induced egress promote the bradyzoite differentiation (Nagamune et al., 2008b).

It is worth mentioning that there are already several genetically-attenuated parasite strains described in the literature, which efficiently protect against a lethal challenge with hypervirulent strains of *T. gondii* in murine models (Behnke et al., 2012; Huynh and Carruthers, 2006; Kafsack et al., 2009; Meissner et al., 2002; Mercier et al., 1998). Going further, the importance of genetically-attenuated vaccines as the *Δtgpts* mutant in preventing toxoplasmosis, is exemplified by the uracil auxotroph *cps 1-1* strain, which also can protect mice against lethal challenge with virulent type I strains or chronic type II strains (Fox and Bzik, 2002; Gigley et al., 2009).

Nevertheless, there are many pitfalls to be taken into account when considering *Δtgpts* parasites in a real vaccination setup. The major one regards to the safety of a live attenuated vaccine, which may not only produce serious side-effects but also potentially revert to a pathogenic form, as has been described for the currently available S48, although in very few cases (Kur et al., 2009). In this regard, the development of safer recombinant DNA and antigen vaccines in animal models has been established, however only partial protection rates have been achieved with (Echeverria et al., 2006; Li et al., 2014; Mendes et al., 2013). One of the most potent recombinant anti-cyst vaccines described is a *Toxoplasma* ROP2-*Leishmania* HSP83 protein fusion; however it only elicited a modest delay in mortality after challenge with the highly virulent RH strain (Echeverria et al., 2006).

5. Conclusions

This work shows the natural and abundant occurrence of PtdThr, an otherwise rare PtdSer analogue, in *T. gondii* and establishes the functional speciation of the closely-related phospholipids during the lytic cycle of the parasite.

Furthermore this work also identifies the enzymes realizing the synthesis of both, PtdSer and PtdThr, in the parasite ER and establishes a method to study spatiotemporal calcium signaling in intracellular pathogens.

Finally, this thesis also reveals the importance of PdThr at regulating the virulence of a pathogen and exposes the exploitation of parasite-specific lipid pathways to develop effective vaccines against both the acute and the yet incurable chronic toxoplasmosis.

Appendix 1

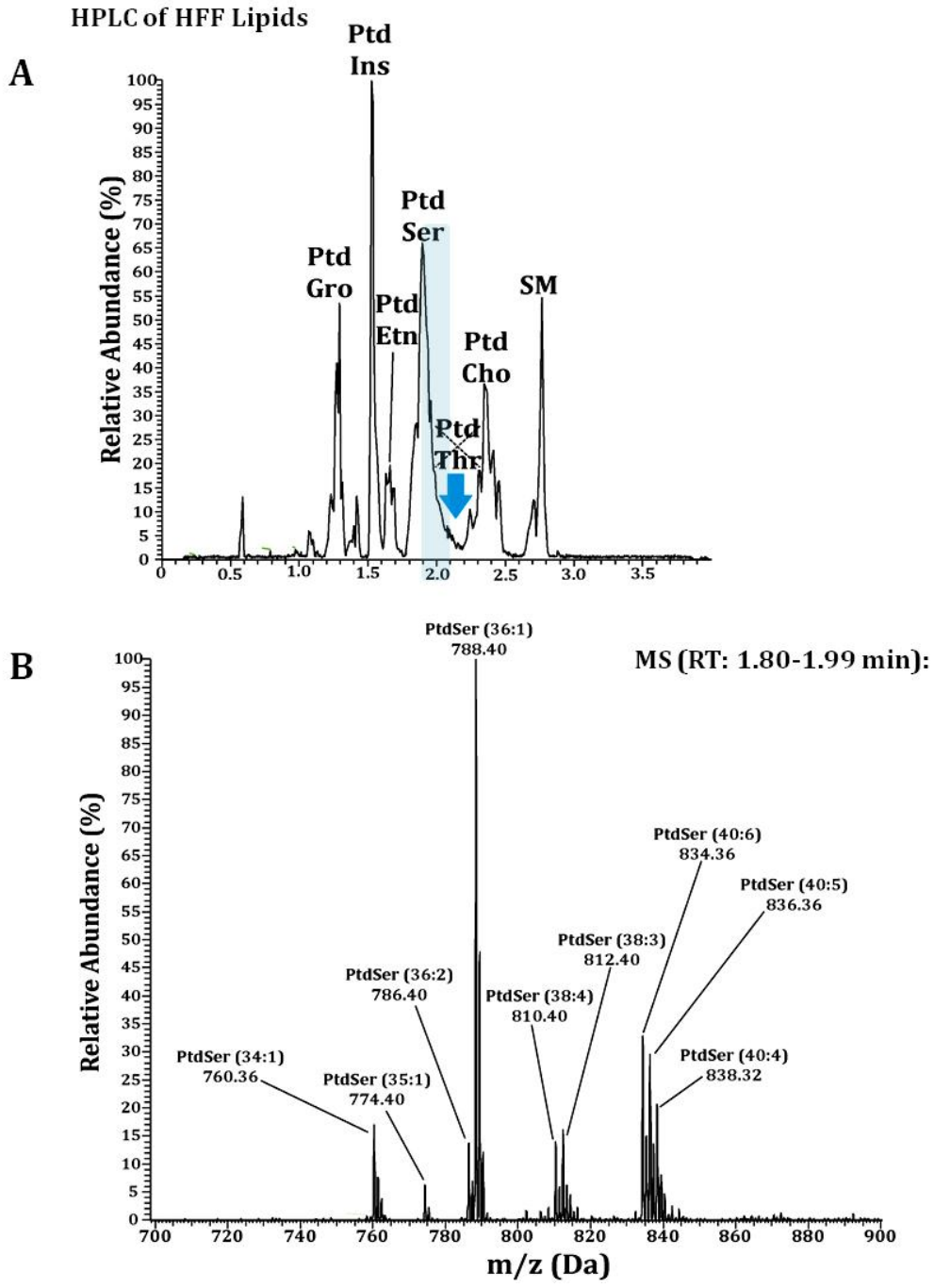

Human foreskin fibroblast cells do not contain detectable amounts of phosphatidylthreonine. **(A)** HPLC elution profile showing the retention times and peak intensities of phospholipids isolated from host fibroblasts. **(B)** MS analysis of the indicated HPLC fraction revealing predominantly PtdSer species and lack of detectable PtdThr species. Fibroblast lipids were detected in negative mode using electrospray ionization using an LTQ-XL (Thermo Scientific, Hampton, NH) mass spectrometer.

Appendix 2

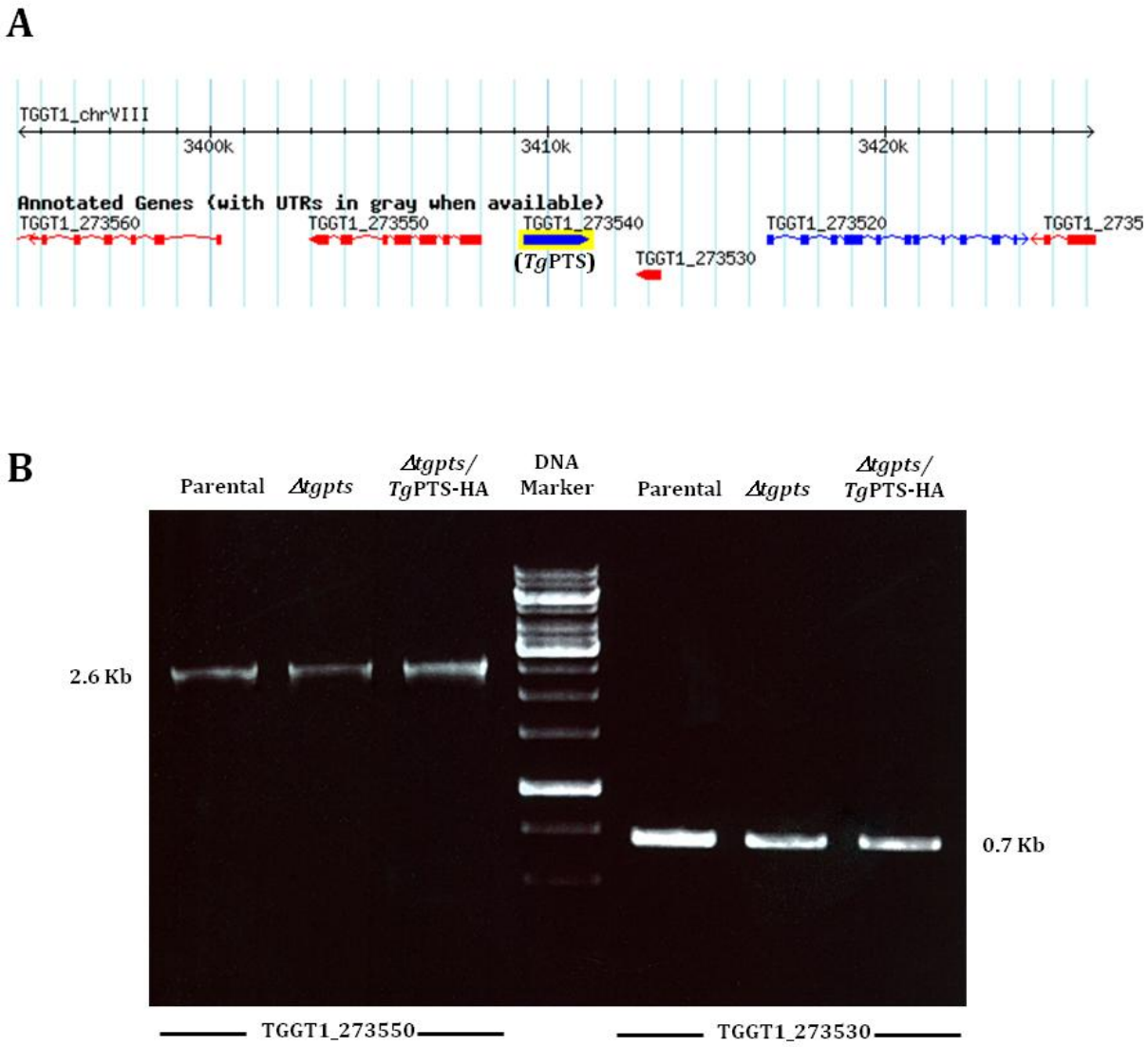

TgPTS gene disruption does not affect transcription of neighboring genes. **(A)** Genome browser view of *Tg*PTS (TGGT1_273540) on the chromosome VIII of *T. gondii* (www.ToxoDB.org). **(B)** ORF-specific RT-PCR of TGGT1_273550 and TGGT1_273530 amplified from total RNA (100 ng) isolated from the parental, *Δtgpts* mutant and complemented strains.

Appendix 3

A.

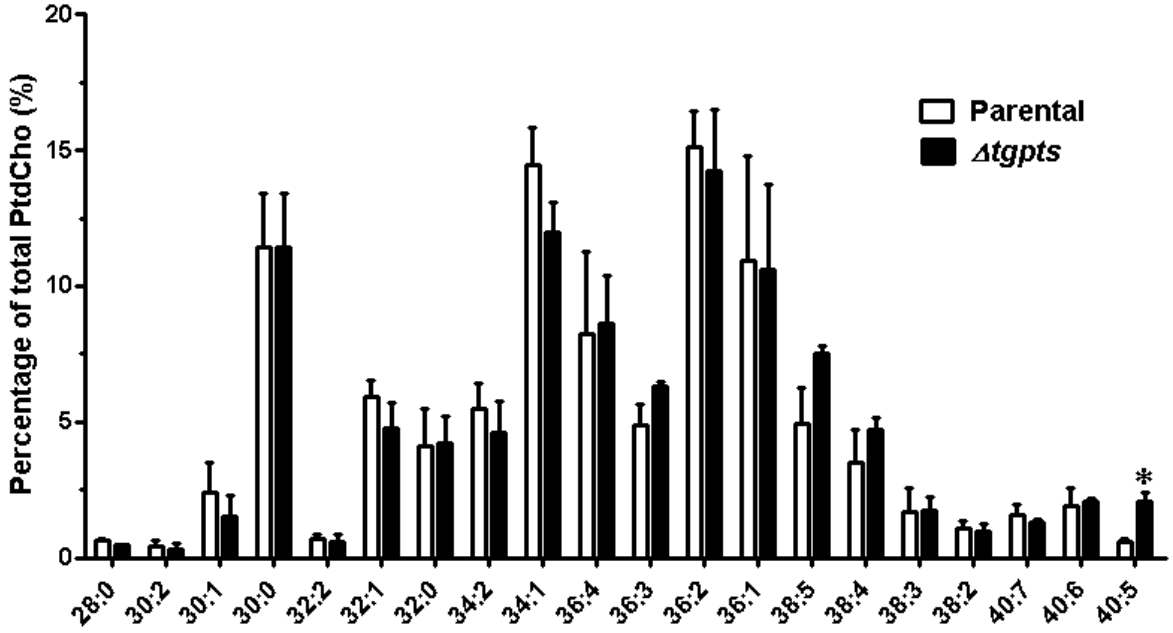

B.

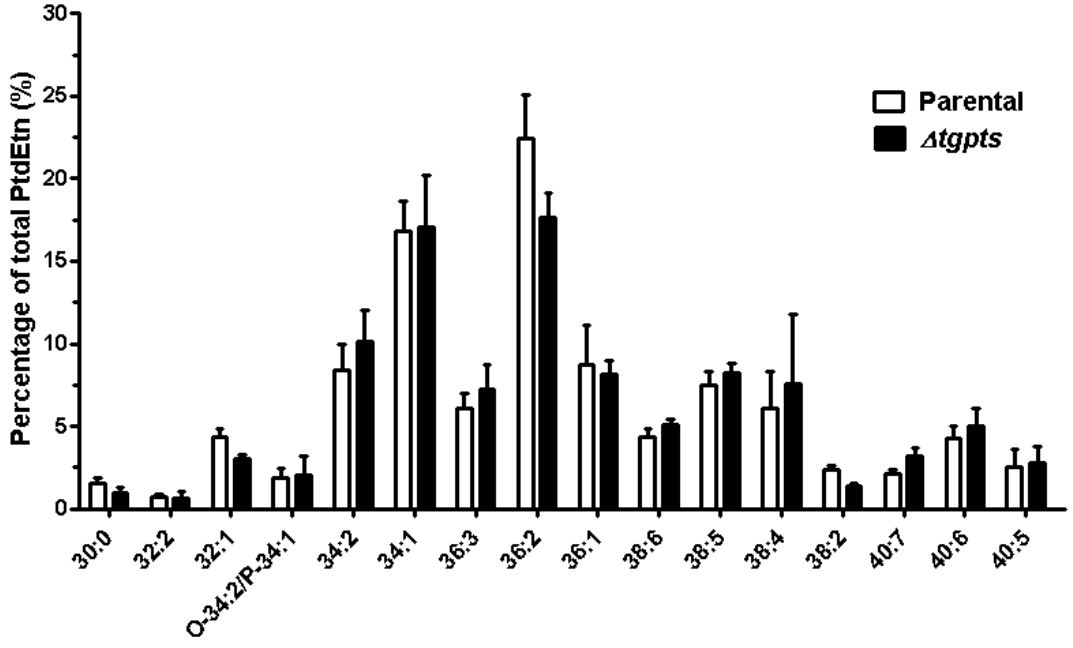

C.

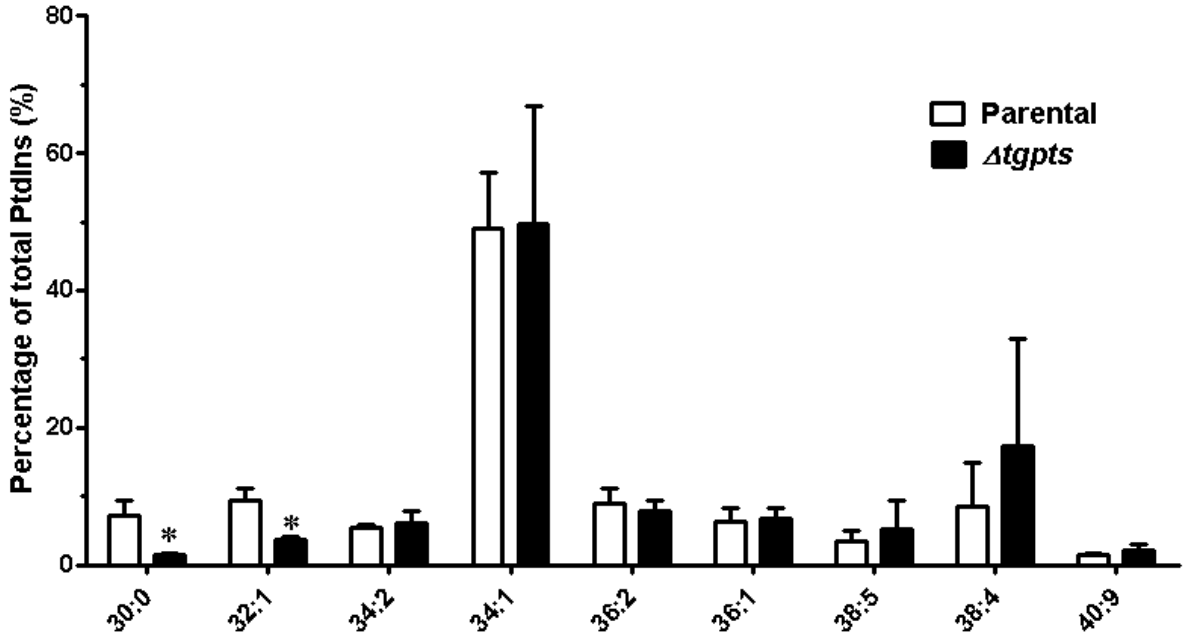

Fatty acyl distribution of PtdCho, PtdEtn and PtdIns in parental and Δtgpts strains. Lipid species were identified by their *m/z* ratios in the positive (PtdCho **(A)**) and negative (PtdEtn **(B)** and PtdIns **(C)**) ionization modes. Magnitude of each lipid species was determined by their peak intensity. (n = 3 assays; *, $p<0.05$; **, $p < 0.01$; ***, $p < 0.001$). Error bars, S.E.

Appendix 4

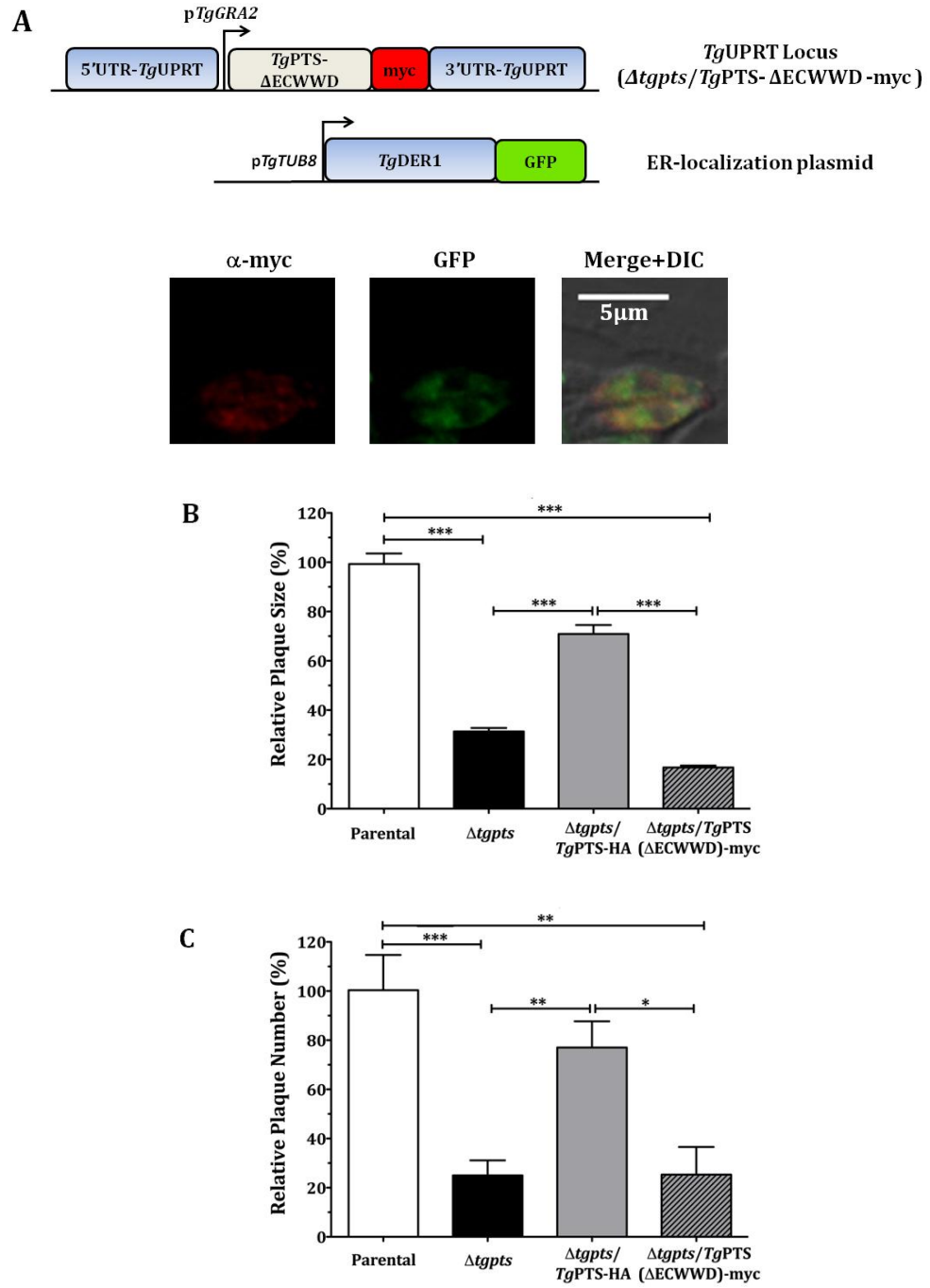

Catalytic activity of TgPTS is crucial for the lytic cycle of T. gondii. Expression of a mutagenized isoform of *Tg*PTS without catalityc activity (*Tg*PTS(ΔECWWD)-myc, see Fig. 20D) does not recover the growth phenotype of *Δtgpts* parasites as determined by plaque assays, despite normal ER localization **(A)**. Notice, in contrast, effective complementation with expression of full length *Tg*PTS-HA. **(B)** Size of plaques and **(C)** number of plaques formed by the indicated strains. (n = 3 assays; *, $p<0.05$; **, $p < 0.01$; ***, $p < 0.001$). Error bars, S.E.

Appendix 5

A **Targeted Gene replacement of *Tg*PSS by a Dihydrofolate reductase (DHFR-TS):**

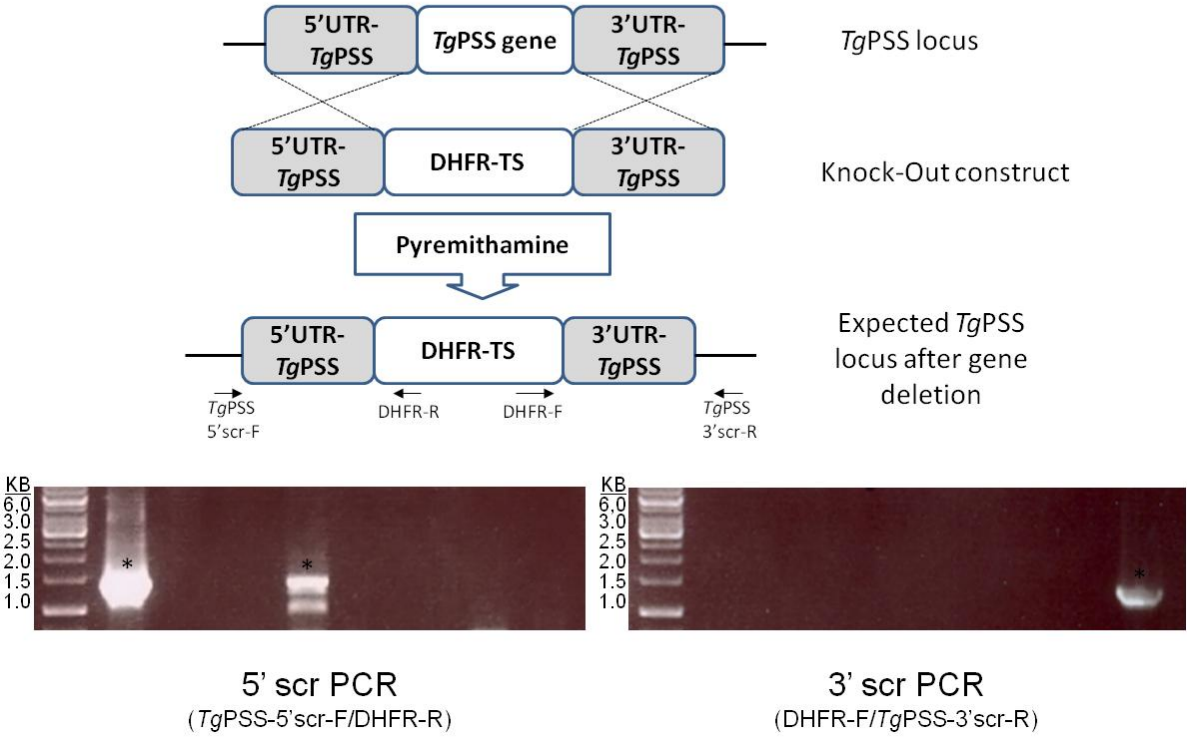

B **Targeted Gene replacement of *Tg*PSS by a Chloramphenicol Acetyl Transferase (CAT-RC):**

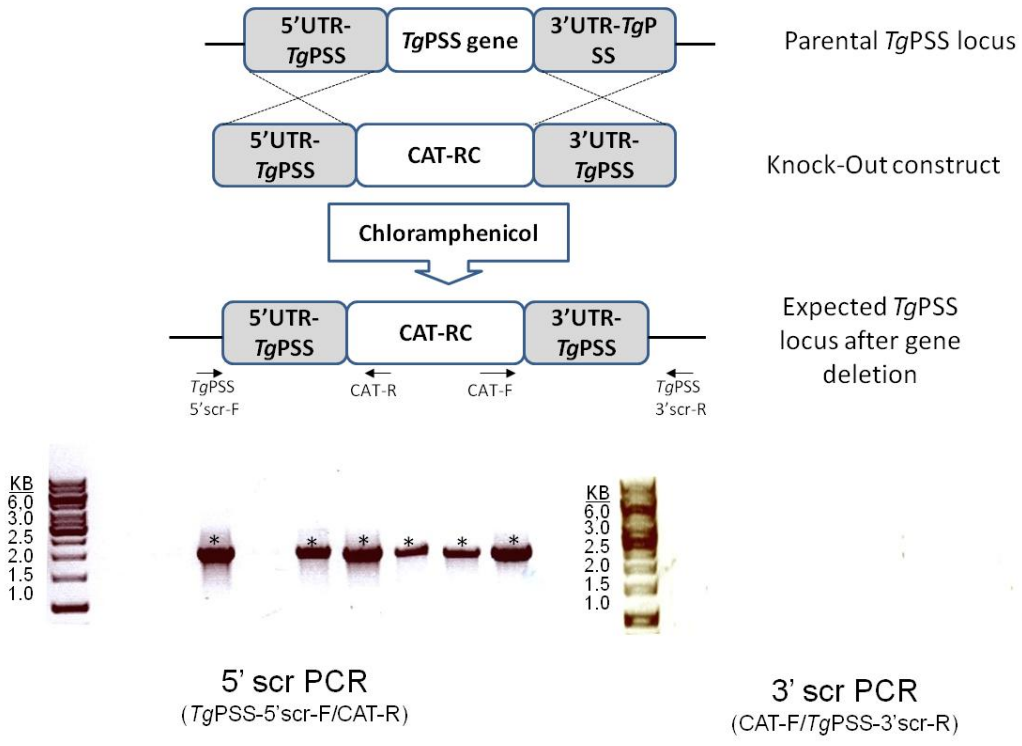

C **Targeted Gene Disruption of catalytic site of *Tg*PSS by a hypoxanthine-xanthine-guanine phosphoribosyl transferase (HXGPRT):**

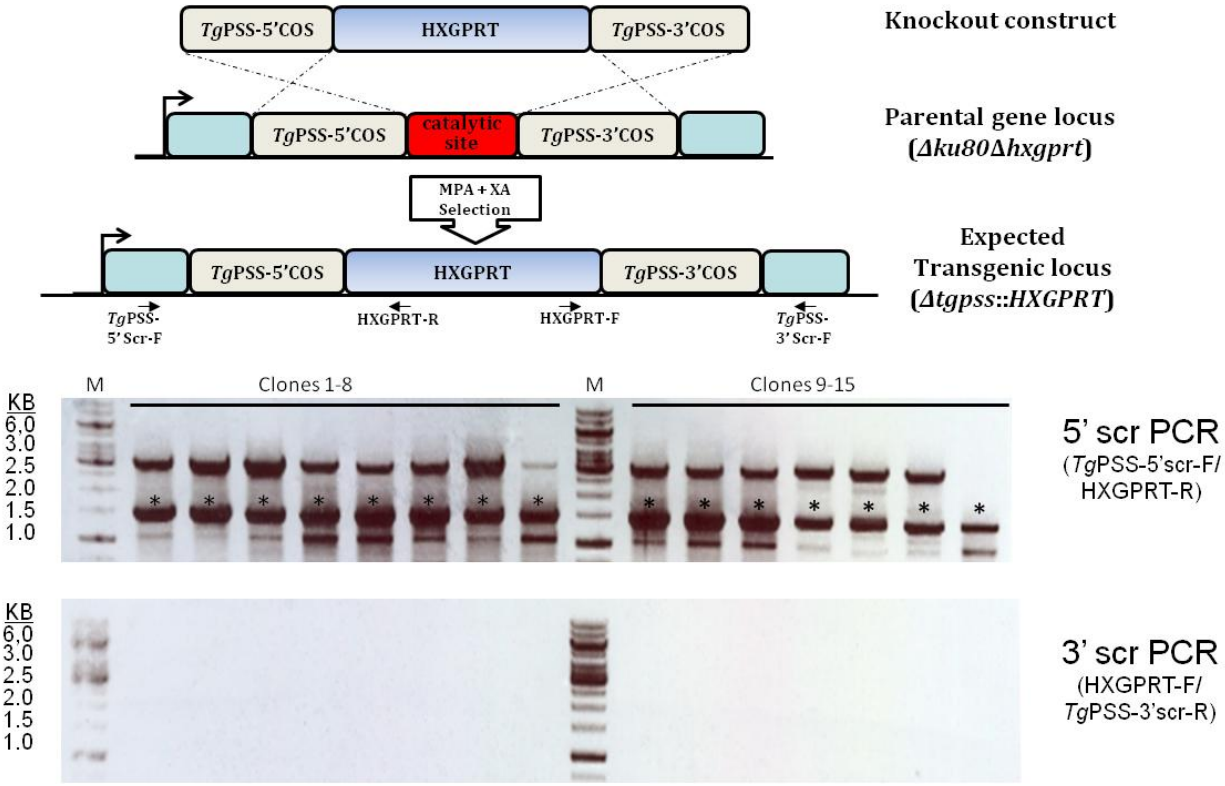

Conventional gene replacement or disruption of TgPSS is not feasible. **(A)** Strategy for targeted gene replacement at the *Tg*PSS locus by double homologous recombination of a pyrimethamine-resistant dihydrofolate reductase cassette. Notice that 5' or 3' crossover events (*) only occurred in single clones and were never simultaneous as evidenced by specific screening PCR bands. **(B)** The same strategy was applied to replace *Tg*PSS gene with Chloramphenicol Acetyl transferase (CAT-RC) as selection marker. Only 5' (*), and none 3' crossover events were detected after clonal selection. **(C)** Strategy for targeted gene disruption of *Tg*PSS by replacing the catalytic domain ECWWD with a hypoxanthine-xanthine-guanine phosphoribosyl transferase resistance cassette. Contrary to the case of *Tg*PTS (see Fig. 18), none clone showed evidence for double homologous recombination, and instead they all underwent single 5'crossover events (*) after selection.

Appendix 6

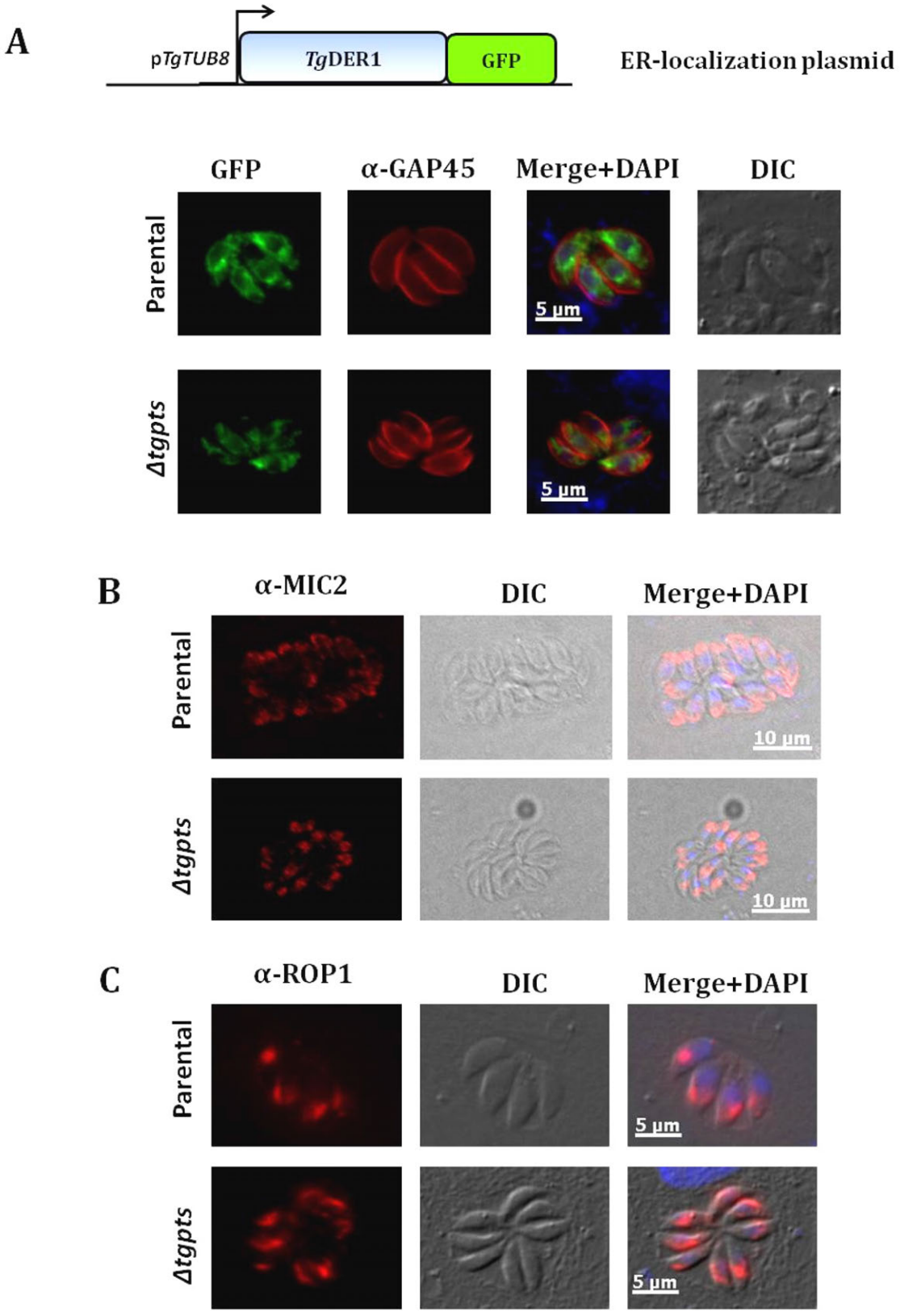
A
pTgTUB8
TgDER1
GFP
ER-localization plasmid
GFP
α-GAP45
Merge+DAPI
DIC
Parental
Δtgpts
5 μm
5 μm
B
α-MIC2
DIC
Merge+DAPI
Parental
Δtgpts
10 μm
10 μm
C
α-ROP1
DIC
Merge+DAPI
Parental
Δtgpts
5 μm
5 μm

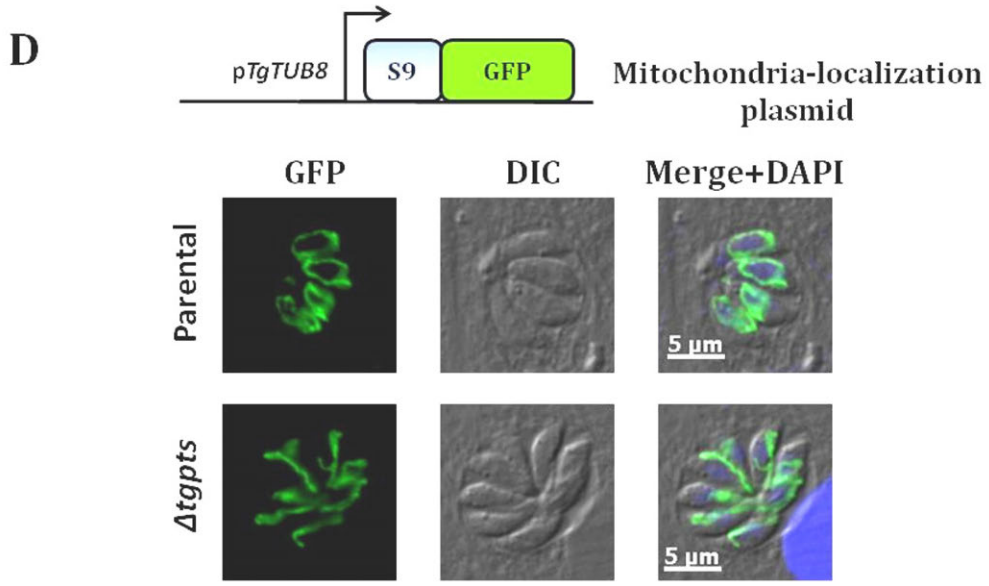

Δtgpts parasites have normal organelle morphology. **(A)** ER staining as detected with the ER-marker Der1-GFP (Agrawal et al., 2009), α-GAP45 was used as an IMC marker. **(B)** Microneme staining as detected with the α-MIC2 antibody. **(C)** Roptrhy staining as detected with the α-ROP1 antibody. **(D)** Mitochondrion staining as detected with the mitochondrial marker S9-GFP (DeRocher et al., 2000).

Appendix 7

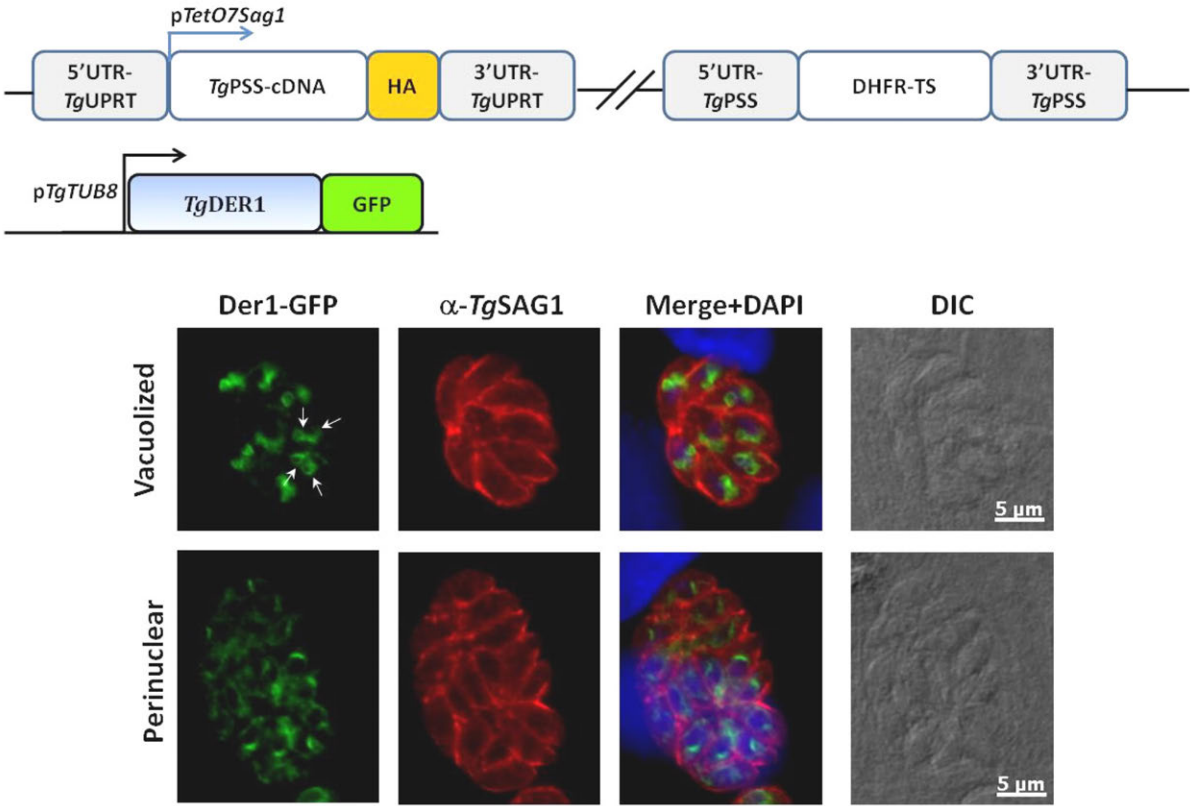

Overexpression of TgPSS under pTetO7sag1 promoter causes ER-vacuolization. Fluorescence images showing the "vacuolized" ER-pattern (arrows) found in some instances in the *Δtgpss*/*Tg*PSS-HAi strain. Below the normal perinuclear pattern expected for the ER and observed in most cases. All images were taken in absence of anydrotetracycline.

Appendix 8

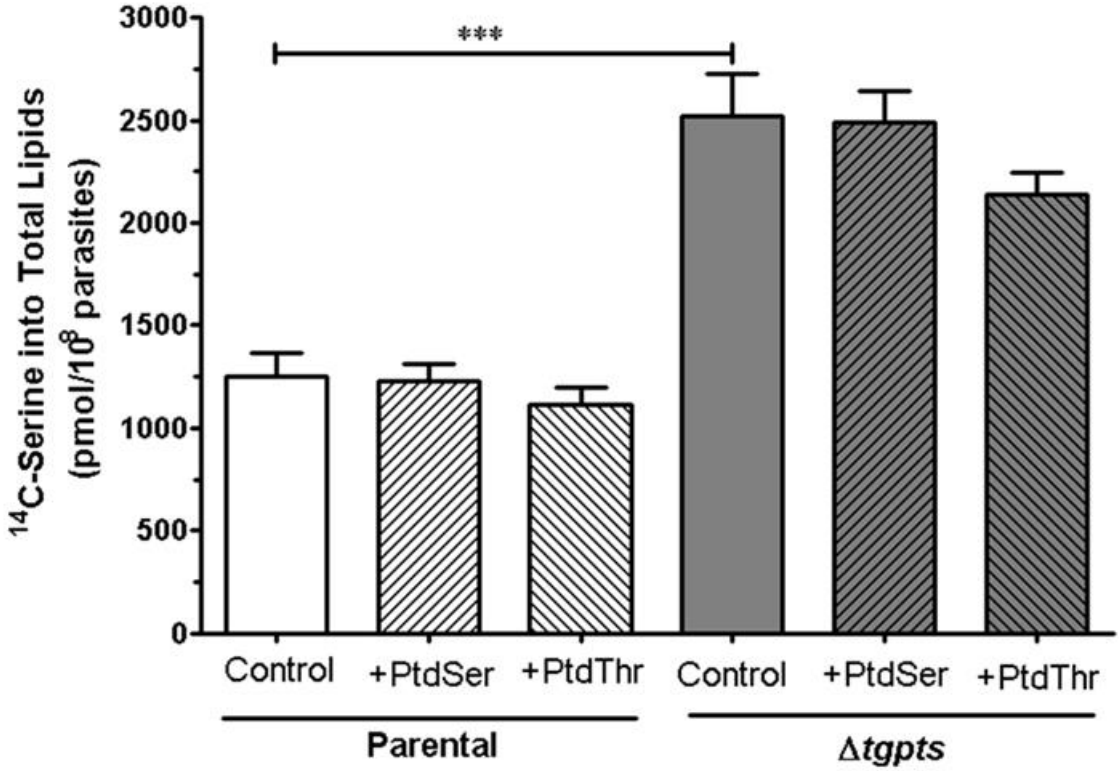

Incorporation of ^{14}C-serine into lipid fraction in presence of exogenously provided PtdSer and PtdThr is not significanlty altered. Freshly syringe-released extracellular tachyzoites of the indicated strains labeled with ^{14}C-Serine (2 μCi, 2hrs, 37°C, 5x10^7 parasites each) in presence or absence of PtdSer (40μM, Avantis) or PtdThr (~40μM) isolated from wild-type *T. gondii*. (n = 3 assays; *, $p<0.05$; **, $p < 0.01$; ***, $p < 0.001$). Error bars, S.E.

Appendix 9

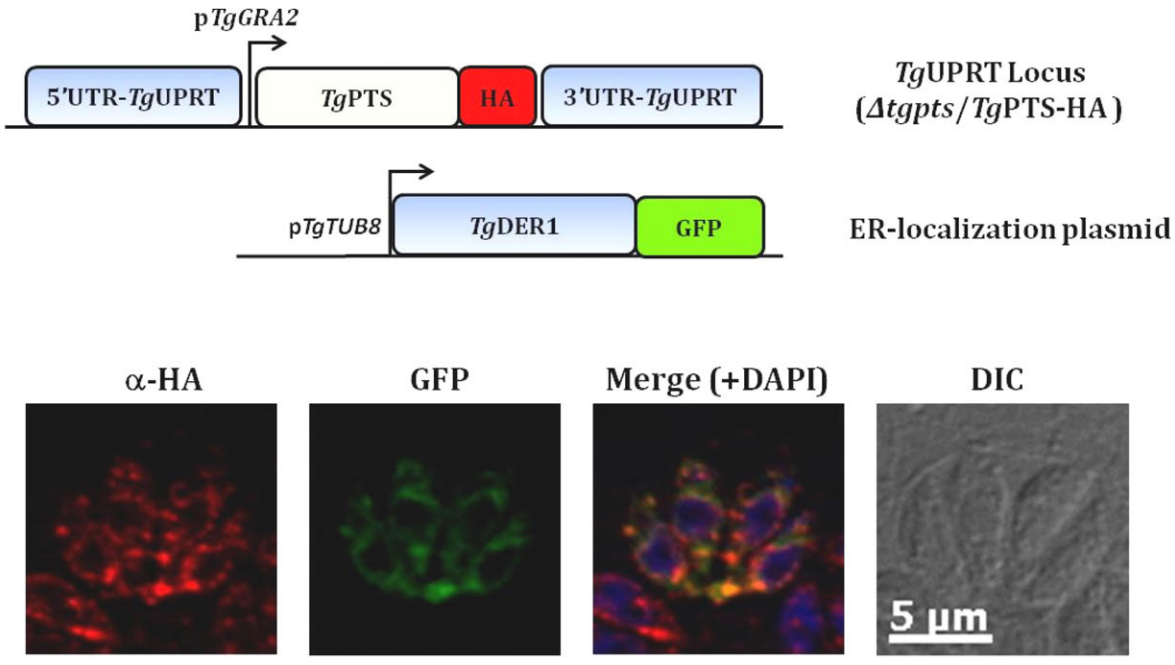

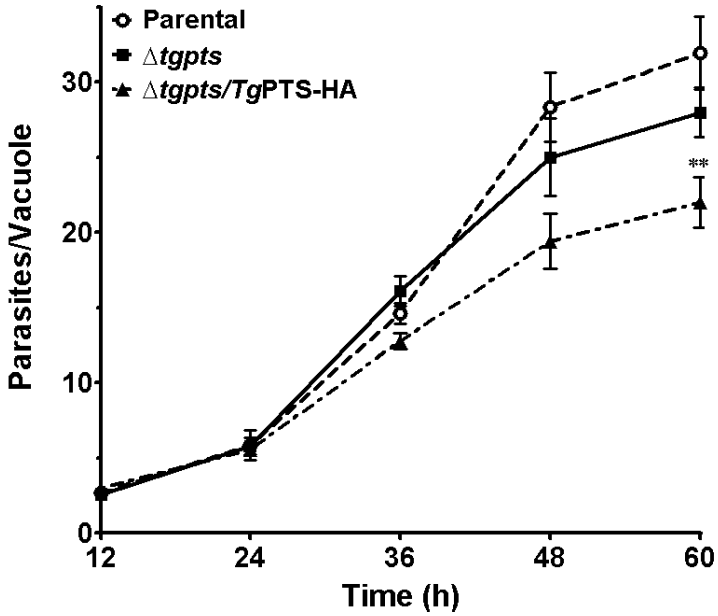

Foreign complementation of the Δtgpts strain under the pTgGRA2 promoter causes a slight replication defect despite a normal localization. The mean number of parasites per vacuole of each indicated strain was calculated every 12 hrs after infection by immunofluorescence staining (see methods). The ER-localization of *Tg*PTS under the *Tg*GRA2 promoter was corroborated by a similar staining pattern to the ER marker Der1-GFP. (n=3 assays; **p<0.01). Error bars, S.E.

Appendix 10

A

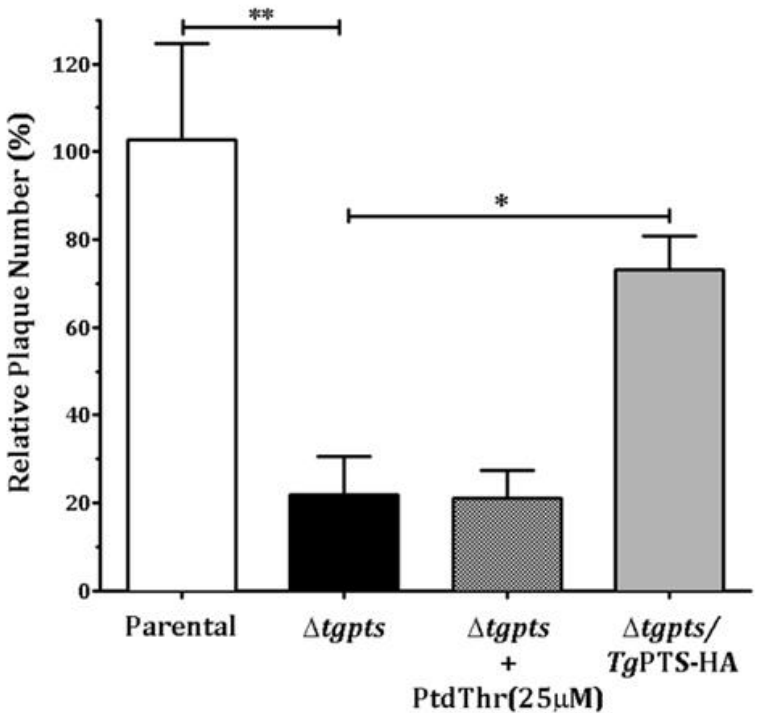

B

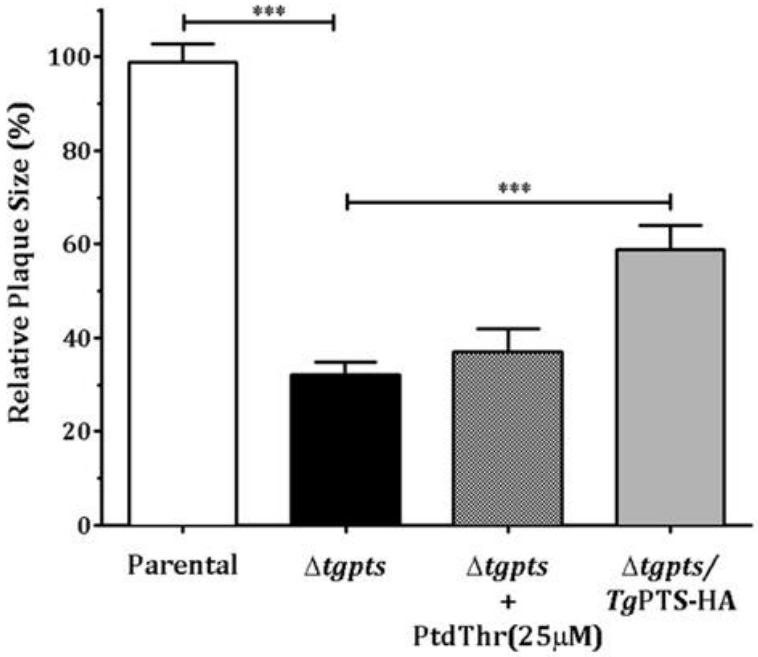

Exogenously provided PtdThr does not recover the growth phenotype of the Δtgpts strain. Growth phenotype of the indicated strains as evaluated by plaque assays. Neither plaque size **(A)** nor number **(B)** were recovered in the *Δtgpts* strain by exogenously provided PtdThr isolated from wild-type parasites. (n = 3 assays; *, $p<0.05$; **, $p < 0.01$; ***, $p < 0.001$). Error bars, S.E.

Appendix 11

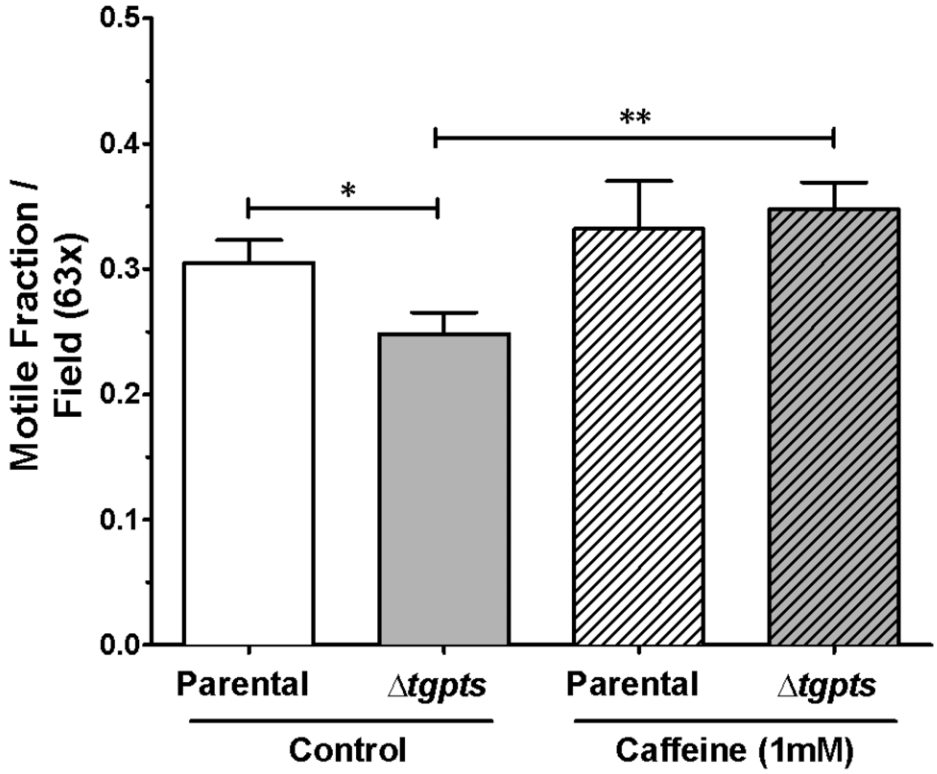

Stimulation of ryanodine-receptor (RyR)-type Ca^{2+}channels recovers the motility of the Δtgpts strain. Caffeine, a RyR activator and microneme inducer (Wetzel et al., 2004), also normalizes motility defect of extracellular *Δtgpts* parasites. (n=6 random fields, 100-200 parasites; *p<0.05, **p<0.01). Error bars, S.E.

Appendix 12

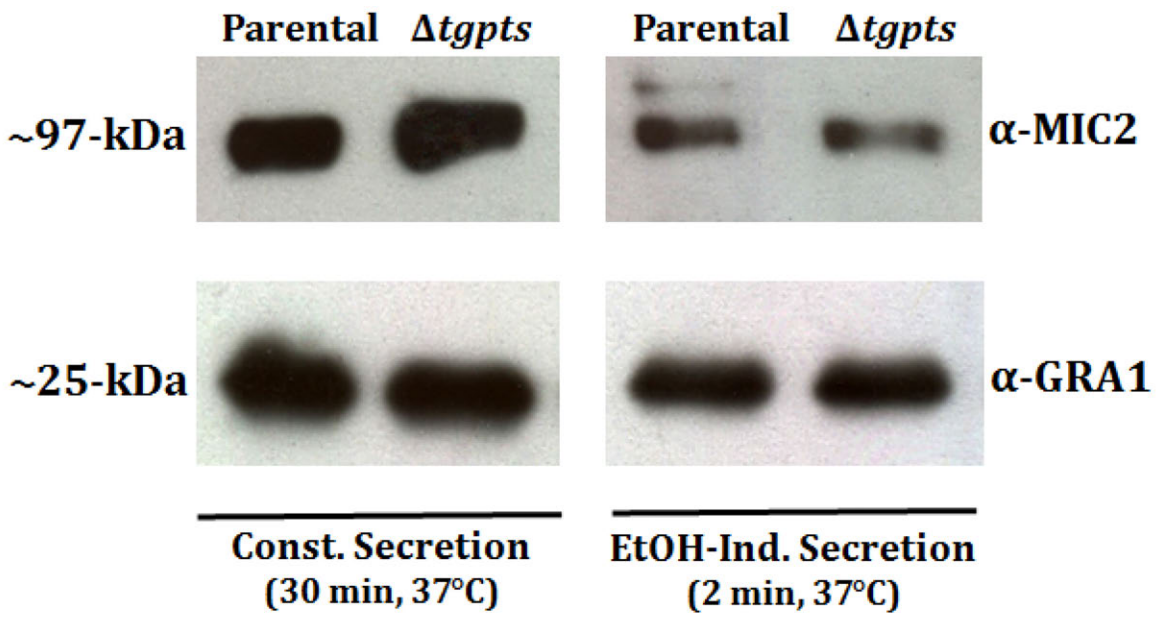

Loss of PtdThr does not affect the microneme secretion of extracellular parasites. 2x 10^6 freshly syringe-released tachyzoites of each strain were incubated for 30 min at 37°C in the absence of drug (constitutive secretion) or stimulated with 1% ethanol (EtOH) for 2 minutes. Parasites were removed by centrifugation and supernatants were analysed by Western blotting with antibodies specific for the shown markers. MIC2 served as micronemal secretion marker while GRA1 as a dense granule secretion and loading control.

Appendix 13

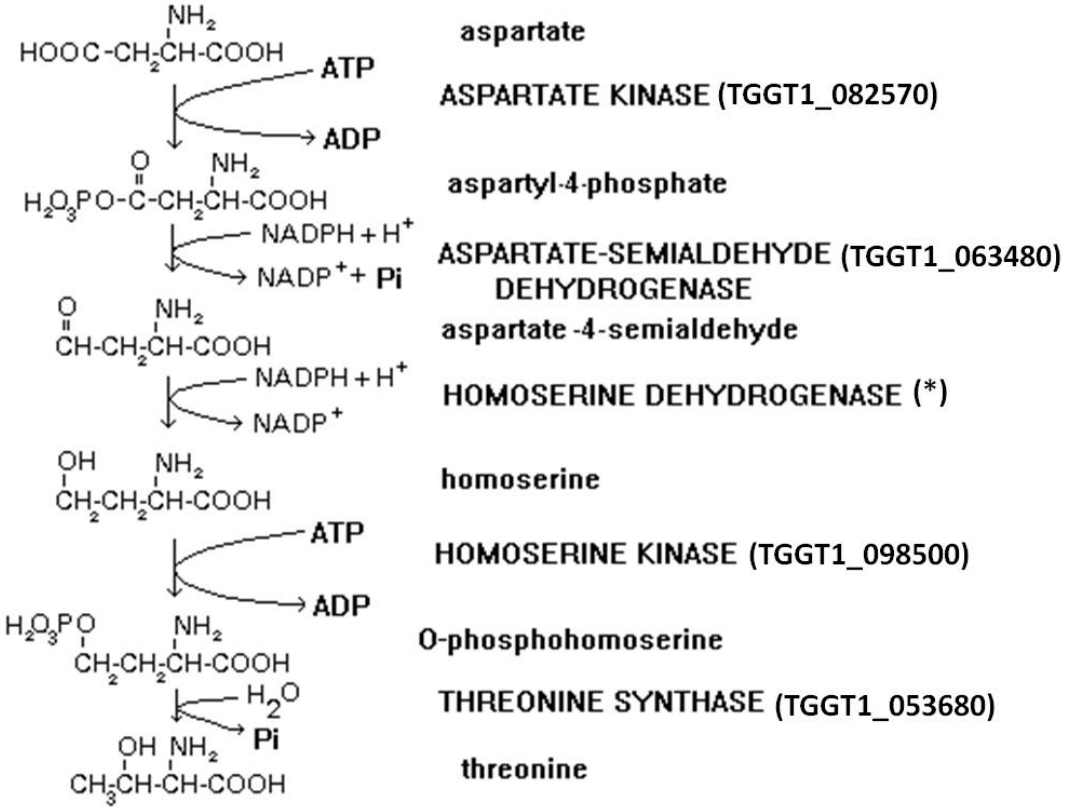

T. gondii harbors a threonine biosynthetic pathway. Typical threonine biosynthesis pathway found in plants in bacteria (Adapted from (Bryan, 1980). Putative homolog enzymes in *T. gondii* were identified in www.ToxoDB.org (accession numbers in brackets). An homolog for homoserine dehydrogenase (*) was not found, although it is known that some aspartate kinases (e.g. *Arabidopsis thaliana*) also show such activity (Zhu-Shimoni and Galili, 1998).

Appendix 14

A.

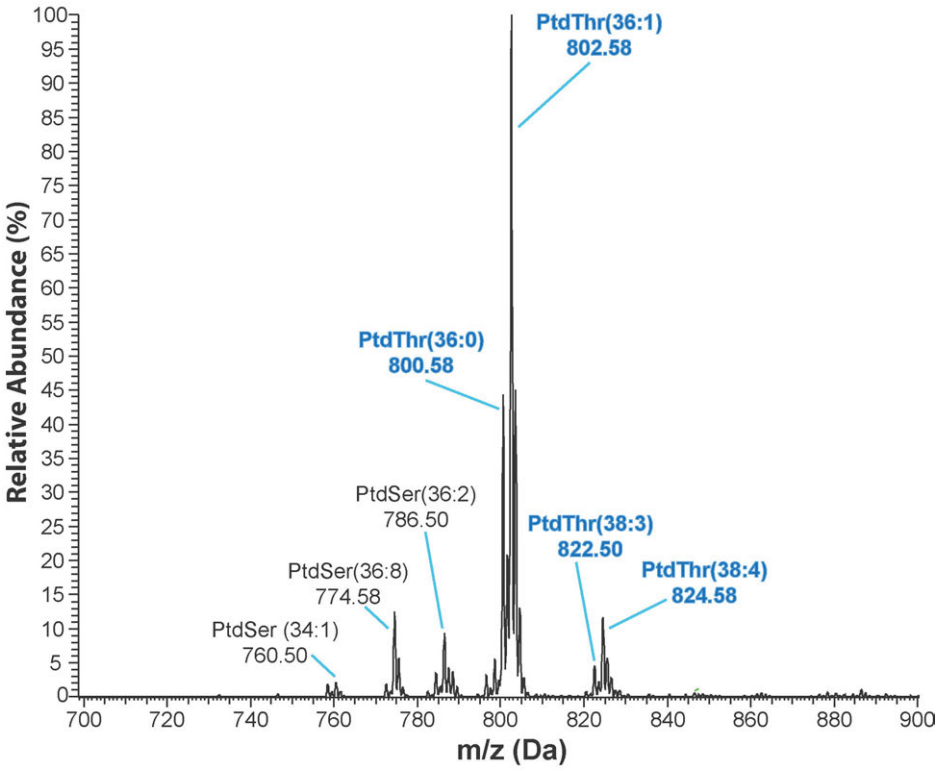

B.

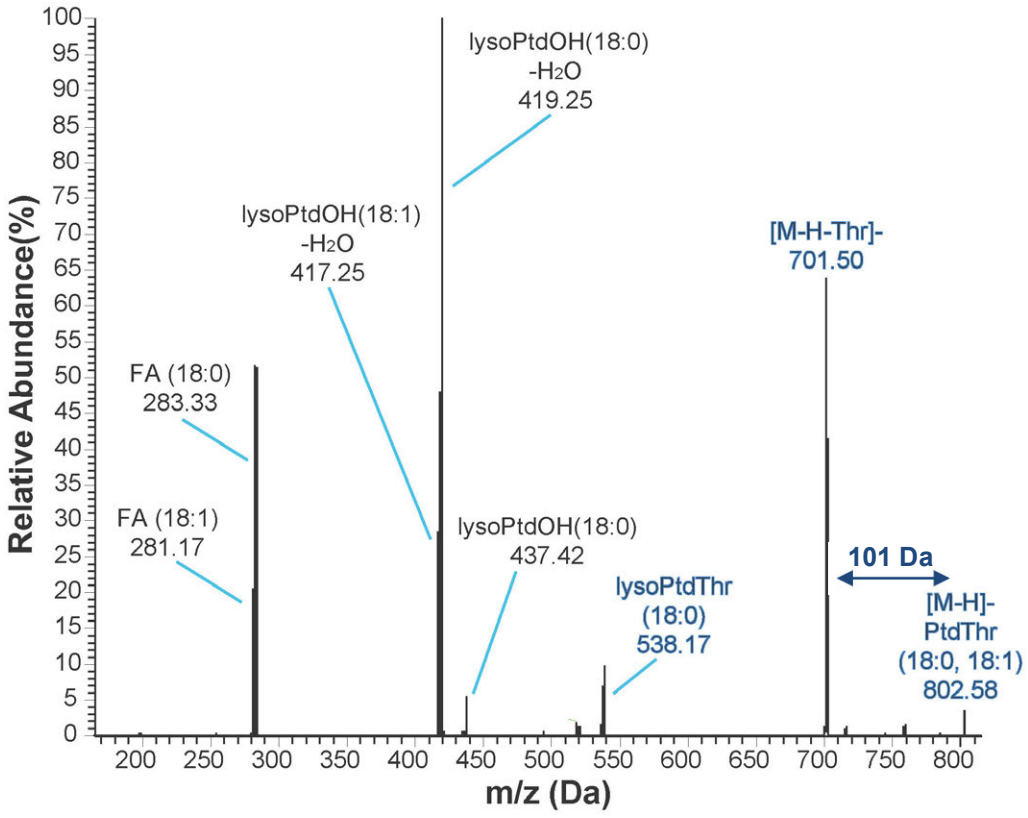

C.

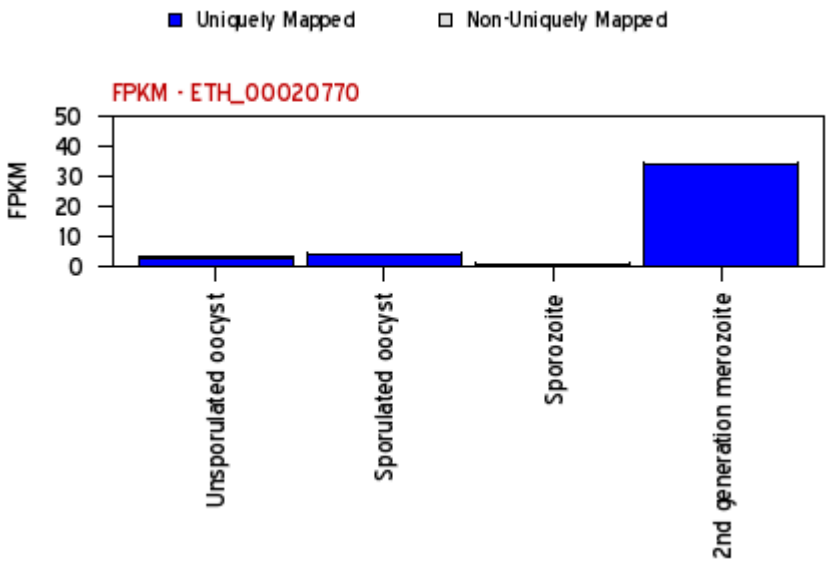

D.

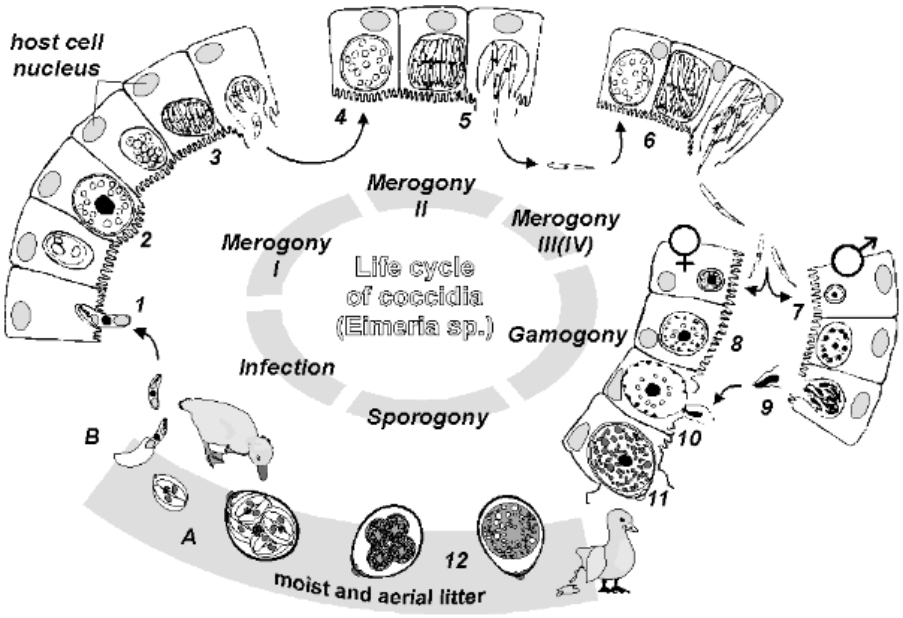

PtdThr is present in the coccidian parasite Eimeria tenella. **(A)** MS spectra of the HPLC-derived fraction containing PtdThr in lipids of *Eimeria tenella* sporozoites (donated by Dr. Damer Blake, Royal Veterinary College, University of London). Observe dominance of PtdThr (36:1) species. **(B)** MS/MS spectra identifying PtdThr (18:0/18:1) in *E. tenella*. Threonine as polar head group was identified by the neutral loss of 101 Da, and fatty acyl chains by their *m/z* ratios. **(C)** Transcriptomic profile of putative *Et*PTS (ETH_00020770) during *E. tenella* life cycle (taken from ToxoDB.org). **(D)** Life cycle of *Eimeria* species (Adapted from http://www.saxonet.de/coccidia/coccid02.htm).

References

Agop-Nersesian, C., Egarter, S., Langsley, G., Foth, B.J., Ferguson, D.J.P., and Meissner, M. (2010). Biogenesis of the inner membrane complex is dependent on vesicular transport by the alveolate specific GTPase Rab11B. PLoS Pathog. *6*, e1001029.

Agrawal, S., van Dooren, G.G., Beatty, W.L., and Striepen, B. (2009). Genetic evidence that an endosymbiont-derived endoplasmic reticulum-associated protein degradation (ERAD) system functions in import of apicoplast proteins. J. Biol. Chem. *284*, 33683–33691.

An, D., Na, C., Bielawski, J., Hannun, Y.A., and Kasper, D.L. (2011). Membrane sphingolipids as essential molecular signals for Bacteroides survival in the intestine. Proc. Natl. Acad. Sci. U. S. A. *108 Suppl* , 4666–4671.

Andenmatten, N., Egarter, S., Jackson, A.J., Jullien, N., Herman, J.-P., and Meissner, M. (2013). Conditional genome engineering in Toxoplasma gondii uncovers alternative invasion mechanisms. Nat. Methods *10*, 125–127.

Armstrong, C.M., and Goldberg, D.E. (2007). An FKBP destabilization domain modulates protein levels in Plasmodium falciparum. Nat. Methods *4*, 1007–1009.

Arrizabalaga, G., and Boothroyd, J.C. (2004). Role of calcium during Toxoplasma gondii invasion and egress. Int. J. Parasitol. *34*, 361–368.

Baldauf, S.L. (2003). The deep roots of eukaryotes. Science *300*, 1703–1706.

Banaszynski, L.A., Chen, L.-C., Maynard-Smith, L.A., Ooi, A.G.L., and Wandless, T.J. (2006). A rapid, reversible, and tunable method to regulate protein function in living cells using synthetic small molecules. Cell *126*, 995–1004.

Behnke, M.S., Fentress, S.J., Mashayekhi, M., Li, L.X., Taylor, G.A., and Sibley, L.D. (2012). The polymorphic pseudokinase ROP5 controls virulence in Toxoplasma gondii by regulating the active kinase ROP18. PLoS Pathog. *8*, e1002992.

Bereswill, S., Kühl, A.A., Alutis, M., Fischer, A., Möhle, L., Struck, D., Liesenfeld, O., Göbel, U.B., Dunay, I.R., and Heimesaat, M.M. (2014). The impact of Toll-like-receptor-9 on intestinal microbiota composition and extra-intestinal sequelae in experimental Toxoplasma gondii induced ileitis. Gut Pathog. *6*, 19.

Billker, O., Lourido, S., and Sibley, L.D. (2009). Calcium-dependent signaling and kinases in apicomplexan parasites. Cell Host Microbe *5*, 612–622.

Black, M.W., and Boothroyd, J.C. (2000). Lytic cycle of Toxoplasma gondii. Microbiol. Mol. Biol. Rev. *64*, 607–623.

Bligh, E.G., and Dyer, W.J. (1959). A rapid method of total lipid extraction and purification. Can. J. Biochem. Physiol. *37*, 911–917.

Blume, M., Rodriguez-Contreras, D., Landfear, S., Fleige, T., Soldati-Favre, D., Lucius, R., and Gupta, N. (2009). Host-derived glucose and its transporter in the obligate intracellular pathogen Toxoplasma gondii are dispensable by glutaminolysis. Proc. Natl. Acad. Sci. U. S. A. *106*, 12998–13003.

Bryan, J.K. (1980). Synthesis of the aspartate family and branched chain amino-acids: The Biochemistry of Plants (New York, NY: Academic Press).

Buxton, D. (1993). Toxoplasmosis: the first commercial vaccine. Parasitol. Today *9*, 335–337.

Cavaillès, P., Sergent, V., Bisanz, C., Papapietro, O., Colacios, C., Mas, M., Subra, J.-F., Lagrange, D., Calise, M., Appolinaire, S., et al. (2006). The rat Toxo1 locus directs toxoplasmosis outcome and controls parasite proliferation and spreading by macrophage-dependent mechanisms. Proc. Natl. Acad. Sci. U. S. A. *103*, 744–749.

Charron, A.J., and Sibley, L.D. (2002). Host cells: mobilizable lipid resources for the intracellular parasite Toxoplasma gondii. J. Cell Sci. *115*, 3049–3059.

Chaudhary, K., Darling, J.A., Fohl, L.M., Sullivan, W.J., Donald, R.G.K., Pfefferkorn, E.R., Ullman, B., and Roos, D.S. (2004). Purine salvage pathways in the apicomplexan parasite Toxoplasma gondii. J. Biol. Chem. *279*, 31221–31227.

Chen, T.-W., Wardill, T.J., Sun, Y., Pulver, S.R., Renninger, S.L., Baohan, A., Schreiter, E.R., Kerr, R.A., Orger, M.B., Jayaraman, V., et al. (2013). Ultrasensitive fluorescent proteins for imaging neuronal activity. Nature *499*, 295–300.

Chen, Y.-L., Montedonico, A.E., Kauffman, S., Dunlap, J.R., Menn, F.-M., and Reynolds, T.B. (2010). Phosphatidylserine synthase and phosphatidylserine decarboxylase are essential for cell wall integrity and virulence in Candida albicans. Mol. Microbiol. *75*, 1112–1132.

Chini, E.N., Nagamune, K., Wetzel, D.M., and Sibley, L.D. (2005). Evidence that the cADPR signalling pathway controls calcium-mediated microneme secretion in Toxoplasma gondii. Biochem. J. *389*, 269–277.

Choi, H.-S., Han, G.-S., and Carman, G.M. (2010). Phosphorylation of yeast phosphatidylserine synthase by protein kinase A: identification of Ser46 and Ser47 as major sites of phosphorylation. J. Biol. Chem. *285*, 11526–11536.

Choi, J.-Y., Martin, W.E., Murphy, R.C., and Voelker, D.R. (2004). Phosphatidylcholine and N-methylated phospholipids are nonessential in Saccharomyces cerevisiae. J. Biol. Chem. *279*, 42321–42330.

Coppens, I., Sinai, A.P., and Joiner, K.A. (2000). Toxoplasma gondii exploits host low-density lipoprotein receptor-mediated endocytosis for cholesterol acquisition. J. Cell Biol. *149*, 167–180.

Crowley, J.J., Treistman, S.N., and Dopico, A.M. (2005). Distinct structural features of phospholipids differentially determine ethanol sensitivity and basal function of BK channels. Mol. Pharmacol. *68*, 4–10.

Dalton, K.A., Pilot, J.D., Mall, S., East, J.M., and Lee, A.G. (1999). Anionic phospholipids decrease the rate of slippage on the Ca(2+)-ATPase of sarcoplasmic reticulum. Biochem. J. *342 (Pt 2*, 431–438.

Daum, G. (1985). Lipids of mitochondria. Biochim. Biophys. Acta *822*, 1–42.

DeRocher, A., Hagen, C.B., Froehlich, J.E., Feagin, J.E., and Parsons, M. (2000). Analysis of targeting sequences demonstrates that trafficking to the Toxoplasma gondii plastid branches off the secretory system. J. Cell Sci. *113 (Pt 2*, 3969–3977.

Donald, R.G., and Roos, D.S. (1993). Stable molecular transformation of Toxoplasma gondii: a selectable dihydrofolate reductase-thymidylate synthase marker based on drug-resistance mutations in malaria. Proc. Natl. Acad. Sci. U. S. A. *90*, 11703–11707.

Donald, R.G., and Roos, D.S. (1995). Insertional mutagenesis and marker rescue in a protozoan parasite: cloning of the uracil phosphoribosyltransferase locus from Toxoplasma gondii. Proc. Natl. Acad. Sci. U. S. A. *92*, 5749–5753.

Dubey, J.. (1998). Advances in the life cycle of Toxoplasma gondii. Int. J. Parasitol. *28*, 1019–1024.

Echeverria, P.C., Matrajt, M., Harb, O.S., Zappia, M.P., Costas, M.A., Roos, D.S., Dubremetz, J.F., and Angel, S.O. (2005). Toxoplasma gondii Hsp90 is a potential drug target whose expression and subcellular localization are developmentally regulated. J. Mol. Biol. *350*, 723–734.

Echeverria, P.C., de Miguel, N., Costas, M., and Angel, S.O. (2006). Potent antigen-specific immunity to Toxoplasma gondii in adjuvant-free vaccination system using Rop2-Leishmania infantum Hsp83 fusion protein. Vaccine *24*, 4102–4110.

Endo, T., and Yagita, K. Effect of extracellular ions on motility and cell entry in Toxoplasma gondii. J. Protozool. *37*, 133–138.

Fadok, V.A., Voelker, D.R., Campbell, P.A., Cohen, J.J., Bratton, D.L., and Henson, P.M. (1992). Exposure of phosphatidylserine on the surface of apoptotic lymphocytes triggers specific recognition and removal by macrophages. J. Immunol. *148*, 2207–2216.

Fang, J., Marchesini, N., and Moreno, S.N.J. (2006). A Toxoplasma gondii phosphoinositide phospholipase C (TgPI-PLC) with high affinity for phosphatidylinositol. Biochem. J. *394*, 417–425.

Flegr, J., Klapilová, K., and Kaňková, S. (2014). Toxoplasmosis can be a sexually transmitted infection with serious clinical consequences. Not all routes of infection are created equal. Med. Hypotheses.

Florin-Christensen, J., Suarez, C.E., Florin-Christensen, M., Hines, S.A., McElwain, T.F., and Palmer, G.H. (2000). Phosphatidylcholine formation is the predominant lipid biosynthetic event in the hemoparasite Babesia bovis. Mol. Biochem. Parasitol. *106*, 147–156.

Foussard, F., Gallois, Y., Girault, A., and Menez, J.F. (1991). Lipids and fatty acids of tachyzoites and purified pellicles of Toxoplasma gondii. Parasitol. Res. *77*, 475–477.

Fox, B.A., and Bzik, D.J. (2002). De novo pyrimidine biosynthesis is required for virulence of Toxoplasma gondii. Nature *415*, 926–929.

Fox, B.A., Ristuccia, J.G., Gigley, J.P., and Bzik, D.J. (2009). Efficient Gene Replacements in Toxoplasma gondii Strains Deficient for Nonhomologous End Joining. Eukaryot. Cell *8*, 520–529.

Fox, B.A., Falla, A., Rommereim, L.M., Tomita, T., Gigley, J.P., Mercier, C., Cesbron-Delauw, M.-F., Weiss, L.M., and Bzik, D.J. (2011). Type II Toxoplasma gondii KU80 knockout strains enable functional analysis of genes required for cyst development and latent infection. Eukaryot. Cell *10*, 1193–1206.

Fruth, I.A., and Arrizabalaga, G. (2007). Toxoplasma gondii: induction of egress by the potassium ionophore nigericin. Int. J. Parasitol. *37*, 1559–1567.

Gigley, J.P., Fox, B.A., and Bzik, D.J. (2009). Long-term immunity to lethal acute or chronic type II Toxoplasma gondii infection is effectively induced in genetically susceptible C57BL/6 mice by immunization with an attenuated type I vaccine strain. Infect. Immun. *77*, 5380–5388.

Gupta, N., Zahn, M.M., Coppens, I., Joiner, K. a, and Voelker, D.R. (2005). Selective disruption of phosphatidylcholine metabolism of the intracellular parasite Toxoplasma gondii arrests its growth. J. Biol. Chem. *280*, 16345–16353.

Gupta, N., Hartmann, A., Lucius, R., and Voelker, D.R. (2012). The obligate intracellular parasite Toxoplasma gondii secretes a soluble phosphatidylserine decarboxylase. J. Biol. Chem. *287*, 22938–22947.

Håkansson, S., Charron, A.J., and Sibley, L.D. (2001). Toxoplasma evacuoles: a two-step process of secretion and fusion forms the parasitophorous vacuole. EMBO J. *20*, 3132–3144.

Hartmann, A., Arroyo-Olarte, R.D., Imkeller, K., Hegemann, P., Lucius, R., and Gupta, N. (2013). Optogenetic modulation of an adenylate cyclase in Toxoplasma gondii demonstrates a requirement of the parasite cAMP for host-cell invasion and stage differentiation. J. Biol. Chem.

Hartmann, A., Hellmund, M., Lucius, R., Voelker, D.R., and Gupta, N. (2014). Phosphatidylethanolamine synthesis in the parasite mitochondrion is required for efficient growth but dispensable for survival of Toxoplasma gondii. J. Biol. Chem.

Hasegawa, K., Kuge, O., Nishijima, M., and Akamatsu, Y. (1989). Isolation and characterization of a Chinese hamster ovary cell mutant with altered regulation of phosphatidylserine biosynthesis. J. Biol. Chem. *264*, 19887–19892.

Heaslip, A.T., Nishi, M., Stein, B., and Hu, K. (2011). The Motility of a Human Parasite, Toxoplasma gondii, Is Regulated by a Novel Lysine Methyltransferase. PLoS Pathog. *7*, e1002201.

Heikinheimo, L., and Somerharju, P. (2002). Translocation of phosphatidylthreonine and -serine to mitochondria diminishes exponentially with increasing molecular hydrophobicity. Traffic *3*, 367–377.

Herm-Götz, A., Agop-Nersesian, C., Münter, S., Grimley, J.S., Wandless, T.J., Frischknecht, F., and Meissner, M. (2007). Rapid control of protein level in the apicomplexan Toxoplasma gondii. Nat. Methods *4*, 1003–1005.

Hikiji, T., Miura, K., Kiyono, K., Shibuya, I., and Ohta, A. (1988). Disruption of the CHO1 gene encoding phosphatidylserine synthase in Saccharomyces cerevisiae. J. Biochem. *104*, 894–900.

Hoek, J.B., Thomas, A.P., Rubin, R., and Rubin, E. (1987). Ethanol-induced mobilization of calcium by activation of phosphoinositide-specific phospholipase C in intact hepatocytes. J. Biol. Chem. *262*, 682–691.

Hsiao, L.L., Howard, R.J., Aikawa, M., and Taraschi, T.F. (1991). Modification of host cell membrane lipid composition by the intra-erythrocytic human malaria parasite Plasmodium falciparum. Biochem. J. *274*, 121–132.

Hubbard, S.C., and Brody, S. (1975). Glycerophospholipid variation in choline and inositol auxotrophs of Neurospora crassa. Internal compensation among zwitterionic and anionic species. J. Biol. Chem. *250*, 7173–7181.

Huynh, M.-H., and Carruthers, V.B. (2006). Toxoplasma MIC2 is a major determinant of invasion and virulence. PLoS Pathog. *2*, e84.

Ikeda, M., Kihara, A., and Igarashi, Y. (2006). Lipid asymmetry of the eukaryotic plasma membrane: functions and related enzymes. Biol. Pharm. Bull. *29*, 1542–1546.

Iltzsch, M.H. (1993). Pyrimidine salvage pathways in Toxoplasma gondii. J. Eukaryot. Microbiol. *40*, 24–28.

Ivanova, P.T., Milne, S.B., and Brown, H.A. (2010). Identification of atypical ether-linked glycerophospholipid species in macrophages by mass spectrometry. J. Lipid Res. *51*, 1581–1590.

Iwashita, M., Makide, K., Nonomura, T., Misumi, Y., Otani, Y., Ishida, M., Taguchi, R., Tsujimoto, M., Aoki, J., Arai, H., et al. (2009). Synthesis and evaluation of lysophosphatidylserine analogues as inducers of mast cell degranulation. Potent activities of lysophosphatidylthreonine and its 2-deoxy derivative. J. Med. Chem. *52*, 5837–5863.

Janmey, P. a, and Kinnunen, P.K.J. (2006). Biophysical properties of lipids and dynamic membranes. Trends Cell Biol. *16*, 538–546.

Janouskovec, J., Horák, A., Oborník, M., Lukes, J., and Keeling, P.J. (2010). A common red algal origin of the apicomplexan, dinoflagellate, and heterokont plastids. Proc. Natl. Acad. Sci. U. S. A. *107*, 10949–10954.

Jensen, K.D.C., Hu, K., Whitmarsh, R.J., Hassan, M.A., Julien, L., Lu, D., Chen, L., Hunter, C.A., and Saeij, J.P.J. (2013). Toxoplasma gondii rhoptry 16 kinase promotes host resistance to oral infection and intestinal inflammation only in the context of the dense granule protein GRA15. Infect. Immun. *81*, 2156–2167.

Jiménez-Ruiz, E., Wong, E.H., Pall, G.S., and Meissner, M. (2014). Advantages and disadvantages of conditional systems for characterization of essential genes in Toxoplasma gondii. Parasitology 1–9.

Kafsack, B.F.C., Beckers, C., and Carruthers, V.B. (2004). Synchronous invasion of host cells by Toxoplasma gondii. Mol. Biochem. Parasitol. *136*, 309–311.

Kafsack, B.F.C., Pena, J.D.O., Coppens, I., Ravindran, S., Boothroyd, J.C., and Carruthers, V.B. (2009). Rapid membrane disruption by a perforin-like protein facilitates parasite exit from host cells. Science (80-.). *323*, 530–533.

Kasimova, M.A., Tarek, M., Shaytan, A.K., Shaitan, K. V, and Delemotte, L. (2014). Voltage-gated ion channel modulation by lipids: insights from molecular dynamics simulations. Biochim. Biophys. Acta *1838*, 1322–1331.

Kaufusi, P.H., Kelley, J.F., Yanagihara, R., and Nerurkar, V.R. (2014). Induction of endoplasmic reticulum-derived replication-competent membrane structures by West Nile virus non-structural protein 4B. PLoS One *9*, e84040.

Kay, J.G., and Grinstein, S. (2011). Sensing phosphatidylserine in cellular membranes. Sensors (Basel). *11*, 1744–1755.

Kemen, E., Gardiner, A., and Schultz-Larsen, T. (2011). Gene gain and loss during evolution of obligate parasitism in the white rust pathogen of Arabidopsis thaliana. PLoS Biol. *9*.

Kim, K., and Boothroyd, J.C. (1995). Toxoplasma gondii: stable complementation of sag1 (p30) mutants using SAG1 transfection and fluorescence-activated cell sorting. Exp. Parasitol. *80*, 46–53.

Kim, S.-K., Fouts, A.E., and Boothroyd, J.C. (2007). Toxoplasma gondii dysregulates IFN-gamma-inducible gene expression in human fibroblasts: insights from a genome-wide transcriptional profiling. J. Immunol. *178*, 5154–5165.

Kobayashi, T., Beuchat, M.-H., Chevallier, J., Makino, A., Mayran, N., Escola, J.-M., Lebrand, C., Cosson, P., Kobayashi, T., and Gruenberg, J. (2002). Separation and characterization of late endosomal membrane domains. J. Biol. Chem. *277*, 32157–32164.

Kolter, T., and Sandhoff, K. (2005). Principles of lysosomal membrane digestion: stimulation of sphingolipid degradation by sphingolipid activator proteins and anionic lysosomal lipids. Annu. Rev. Cell Dev. Biol. *21*, 81–103.

Krohn, M., Lange, C., Hofrichter, J., Scheffler, K., Stenzel, J., Steffen, J., Schumacher, T., Brüning, T., Plath, A.-S., Alfen, F., et al. (2011). Cerebral amyloid-β proteostasis is regulated by the membrane transport protein ABCC1 in mice. J. Clin. Invest. *121*, 3924–3931.

Kuge, O., Saito, K., and Nishijima, M. (1997). Cloning of a Chinese hamster ovary (CHO) cDNA encoding phosphatidylserine synthase (PSS) II, overexpression of which suppresses the phosphatidylserine biosynthetic defect of a PSS I-lacking mutant of CHO-K1 cells. J. Biol. Chem. *272*, 19133–19139.

Kuge, O., Hasegawa, K., Saito, K., and Nishijima, M. (1998). Control of phosphatidylserine biosynthesis through phosphatidylserine-mediated inhibition of phosphatidylserine synthase I in Chinese hamster ovary cells. Proc. Natl. Acad. Sci. U. S. A. *95*, 4199–4203.

Kur, J., Holec-Gasior, L., and Hiszczyńska-Sawicka, E. (2009). Current status of toxoplasmosis vaccine development. Expert Rev. Vaccines *8*, 791–808.

Leventis, P.A., and Grinstein, S. (2010). The distribution and function of phosphatidylserine in cellular membranes. Annu. Rev. Biophys. *39*, 407–427.

Li, M.O., Sarkisian, M.R., Mehal, W.Z., Rakic, P., and Flavell, R.A. (2003). Phosphatidylserine receptor is required for clearance of apoptotic cells. Science *302*, 1560–1563.

Li, Z.-Y., Chen, J., Petersen, E., Zhou, D.-H., Huang, S.-Y., Song, H.-Q., and Zhu, X.-Q. (2014). Synergy of mIL-21 and mIL-15 in enhancing DNA vaccine efficacy against acute and chronic Toxoplasma gondii infection in mice. Vaccine *32*, 3058–3065.

Liu, Y.-C., and Singh, U. (2014). Destabilization domain approach adapted for regulated protein expression in the protozoan parasite Entamoeba histolytica. Int. J. Parasitol.

Lopes, W.D.Z., Rodriguez, J.D., Souza, F.A., dos Santos, T.R., dos Santos, R.S., Rosanese, W.M., Lopes, W.R.Z., Sakamoto, C.A., and da Costa, A.J. (2013). Sexual transmission of Toxoplasma gondii in sheep. Vet. Parasitol. *195*, 47–56.

Lourido, S., Shuman, J., Zhang, C., Shokat, K.M., Hui, R., and Sibley, L.D. (2010). Calcium-dependent protein kinase 1 is an essential regulator of exocytosis in Toxoplasma. Nature *465*, 359–362.

Lovett, J.L., and Sibley, L.D. (2003). Intracellular calcium stores in Toxoplasma gondii govern invasion of host cells. J. Cell Sci. *116*, 3009–3016.

Lovett, J.L., Marchesini, N., Moreno, S.N.J., and Sibley, L.D. (2002). Toxoplasma gondii microneme secretion involves intracellular Ca(2+) release from inositol 1,4,5-triphosphate (IP(3))/ryanodine-sensitive stores. J. Biol. Chem. *277*, 25870–25876.

Makielski, J.C. (1997). Anionic Phospholipids Activate ATP-sensitive Potassium Channels. J. Biol. Chem. *272*, 5388–5395.

Mark-Malchoff, D., Marinetti, G. V, Hare, G.D., and Meisler, A. (1978). Characterization of phosphatidylthreonine in polyoma virus transformed fibroblasts. Biochemistry *17*, 2684–2688.

Martin, T.W., and Lagunoff, D. (1979). Inhibition of mast cell histamine secretion by N-substituteed derivatives of phosphatidylserine. Science *204*, 631–633.

Matsuo, H., Chevallier, J., Mayran, N., Le Blanc, I., Ferguson, C., Fauré, J., Blanc, N.S., Matile, S., Dubochet, J., Sadoul, R., et al. (2004). Role of LBPA and Alix in multivesicular liposome formation and endosome organization. Science *303*, 531–534.

Matsuo, Y., Fisher, E., Patton-Vogt, J., and Marcus, S. (2007). Functional characterization of the fission yeast phosphatidylserine synthase gene, pps1, reveals novel cellular functions for phosphatidylserine. Eukaryot. Cell *6*, 2092–2101.

McCoy, J.M., Whitehead, L., van Dooren, G.G., and Tonkin, C.J. (2012). TgCDPK3 regulates calcium-dependent egress of Toxoplasma gondii from host cells. PLoS Pathog. *8*, e1003066.

McCOY, R.H., MEYER, C.E., and ROSE, W.C. (1974). FEEDING EXPERIMENTS WITH MIXTURES OF HIGHLY PURIFIED AMINO ACIDS. VIII. ISOLATION AND IDENTIFICATION OF A NEW ESSENTIAL AMINO ACID*. Nutr. Rev. *32*, 16–18.

Van Meer, G., and de Kroon, A.I.P.M. (2011). Lipid map of the mammalian cell. J. Cell Sci. *124*, 5–8.

Van Meer, G., Voelker, D.R., Feigenson, G.W., and Meer, G. (2008). Membrane lipids: where they are and how they behave. Nat. Rev. Mol. Cell Biol. *9*, 112–124.

Meissner, M., Schlüter, D., and Soldati, D. (2002). Role of Toxoplasma gondii myosin A in powering parasite gliding and host cell invasion. Science *298*, 837–840.

Mendes, É.A., Fonseca, F.G., Casério, B.M., Colina, J.P., Gazzinelli, R.T., and Caetano, B.C. (2013). Recombinant vaccines against T. gondii: comparison between homologous and heterologous vaccination protocols using two viral vectors expressing SAG1. PLoS One *8*, e63201.

Mercier, C., Howe, D.K., Mordue, D., Lingnau, M., and Sibley, L.D. (1998). Targeted disruption of the GRA2 locus in Toxoplasma gondii decreases acute virulence in mice. Infect. Immun. *66*, 4176–4182.

Mital, J., Meissner, M., Soldati, D., and Ward, G.E. (2005). Conditional expression of Toxoplasma gondii apical membrane antigen-1 (TgAMA1) demonstrates that TgAMA1 plays a critical role in host cell invasion. Mol. Biol. Cell *16*, 4341–4349.

Mitoma, J., Kasama, T., Furuya, S., and Hirabayashi, Y. (1998). Occurrence of an unusual phospholipid, phosphatidyl-L-threonine, in cultured hippocampal neurons. Exogenous L-serine is required for the synthesis of neuronal phosphatidyl-L-serine and sphingolipids. J. Biol. Chem. *273*, 19363–19366.

Möhle, L., Parlog, A., Pahnke, J., and Dunay, I.R. (2014). Spinal cord pathology in chronic experimental Toxoplasma gondii infection. Eur. J. Microbiol. Immunol. (Bp). *4*, 65–75.

Mordue, D.G., Monroy, F., La Regina, M., Dinarello, C.A., and Sibley, L.D. (2001). Acute toxoplasmosis leads to lethal overproduction of Th1 cytokines. J. Immunol. *167*, 4574–4584.

Moreno, S.N.J., Ayong, L., and Pace, D.A. (2011). NIH Public Access. Essays Biochem. *51*, 97–110.

Moudy, R., Manning, T.J., and Beckers, C.J. (2001). The loss of cytoplasmic potassium upon host cell breakdown triggers egress of Toxoplasma gondii. J. Biol. Chem. *276*, 41492–41501.

Nagamune, K., and Sibley, L.D. (2006). Comparative genomic and phylogenetic analyses of calcium ATPases and calcium-regulated proteins in the apicomplexa. Mol. Biol. Evol. *23*, 1613–1627.

Nagamune, K., Moreno, S.N.J., Chini, E.N., and Sibley, L.D. (2008a). Molecular Mechanisms of Parasite Invasion. Chapter 5: Calcium Regulation and Signaling in Apicomplexan Parasites (New York, NY: Springer New York).

Nagamune, K., Hicks, L.M., Fux, B., Brossier, F., Chini, E.N., and Sibley, L.D. (2008b). Abscisic acid controls calcium-dependent egress and development in Toxoplasma gondii. Nature *451*, 207–210.

Navia, B.A., Petito, C.K., Gold, J.W., Cho, E.S., Jordan, B.D., and Price, R.W. (1986). Cerebral toxoplasmosis complicating the acquired immune deficiency syndrome: clinical and neuropathological findings in 27 patients. Ann. Neurol. *19*, 224–238.

Niedelman, W., Gold, D.A., Rosowski, E.E., Sprokholt, J.K., Lim, D., Farid Arenas, A., Melo, M.B., Spooner, E., Yaffe, M.B., and Saeij, J.P.J. (2012). The rhoptry proteins ROP18 and ROP5 mediate Toxoplasma gondii evasion of the murine, but not the human, interferon-gamma response. PLoS Pathog. *8*, e1002784.

Oborník, M., Janouskovec, J., Chrudimský, T., and Lukes, J. (2009). Evolution of the apicoplast and its hosts: from heterotrophy to autotrophy and back again. Int. J. Parasitol. *39*, 1–12.

Ohsawa, T., Nishijima, M., and Kuge, O. (2004). Functional analysis of Chinese hamster phosphatidylserine synthase 1 through systematic alanine mutagenesis. Biochem. J. *381*, 853–859.

Pace, D.A., McKnight, C.A., Liu, J., Jimenez, V., and Moreno, S.N.J. (2014). Calcium Entry in Toxoplasma gondii and Its Enhancing Effect of Invasion-linked Traits. J. Biol. Chem. *289*, 19637–19647.

Parlog, A., Harsan, L.-A., Zagrebelsky, M., Weller, M., von Elverfeldt, D., Mawrin, C., Korte, M., and Dunay, I.R. (2014). Chronic murine toxoplasmosis is defined by subtle changes in neuronal connectivity. Dis. Model. Mech. *7*, 459–469.

Pfefferkorn, E.R., and Kasper, L.H. (1983). Toxoplasma gondii: genetic crosses reveal phenotypic suppression of hydroxyurea resistance by fluorodeoxyuridine resistance. Exp. Parasitol. *55*, 207–218.

Pfefferkorn, E.R., and Pfefferkorn, L.C. (1976). Arabinosyl nucleosides inhibit Toxoplasma gondii and allow the selection of resistant mutants. J. Parasitol. *62*, 993–999.

Plattner, F., Yarovinsky, F., Romero, S., Didry, D., Carlier, M.-F., Sher, A., and Soldati-Favre, D. (2008). Toxoplasma profilin is essential for host cell invasion and TLR11-dependent induction of an interleukin-12 response. Cell Host Microbe *3*, 77–87.

Plattner, H., Sehring, I.M., Mohamed, I.K., Miranda, K., De Souza, W., Billington, R., Genazzani, A., and Ladenburger, E.-M. (2012). Calcium signaling in closely related protozoan groups (Alveolata): non-parasitic ciliates (Paramecium, Tetrahymena) vs. parasitic Apicomplexa (Plasmodium, Toxoplasma). Cell Calcium *51*, 351–382.

Radke, J.R., and White, M.W. (1998). A cell cycle model for the tachyzoite of Toxoplasma gondii using the Herpes simplex virus thymidine kinase. Mol. Biochem. Parasitol. *94*, 237–247.

Ramakrishnan, S., Serricchio, M., Striepen, B., and Bütikofer, P. (2013). Lipid synthesis in protozoan parasites: a comparison between kinetoplastids and apicomplexans. Prog. Lipid Res. *52*, 488–512.

Raykhel, I., Alanen, H., Salo, K., Jurvansuu, J., Nguyen, V.D., Latva-Ranta, M., and Ruddock, L. (2007). A molecular specificity code for the three mammalian KDEL receptors. J. Cell Biol. *179*, 1193–1204.

Roiko, M.S., and Carruthers, V.B. (2013). Functional dissection of Toxoplasma gondii perforin-like protein 1 reveals a dual domain mode of membrane binding for cytolysis and parasite egress. J. Biol. Chem. *288*, 8712–8725.

Romano, J.D., de Beaumont, C., Carrasco, J.A., Ehrenman, K., Bavoil, P.M., and Coppens, I. (2013a). Fierce competition between Toxoplasma and Chlamydia for host cell structures in dually infected cells. Eukaryot. Cell *12*, 265–277.

Romano, J.D., Sonda, S., Bergbower, E., Smith, M.E., and Coppens, I. (2013b). Toxoplasma gondii salvages sphingolipids from the host Golgi through the rerouting of selected Rab vesicles to the parasitophorous vacuole. Mol. Biol. Cell *24*, 1974–1995.

Rotureau, B., Gego, A., and Carme, B. (2005). Trypanosomatid protozoa: a simplified DNA isolation procedure. Exp. Parasitol. *111*, 207–209.

Rouser, G., Fleischer, S., and Yamamoto, A. (1970). Two dimensional thin layer chromatographic separation of polar lipids and determination of phospholipids by phosphorus analysis of spots. Lipids *5*, 494–496.

Sadak, A., Taghy, Z., Fortier, B., and Dubremetz, J.F. (1988). Characterization of a family of rhoptry proteins of Toxoplasma gondii. Mol. Biochem. Parasitol. *29*, 203–211.

Sampels, V., Hartmann, A., Dietrich, I., Coppens, I., Sheiner, L., Striepen, B., Herrmann, A., Lucius, R., and Gupta, N. (2012). Conditional mutagenesis of a novel choline kinase demonstrates plasticity of phosphatidylcholine biogenesis and gene expression in Toxoplasma gondii. J. Biol. Chem. *287*, 16289–16299.

Sarantis, H., and Grinstein, S. (2012). Monitoring phospholipid dynamics during phagocytosis: application of genetically-encoded fluorescent probes. Methods Cell Biol. *108*, 429–444.

Sato, S. (2011). The apicomplexan plastid and its evolution. Cell. Mol. Life Sci. *68*, 1285–1296.

Sellmyer, M.A., Chen, L., Egeler, E.L., Rakhit, R., and Wandless, T.J. (2012). Intracellular context affects levels of a chemically dependent destabilizing domain. PLoS One *7*, e43297.

Séron, K., Dzierszinski, F., and Tomavo, S. (2000). Molecular cloning, functional complementation in Saccharomyces cerevisiae and enzymatic properties of phosphatidylinositol synthase from the protozoan parasite Toxoplasma gondii. Eur. J. Biochem. *267*, 6571–6579.

Singer, S.J., and Nicolson, G.L. (1972). The fluid mosaic model of the structure of cell membranes. Science *175*, 720–731.

Smith, B.N. (1972). Natural Abundance of the Stable Isotopes of Carbon in Biological Systems. Bioscience *22*, 226–231.

Soldati, D., and Boothroyd, J.C. (1993). Transient transfection and expression in the obligate intracellular parasite Toxoplasma gondii. Science (80-.). *260*, 349–352.

Sousa, S.B., Jenkins, D., Chanudet, E., Tasseva, G., Ishida, M., Anderson, G., Docker, J., Ryten, M., Sa, J., Saraiva, J.M., et al. (2014). Gain-of-function mutations in the phosphatidylserine synthase 1 (PTDSS1) gene cause Lenz-Majewski syndrome. Nat. Genet. *46*, 70–76.

Striepen, B. (2007). Switching parasite proteins on and off. Nat. Methods *4*, 999–1000.

Su, C., Howe, D.K., Dubey, J.P., Ajioka, J.W., and Sibley, L.D. (2002). Identification of quantitative trait loci controlling acute virulence in Toxoplasma gondii. Proc. Natl. Acad. Sci. U. S. A. *99*, 10753–10758.

Sullivan, W.J., and Jeffers, V. (2012). Mechanisms of Toxoplasma gondii persistence and latency. FEMS Microbiol. Rev. *36*, 717–733.

Torgerson, P.R., and Mastroiacovo, P. (2013). The global burden of congenital toxoplasmosis: a systematic review. Bull. World Health Organ. *91*, 501–508.

Uchida, Y., Hasegawa, J., Chinnapen, D., Inoue, T., Okazaki, S., Kato, R., Wakatsuki, S., Misaki, R., Koike, M., Uchiyama, Y., et al. (2011). Intracellular phosphatidylserine is essential for retrograde membrane traffic through endosomes. Proc. Natl. Acad. Sci. U. S. A. *108*, 15846–15851.

Vaden, D.L., Gohil, V.M., Gu, Z., and Greenberg, M.L. (2005). Separation of yeast phospholipids using one-dimensional thin-layer chromatography. Anal. Biochem. *338*, 162–164.

Vance, J.E. (2008). Phosphatidylserine and phosphatidylethanolamine in mammalian cells: two metabolically related aminophospholipids. J. Lipid Res. *49*, 1377–1387.

Vance, J.E., and Vance, D.E. (2004). Phospholipid biosynthesis in mammalian cells. Biochem. Cell Biol. *82*, 113–128.

Vial, H.J., and Ancelin, M.L. (1992). Malarial lipids. An overview. Subcell. Biochem. *18*, 259–306.

Vial, H.J., Eldin, P., Tielens, A.G.M., and van Hellemond, J.J. (2003). Phospholipids in parasitic protozoa. Mol. Biochem. Parasitol. *126*, 143–154.

Voelker, D.R. (1984). Phosphatidylserine functions as the major precursor of phosphatidylethanolamine in cultured BHK-21 cells. Proc. Natl. Acad. Sci. U. S. A. *81*, 2669–2673.

Vogler, S., Pahnke, J., Rousset, S., Ricquier, D., Moch, H., Miroux, B., and Ibrahim, S.M. (2006). Uncoupling protein 2 has protective function during experimental autoimmune encephalomyelitis. Am. J. Pathol. *168*, 1570–1575.

Welti, R., Mui, E., Sparks, A., Wernimont, S., Isaac, G., Kirisits, M., Roth, M., Roberts, C.W., Botté, C., Maréchal, E., et al. (2007). Lipidomic analysis of Toxoplasma gondii reveals unusual polar lipids. Biochemistry *46*, 13882–13890.

Wendum, D., Carbonell, N., Svrcek, M., Chazouilléres, O., and Fléjou, J.-F. (2002). Fatal disseminated toxoplasmosis in a toxoplasma seropositive liver transplant recipient. J. Clin. Pathol. *55*, 637.

Wetzel, D.M., Chen, L.A., Ruiz, F.A., Moreno, S.N.J., and Sibley, L.D. (2004). Calcium-mediated protein secretion potentiates motility in Toxoplasma gondii. J. Cell Sci. *117*, 5739–5748.

Yamaji-Hasegawa, A., and Tsujimoto, M. (2006). Asymmetric distribution of phospholipids in biomembranes. Biol. Pharm. Bull. *29*, 1547–1553.

Yamaoka, Y., Yu, Y., Mizoi, J., Fujiki, Y., Saito, K., Nishijima, M., Lee, Y., and Nishida, I. (2011). PHOSPHATIDYLSERINE SYNTHASE1 is required for microspore development in Arabidopsis thaliana. Plant J. *67*, 648–661.

Yeung, T., Gilbert, G.E., Shi, J., Silvius, J., Kapus, A., and Grinstein, S. (2008). Membrane phosphatidylserine regulates surface charge and protein localization. Science (80-.). *319*, 210–213.

Zhou, C., and Roberts, M.F. (1998). Nonessential activation and competitive inhibition of bacterial phosphatidylinositol-specific phospholipase C by short-chain phospholipids and analogues. Biochemistry *37*, 16430–16439.

Zhu-Shimoni, J., and Galili, G. (1998). Expression of an arabidopsis aspartate Kinase/Homoserine dehydrogenase gene is metabolically regulated by photosynthesis-related signals but not by nitrogenous compounds. Plant Physiol. *116*, 1023–1028.

LIST OF PUBLICATIONS AND PRESENTATIONS

The following publications and presentations resulted from the here-presented work:

Articles in international peer-reviewed journals	Ruben D. Arroyo-Olarte, Jos F. Brouwers, J. Bernd Helms, Aindrila Biswas, Ildiko R. Dunay, Richard Lucius and Nishith Gupta. "Phosphatidylthreonine and lipid-mediated control of parasite virulence" (In preparation).
Oral presentations in international conferences	IFoTox-2013: Interdisciplinary Forum on Toxoplasmosis. "Phosphatidylserine Biogenesis in *Toxoplasma gondii*". Universitätsmedizin Göttingen, Göttingen, Germany, March 2013.
Poster presentations in international conferences	XIIth International Congress on Toxoplasmosis. "A novel analog of phosphatidylserine in *Toxoplasma gondii* controls the parasite invasion and egress". St Catherine's College, Oxford. United Kingdom, June 2013 XVIth Gordon Research Conference: Biology of Host-Pathogen Interactions. "Phosphatidylserine Biogenesis in *Toxoplasma gondii*". Salve Regina University, RI, USA, June 2012

Selbstständigkeitserklärung

Hiermit erkläre ich an Eides statt, die vorliegende Dissertation selbstständig angefertigt und keine anderen als die angegebenen Quellen und Hilfsmittel benutzt zu haben.

Weiterhin versichere ich, dass diese Dissertation noch keiner anderen Fakultät oder Universität zur Prüfung vorgelegt wurde.

Ich habe mich nicht anderwärts um einen Doktorgrad beworben und besitze keinen entsprechenden Doktorgrad.

Berlin, den 8.8.2014 Ruben Dario Arroyo Olarte